LUND UNIVERSITY

BORGWARNER

Optimising a Cyclo Drive

Authors:
Eric Larsson, Joakim Persson

Supervisor BorgWarner:
Henrik Nilsson

Examiner:
Lars Vedmar

May 29, 2013

Eric Larsson, Joakim Persson: *Optimising a Cyclo Drive*, BorgWarner

May 2013

Preface

While working on this thesis, we have learned to work independently, to set our own goals and to analyse a problem from many different perspectives. We believe and hope that the results from our work will be of great value to BorgWarner in current as well as future projects.

Great thanks to:

Eric Larsson and **Joakim Persson** great cooperation.

Our examiner **Lars Vedmar** for guidance and help.

Our supervisor at BorgWarner **Henrik Nilsson** for assistance with everything practical that made this thesis possible.

Landskrona, May 2013

Eric Larsson
Joakim Persson

Abstract

In this report the function of an eccentric drive (Cyclo Drive) is evaluated. The drive transfers torque between two parallel axes. The eccentric drive is used in a differential in an all-wheel drive system made by BorgWarner. The purpose of the Cyclo Drive is to transfer torque between two parallel-displaced axles without eccentric rotation.

The mechanism consists of three discs with the middle disc being eccentrically placed relative to the outer ones. During the project, it has become apparent that the middle disc cannot withstand the load, which is the reason a thorough analysis of the system is required. The purpose is to redesign the current mechanism to fulfil the requirements as well as to be of use in future development of similar projects.

The first action in the project is to investigate alternative solutions. The idea is to see if there is any other mechanical solution that could replace the Cyclo Drive. During the research some different mechanisms are suggested. These are then evaluated to establish which one most satisfies the expectations.

The forces and contact pressures are derived analytically by analysing the geometry, while the calculations are carried out with the assist of MATLAB. The different parameters that define the geometry are varied to see how this affects the structure.

The calculated loads are then used to optimise the geometry of structure. A fatigue analysis is conducted on the old and new design to determine whether the changes lead to an improvement.

The modifications made includes a small increase of the outer radius, increased thickness, slightly increased hole radius as well as a reduction of number of holes from twelve to elven. In order to maintain the eccentricity an increase of the pin radius was required.

The improvements made lead to a structure that is improved compared to the old one, however to be sure of the functionality some real life tests will need to be conducted.

Keywords:

Mechanism, eccentric, contact pressure, torque transfer, tolerances

Sammanfattning

Denna rapport avhandlar beräkningar på en excenterväxel, Cyclo Drive, som används av BorgWarner i deras differentialer för fyrhjulsdriftssystem. Tanken är att kunna överföra ett moment mellan två parallellförskjutna axlar utan excentrisk rotation (för att undvika skadliga vibrationer).

Mekanismen är uppbyggd av tre diskar varav den mittersta och de yttre är excentriskt placerade i förhållande till varandra. BorgWarner har under projektet haft problem med att den mittersta disken inte klarar av de uppkomna belastningarna varför en grundlig analys av systemet skall genomföras. Syftet är dels att dimensionera nuvarande konstruktion för att klara belastningarna, dels att tjäna som referens för liknande framtida projekt.

För att lösa problemet göres först en marknadsundersökning för att utröna om det finns mekanismer som kan ersätta den befintliga. Resultatet av denna undersökning utvärderas sen för att få fram den alternativa lösning som klarar av de uppställda kraven bäst.

Beräkningarna på den nuvarande mekaniska lösningen genomförs analytiskt genom att analysera den nuvarande geometrien. Själva beräkningarna utförs huvudsakligen i MATLAB. För att utröna vilka förbättringar som kan göras varieras olika värden i geometrien för att se hur de uppkomna lasterna i konstruktionen påverkas.

När lasterna är beräknade för olika geometrier optimeras konstruktionen av Cyclo Driven utifrån dessa. En utmattningsberäkning körs på den ursprungliga geometrin såväl som den nya för att kontrollera att modifieringen har lett till en förbättring.

De modifieringar, som gjordes, innefattar en liten ökning av den yttre radien, något ökad tjocklek, en minskning av antalet hål från tolv till elva samt ökning av hålradien. För att bibehålla excentriciteten krävs härvid även ökad pinnradie.

De förbättringar som gjorts av utformningen av disken gör att disken nu är avsevärt förbättrad i jämförelse med den ursprungliga varianten, men för att avgöra huruvida den faktiskt uppfyller kraven kommer praktiska tester att krävas.

Table of Contents

Nomenclature

r	*Hole position radius*
r_h	*Hole radius*
r_p	*pin radius*
r_i	*Disc internal radius*
r_y	*Disc external radius*
e	*Eccentricity*
b	*Disc thickness*
θ	*Angle between holes*
φ	*Rotation angle*
Δ	*Vertical displacement*
ψ	*Deformation angle*
α	*Angle between hole centre and hole endpoint*
C	*Rolling resistance coefficient*
μ	*Frictional coefficient*
E	*Young's modulus*
ν	*Poisson's ratio*
η	*Efficiency*
F	*Contact force*
P	*Contact pressure*

1. Introduction

1.1 Background

BorgWarner is a company that designs powertrain solutions. The two groups of BorgWarner is one engine group that optimizes engines for fuel efficiency, while the other group develops transmissions and all-wheel drive systems.

The development and production placed in Landskrona Sweden mainly develops and produces all-wheel drive systems.

BorgWarner in Landskrona has started development on a new torque vectoring system called cTV. The differential is meant to be used in a way that the torque transferred to each individual wheel on the rear axle can be varied, the main reason is to improve handling of the vehicle.

It has been found during tests that a certain part of the cTV called the Cyclo Drive has not fulfilled the requirements, prompting BorgWarner to conduct a thorough analysis of the Cyclo Drive.

1.2 Project description

The Cyclo Drive is essential to the function of the cTV. From the input axis the torque is transferred through the Cyclo Drive which allows the input shaft and the output shaft of the drive to be parallel-displaced. The objective of the drive is to create an offset torque transfer. Therefore the gear ratio is to be as close to one as possible.

The offset created is used to transfer the torque through a couple of internal and external cogwheels to two lamella packages. The possibility to lock and unlock the wheel axis with the lamella packages makes it possible to decide how much torque that is to be transferred to each axis.

During the progress of this project the idea is to conclude if the Cyclo Drive is capable of withstand the forces that the torque creates. The torque and number of revolutions that the drive is to be able to withstand is given from a torque spectrum that is provided by BorgWarner. This spectrum will be used to make fatigue calculations on the mechanism.

The main task of this project is to optimize the Cyclo Drive to withstand the torque put through the gearing. There will also be some time spent investigating different mechanisms that could replace the existing mechanism with the same function and demands.

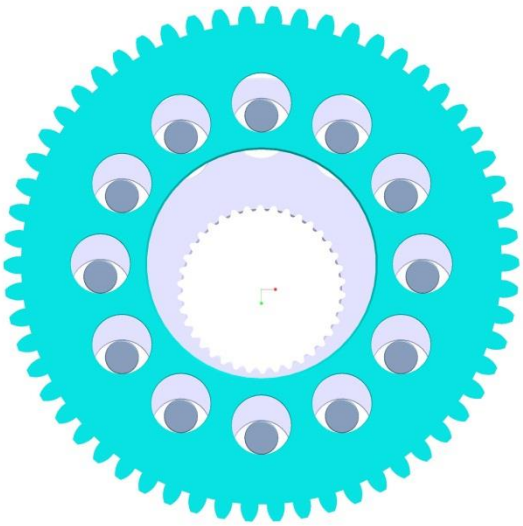

Figure 1.2.1: *Illustration of the Cyclo Drive.*

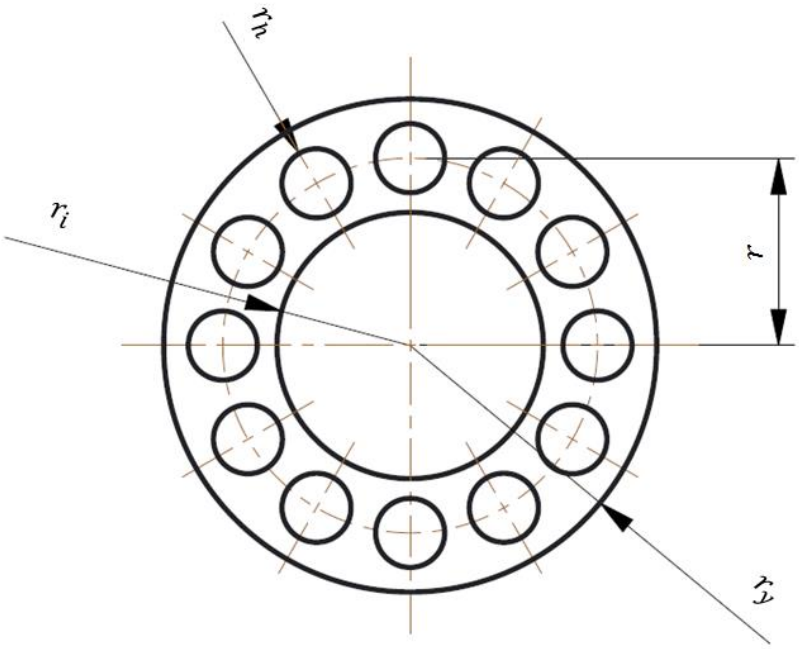

Figure 1.2.2: *Illustration of the Inner disc and parameters.*

1.3 Objectives

The goal with this master thesis is to analyse BorgWarner´s Cyclo Drive, which includes deriving the forces and contact pressures in the existing design, and to provide a basis for redesigning the mechanism, within certain geometrical constraints. The analysis is also supposed to be of use in further development of similar mechanisms, which means every geometric feature will be analysed.

Furthermore, the report includes an investigation of other mechanism with similar function, i.e. transfer of motion between parallel-displaced axes without any eccentric rotation.

1.4 Restrictions

This thesis only covers the theoretical analysis of the Cyclo Drive, which means there will be no practical testing of the proposed improvements. Neither will any attention be given to the mechanisms surrounding the Cyclo Drive, due to time limitations.

There will be no major finite element method analysis (although it may be used to a limited extent for verification purposes) of the structure due to lack of recourses. For the same reason temperature effects will be neglected.

1.5 Method

The calculation on the Cyclo Drive will be carried out without presumptions, meaning packing space is to have no influence what so ever during the calculation part. The calculations will be made with known analytical methods. To ease the calculations and simplify the work progress MATLAB is to be used. To evaluate and verify the calculations some sort of simulation software may be used.

As for the investigation of alternative concepts, it will include searching for alternative solutions. Then a brain storm session will be used to generate concepts. The concepts will then be evaluated briefly with regard to list of demands.

2. Validation

2.1 Background

Initially during the Cyclo Drive calculations project the program Adams was used to analyse the structure. BorgWarner already had an existing model of the Cyclo Drive in Adams (se figure 2.1.1). The main reason to consult this model was to get an initial idea of how the forces act in the Cyclo Drive and the approximate magnitude of the contact forces.
In the Adams model it can be seen that all the frictional forces is pointing in the same direction, which creates some uncertainty as to whether the pins roll or slide during rotation.

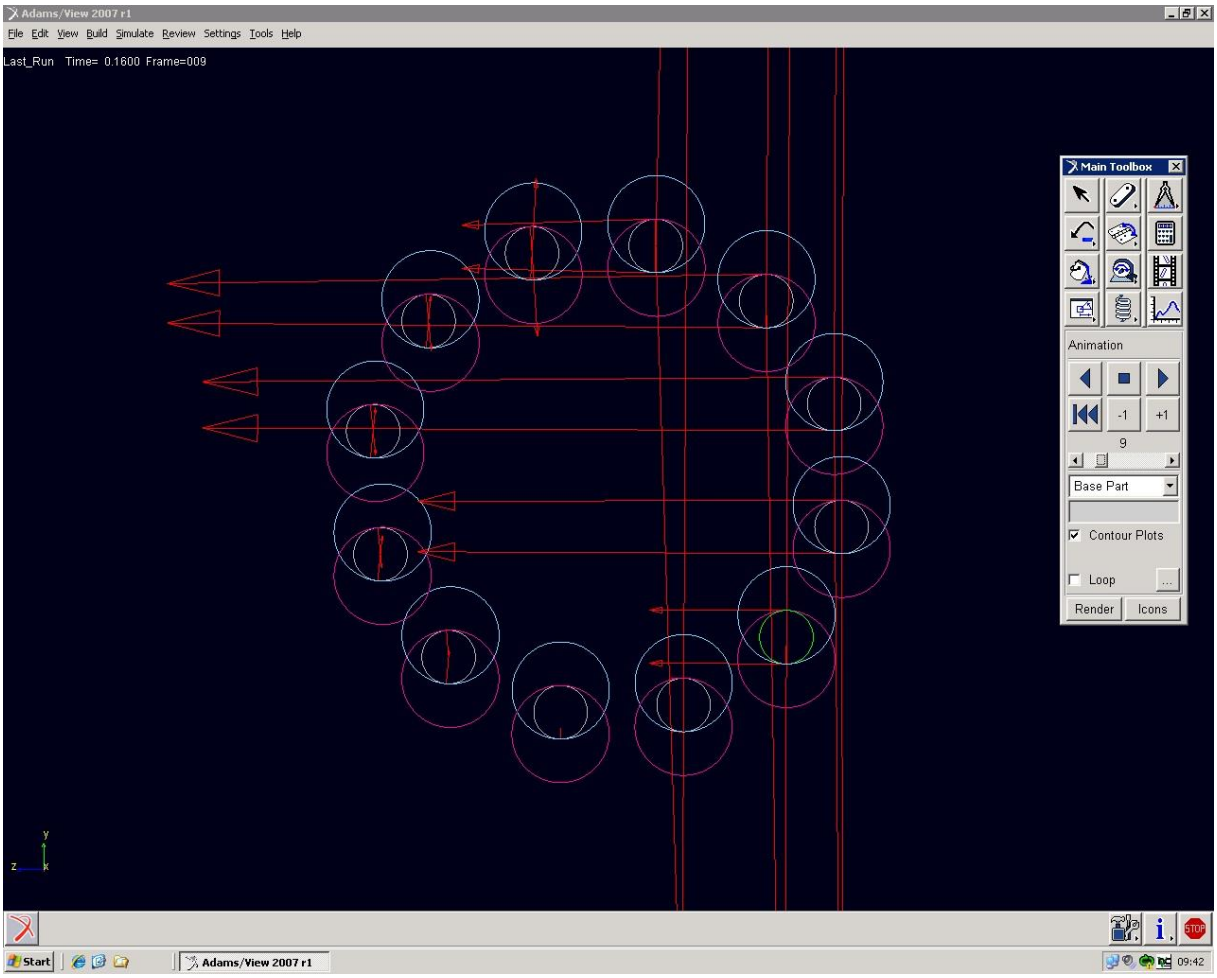

Figure 2.1.1: *Illustration of Adams model with contact forces.*

2.2 Setup

To investigate the behaviour of the pins an experiment was made during the assembly work of the differential. This was made before the differential was completely assembled and closed up. This enabled an inspection of the Cyclo Drive (se figure 2.2.1). Pins as well as the outer disc were marked to enable counting of the revolutions (se figure 2.2.1). The differential was then manually rotated and the revolutions of both the outer disc and the pins were counted (during the rotation there were no load on the Cyclo Drive) . This procedure was made three times with different number of revolutions. The relation between the revolution of the disc and the pin could then be compared to the relation between the hole radius and the pin radius.

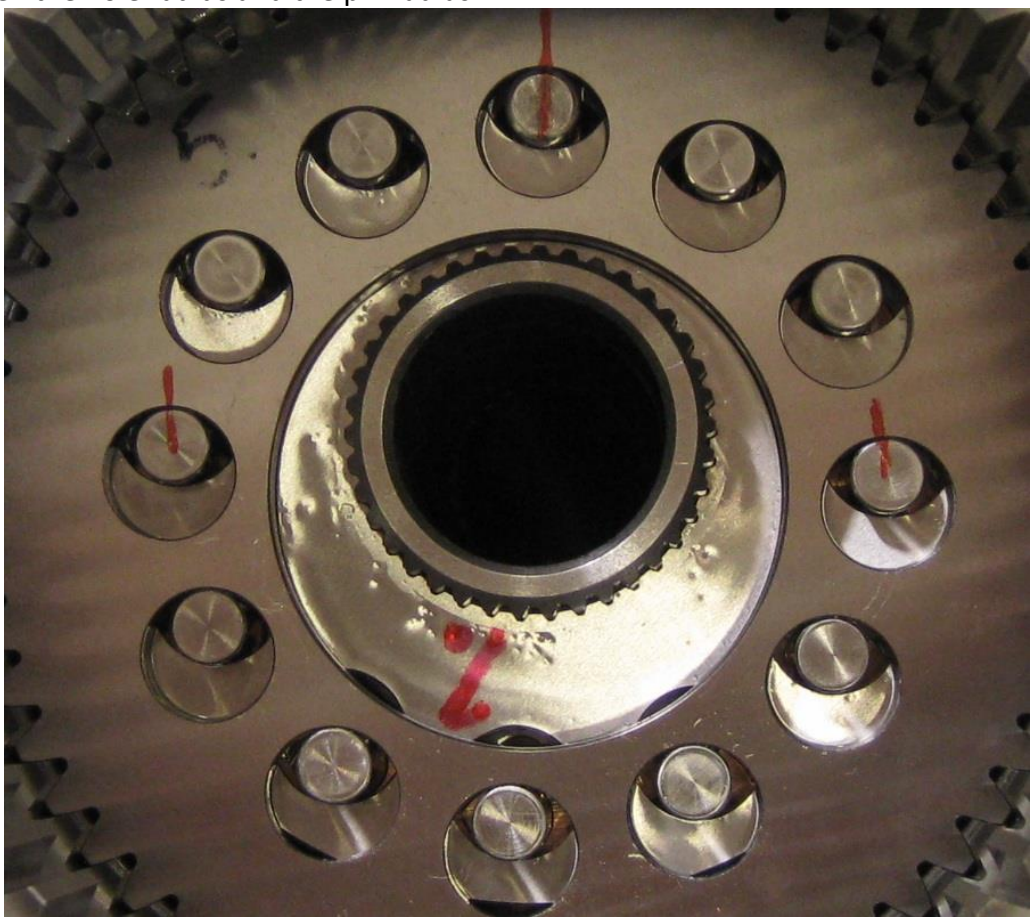

Figure 2.2.1: *The differential with marks on the pins and the outer disc.*

2.3 Result Validation

The relation between the hole radius and the pin radius is:

$$R = \frac{r_h}{r_p} = \frac{7}{4} = 1{,}75 \qquad (2.1.1)$$

From the experimental the following results was received:

Part	Revolutions	Revolutions	Revolutions
Outer disc	1,15	10	20
Pin	2	14	26
Relation Pin/outer disc	1,74	1,4	1,3

Table 2.1.1: *Results from experiment.*

The result shows that the pins are indeed rolling during the revolution. However during some time of the rotation of the differential the pins may slide due to lack of contact force.

3. Contact simulation

3.1 Setup

To get an idea of how the pin behaves during the maximum load a contact simulation was made. The analysis was made in Ansys with some different geometry of the disc. To simplify the analysis the force was added directly at the pin were the outer disc contact would have been.

The aim of the analysis is to assimilate knowledge of the contact between pin and inner disc. The model only includes the geometry that is part of or affects the contact. Figure 3.1.1 below shows the model used in the simulation where $\boldsymbol{F_A}$ *and* $\boldsymbol{F_B}$ is the contact forces created by the torque from the eccentric gearing.

$$\boldsymbol{F_a = F_b = \frac{9.4kN}{2}}$$

In the contact between the pin and the disc the contact condition is set to be frictional with the friction coefficient$\mu = 0.1.$, the surface facing down in figure 3.1.1 is set to fixed position.

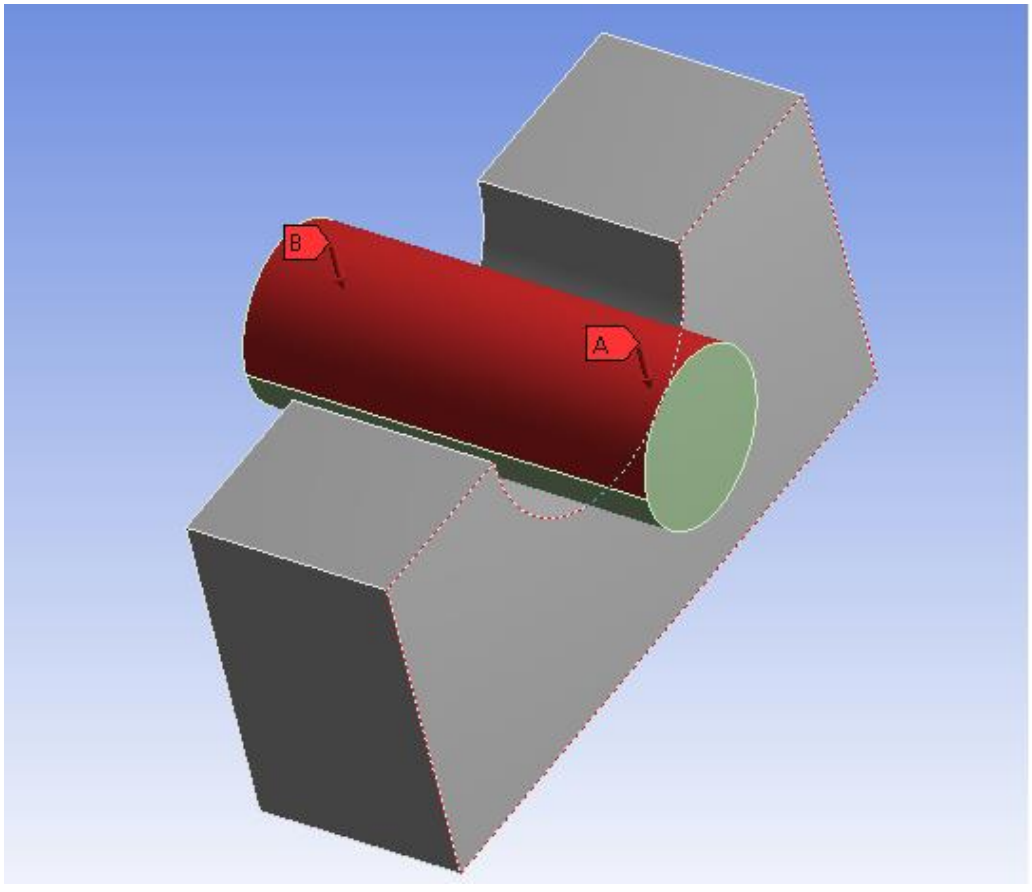

Figure 3.1.1: *Model used in the simulation.*

The edges in the holes will be designed and tested with a round, chamfer and an unmodified edge. The different geometries are tried out to investigate stresses caused by pin deflection (se figure 3.1.2) and to determine if those stresses can be reduced.

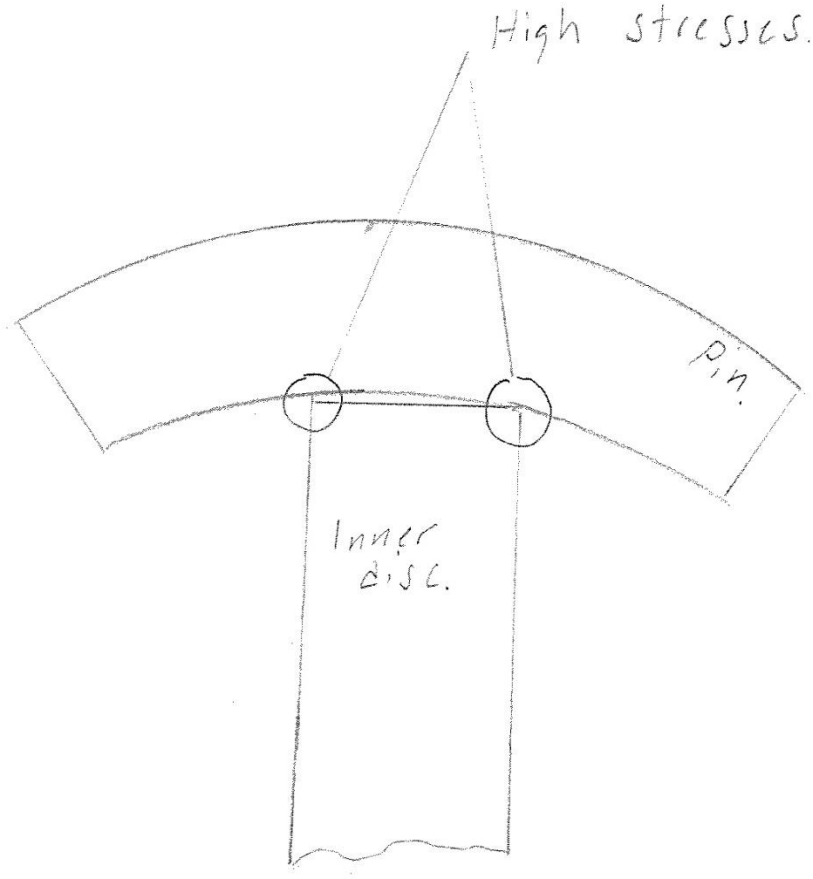

Figure 3.1.2: *Illustration of pin deflection (very exaggerated)*

The simulation was then made for four different configurations on the inner disc see figure 3.1.3 to figure 3.1.5.

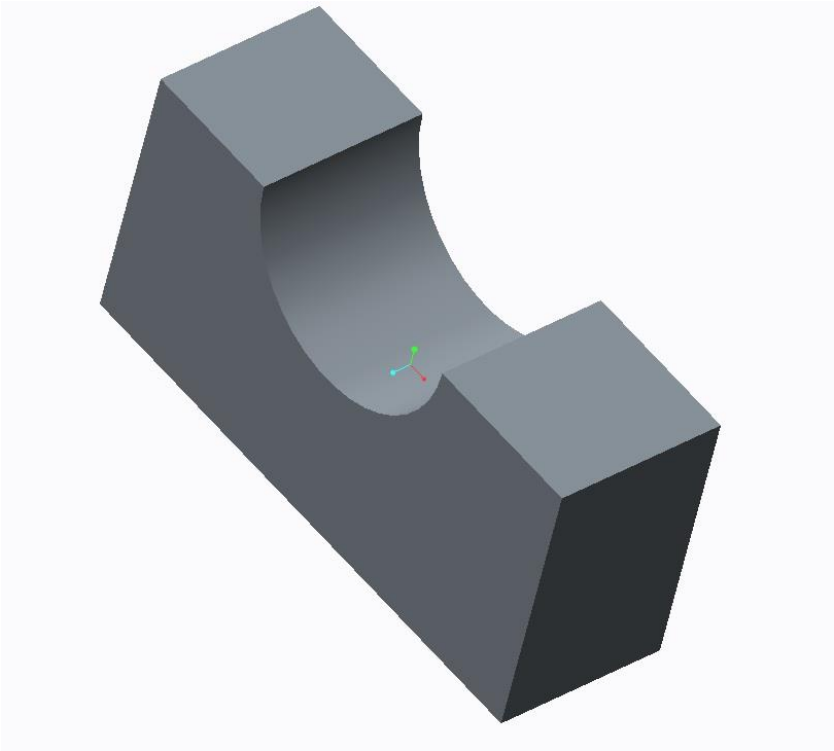

Figure 3.1.3: *Modell of inner disc hole with sharp hole edge.*

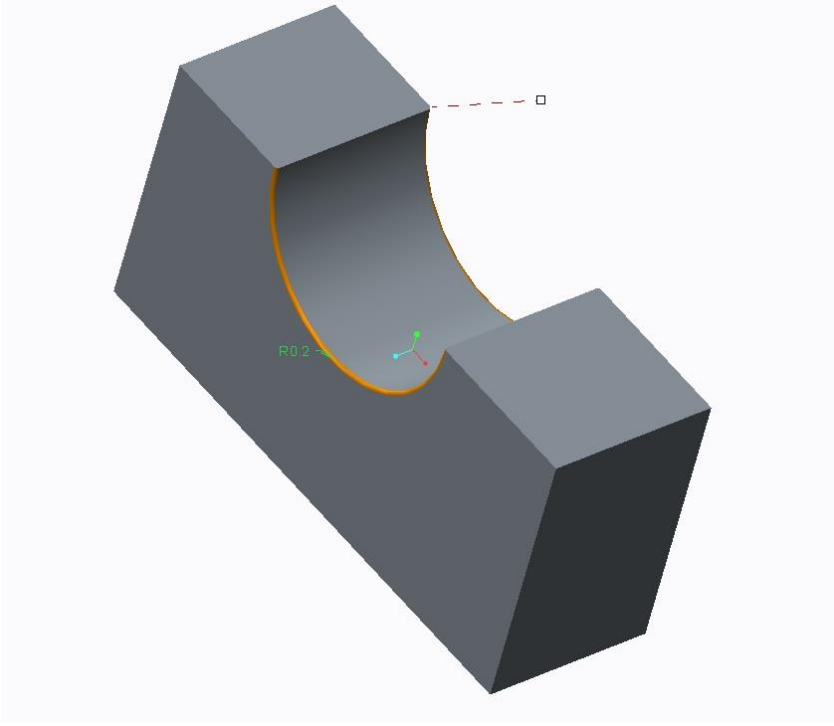

Figure 3.1.4: *Modell of inner disc hole with radius 0.2 mm on the hole edge.*

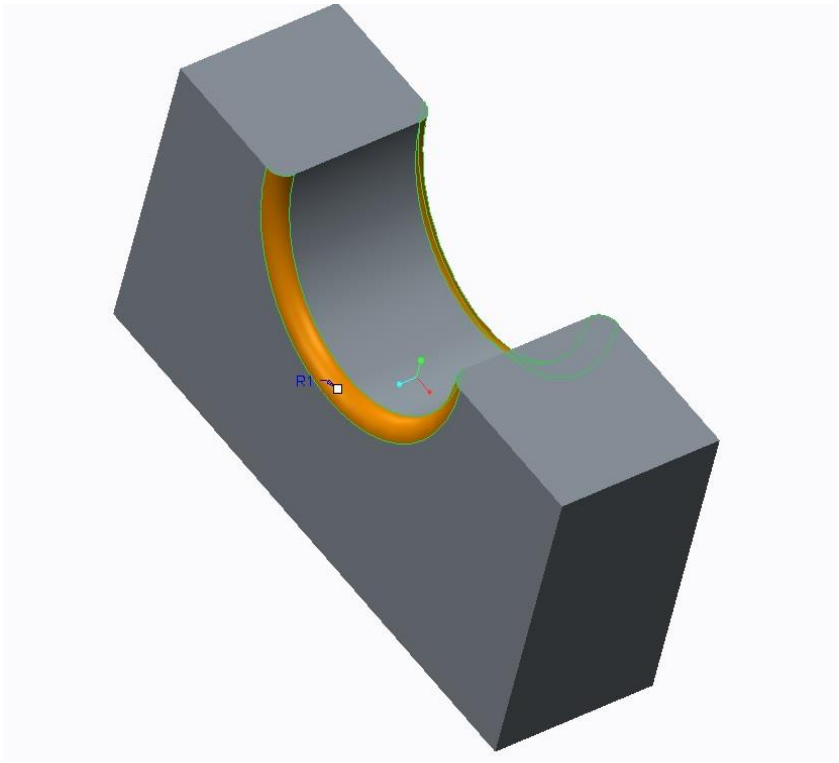

Figure 3.1.4: *Modell of inner disc hole with radius 1 mm on the hole edge.*

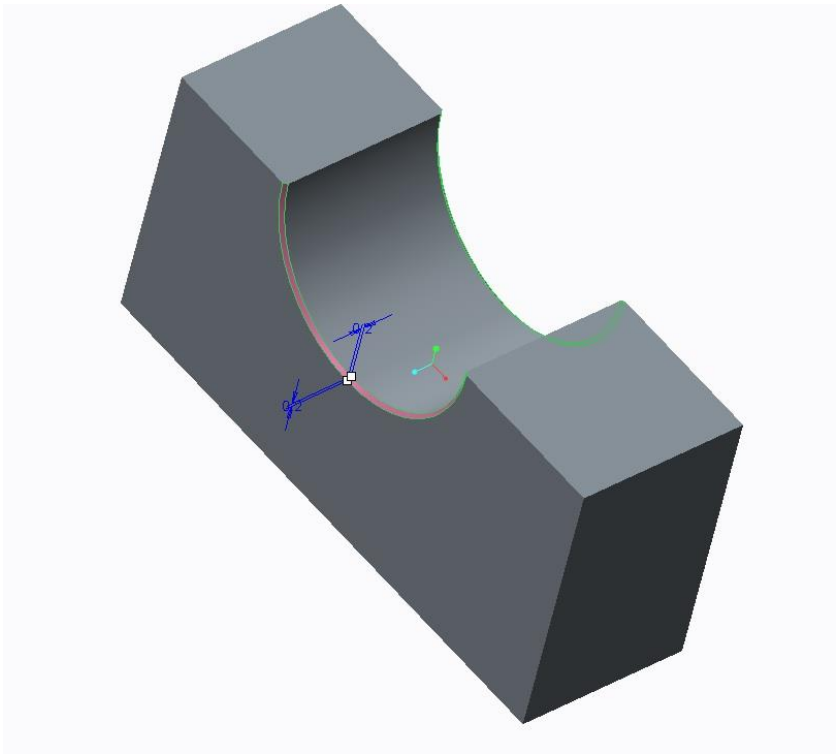

Figure 3.1.5: *Modell of inner disc hole with chamfer 0.2x45^{o} mm on the hole edge.*

3.2 Simulation results

Below the results from the contact simulation is shown. The first figures 3.2.1 to 3.2.4 show the contact pressure in Pa.

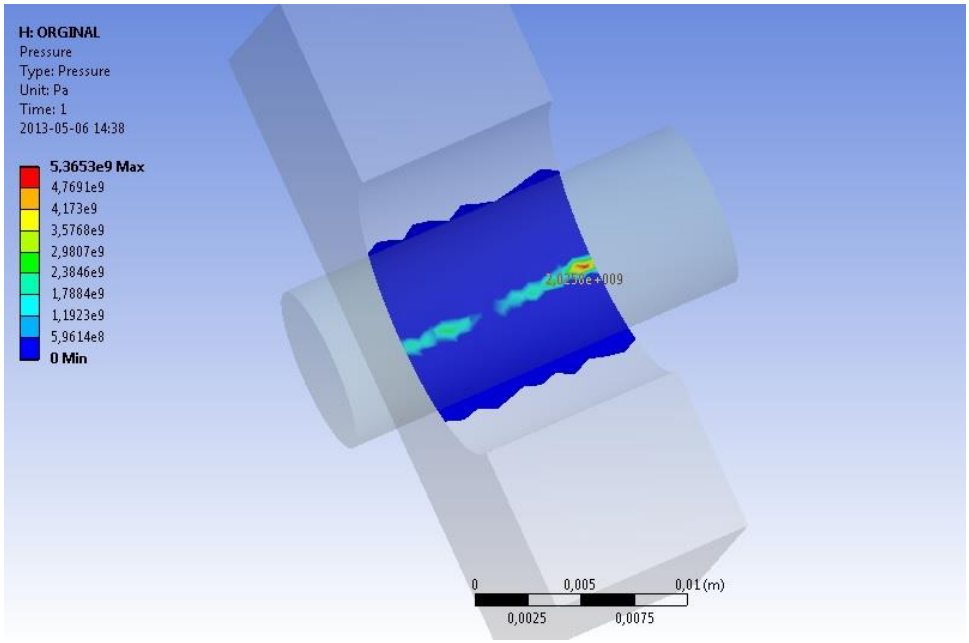

Figure 3.2.1: *Contact pressure for model with sharp edge.*

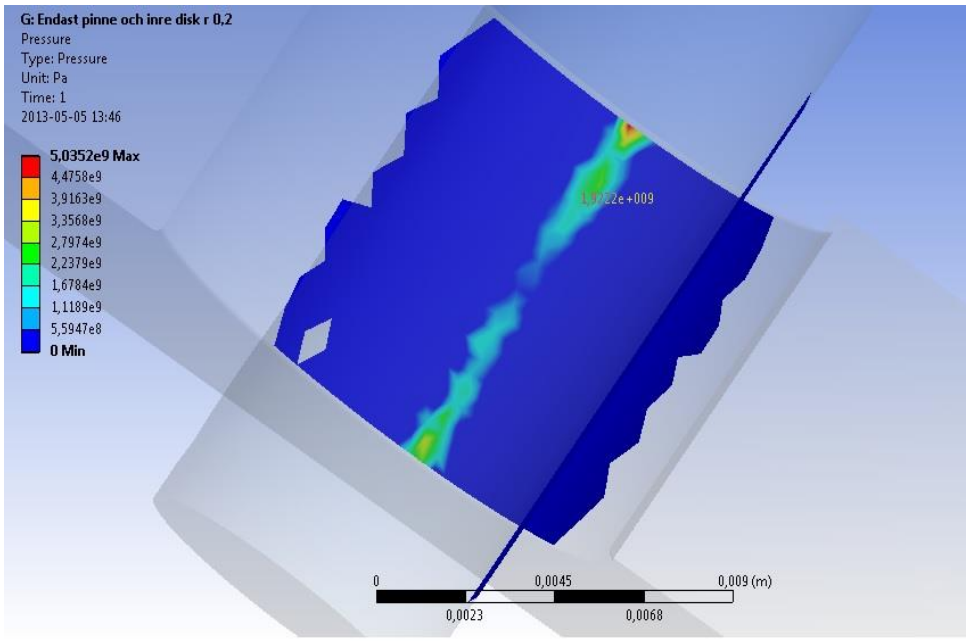

Figure 3.2.2: *Contact pressure for model with an edge radius 0.2 mm.*

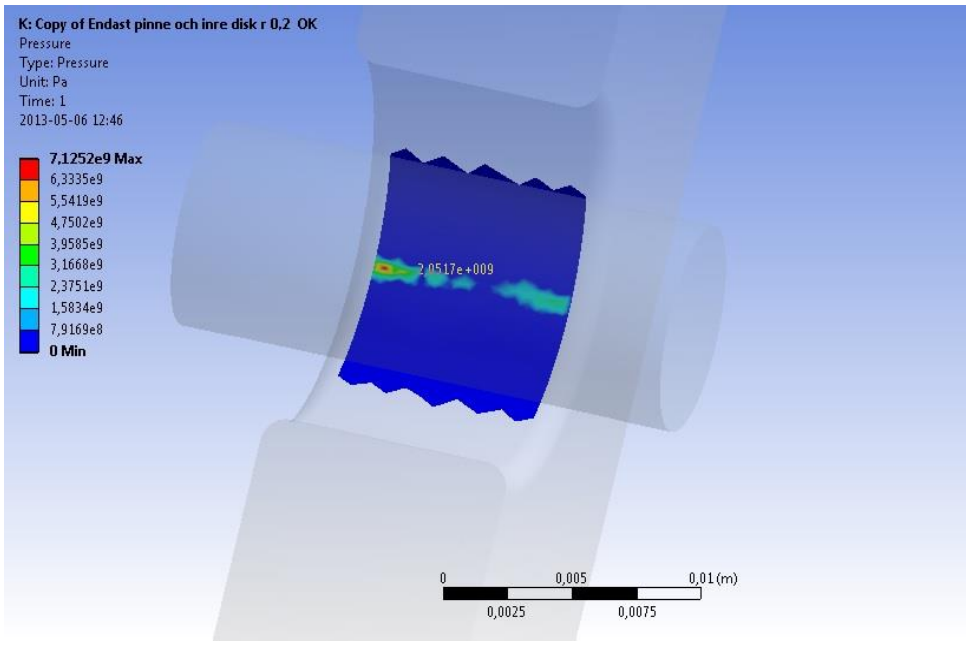

Figure 3.2.3: *Contact pressure for model with an edge radius 1 mm.*

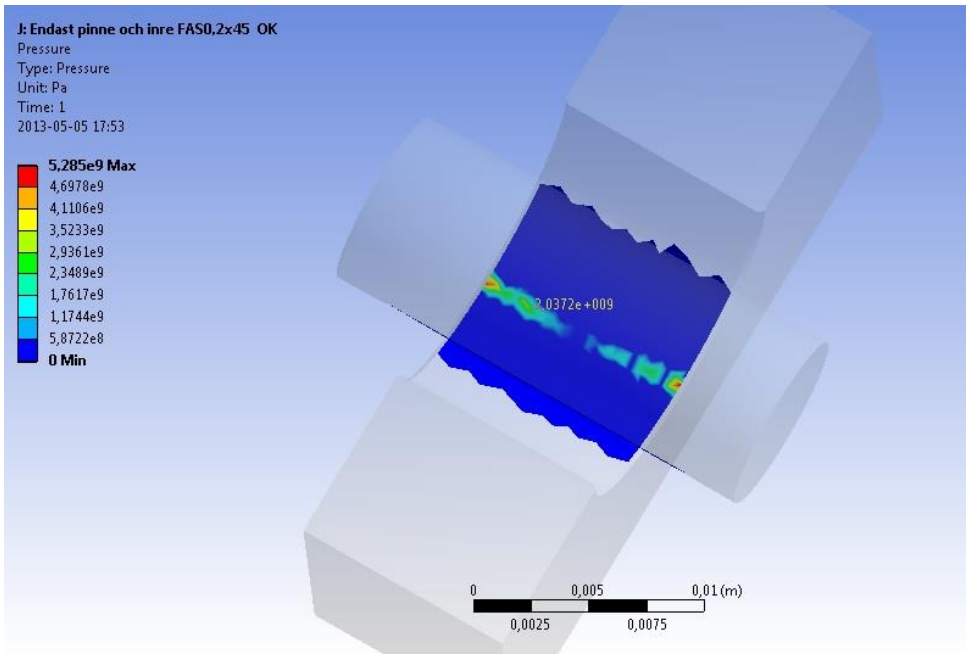

Figure 3.2.4: *Contact pressure for model with an edge chamfer 0.2x45^{o} mm.*

Picture 3.2.5 to 3.2.8. shows the von Mises stresses created by the contact between pin and disc.

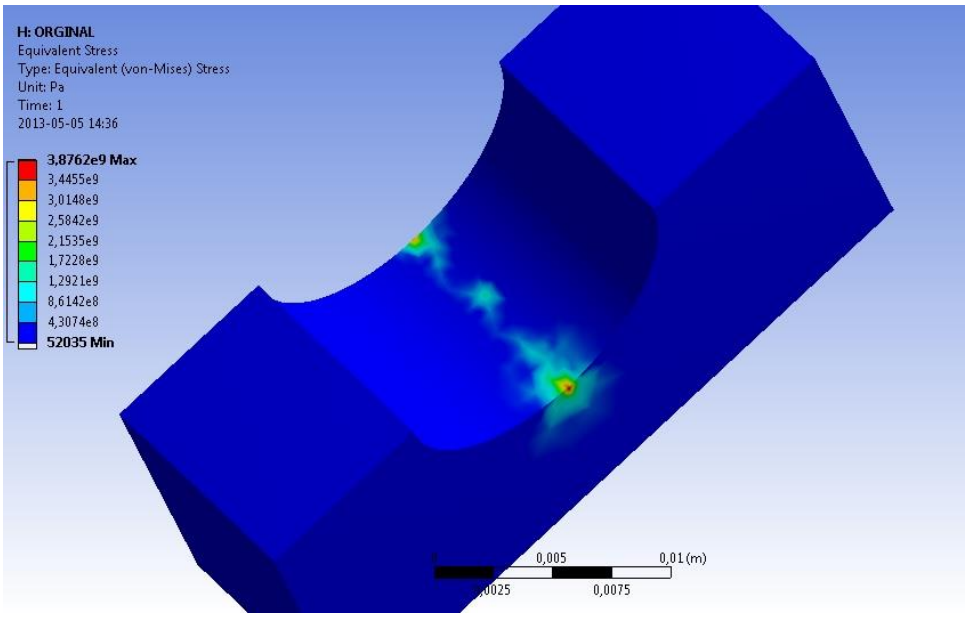

Figure 3.2.5: *Stresses for model with sharp edge.*

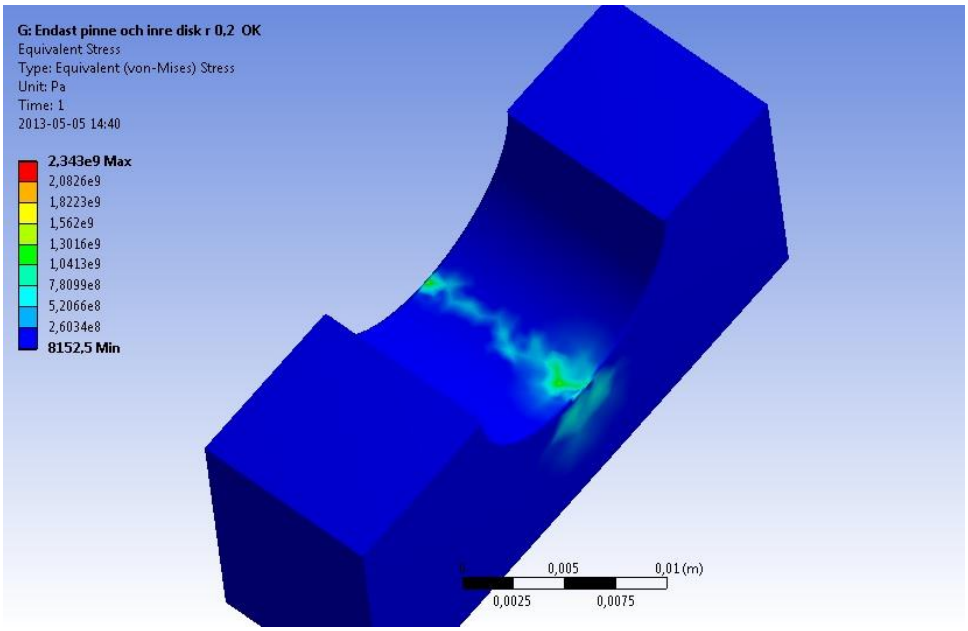

Figure 3.2.6: *Stresses for model with edge radius 0.2 mm.*

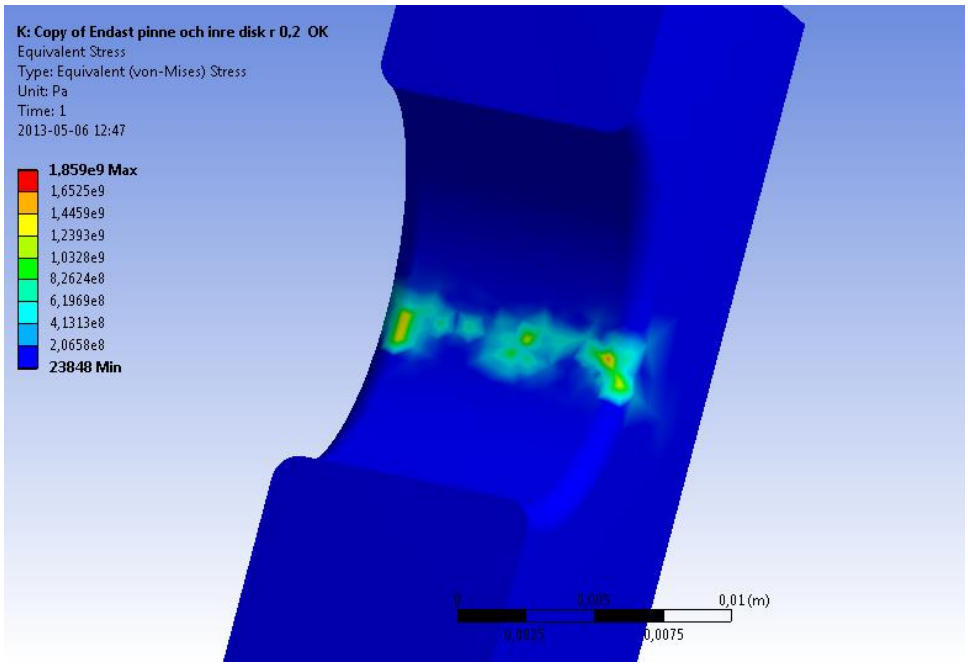

Figure 3.2.7: *Stresses for model with edge radius 1 mm.*

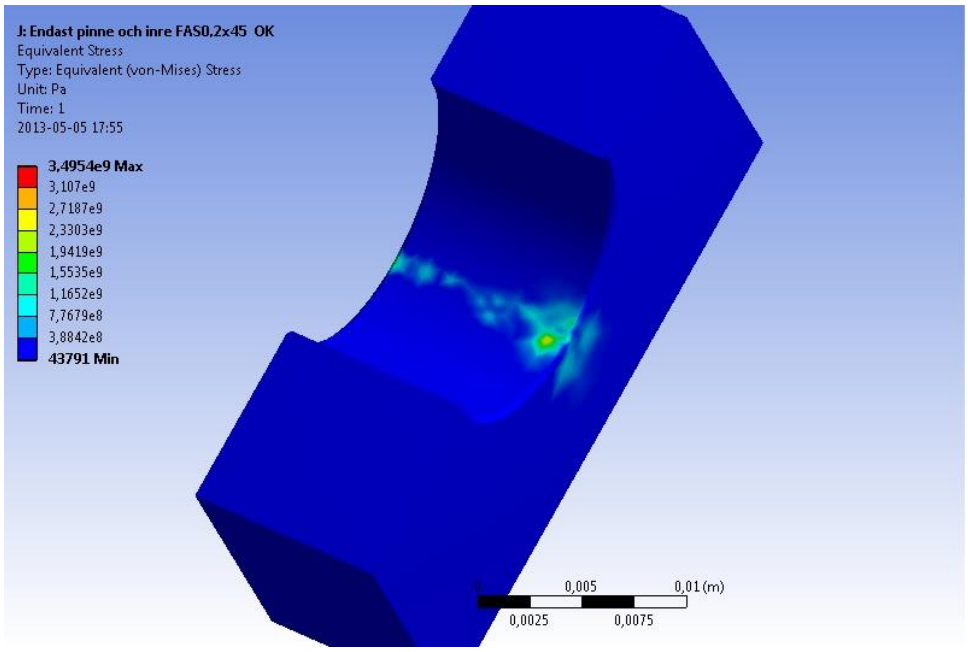

Figure 3.2.8: *Stresses for model with edge chamfer 0.2x45^{o} mm.*

Below the ISO-surface for the stress is shown in the different cases (se figure 3.2.9 to 3.2.12)

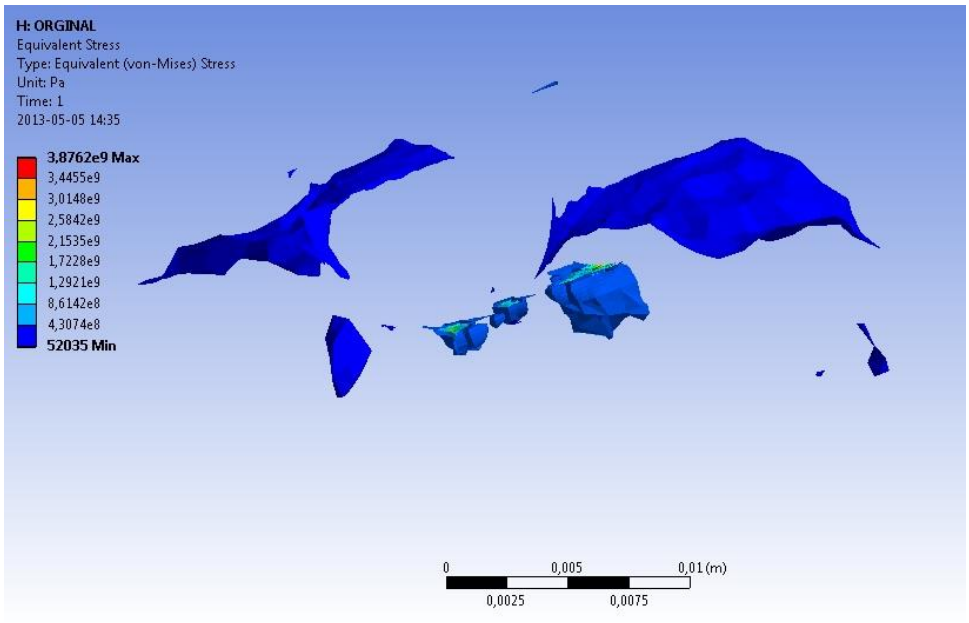

Figure 3.2.9: *Stress ISO-surface for model with sharp edge.*

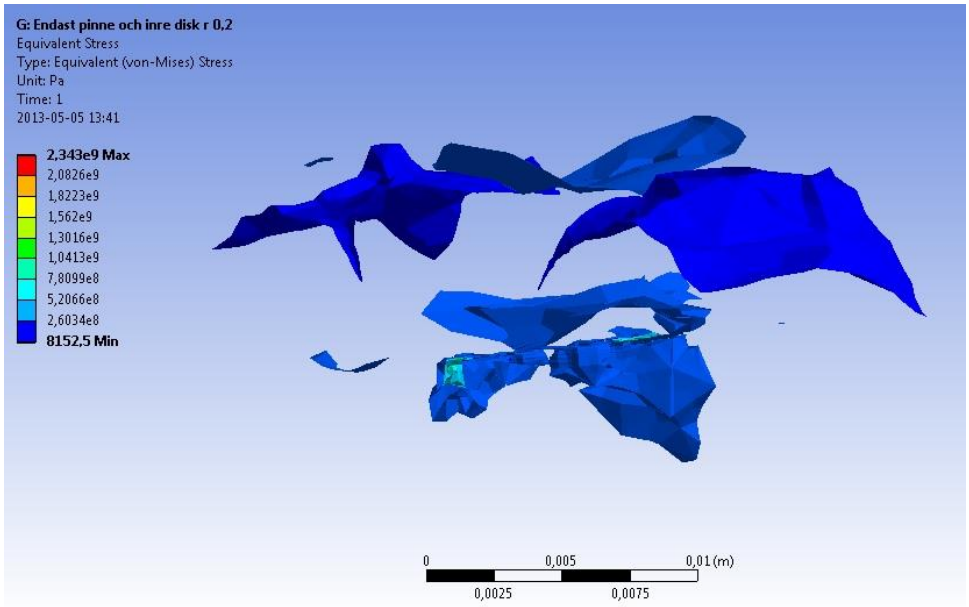

Figure 3.2.10: *Stress ISO-surface for model with edge radius 0.2 mm.*

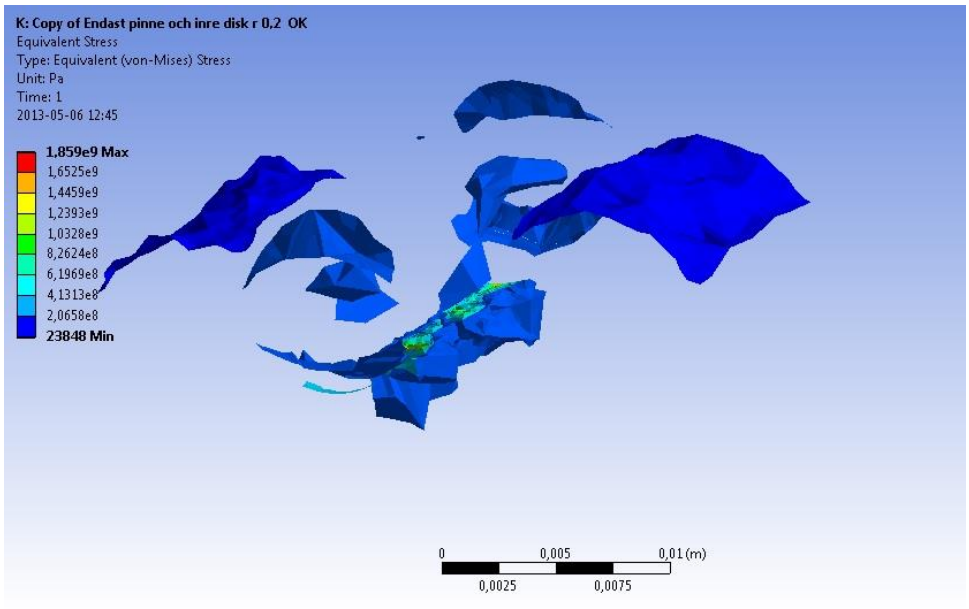

Figure 3.2.11: *Stress ISO-surface for model with edge radius 1 mm.*

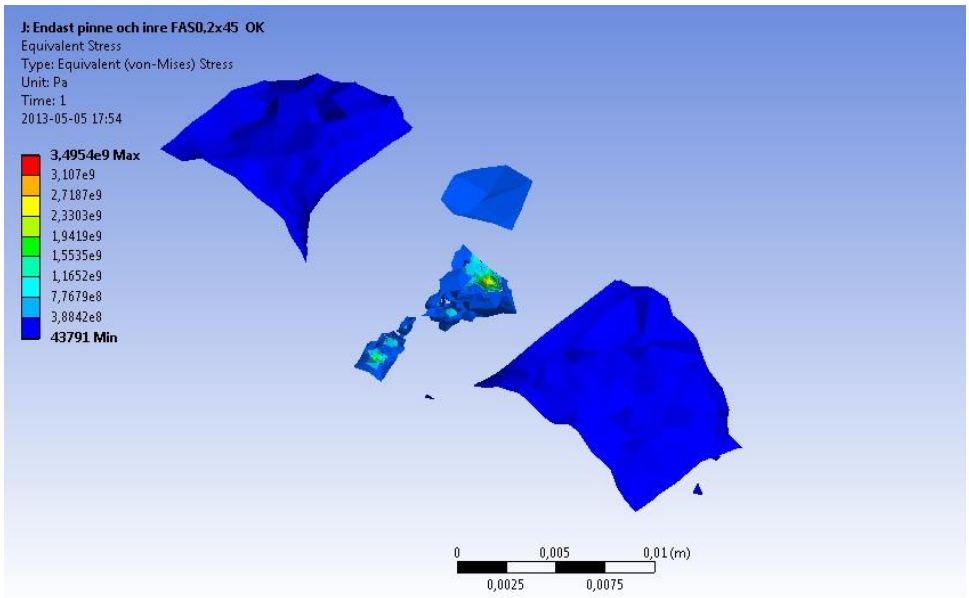

Figure 3.2.12: *Stress ISO-surface for model with edge chamfer 0.2x45^{o} mm.*

The figure below shows the deflection of the pin.

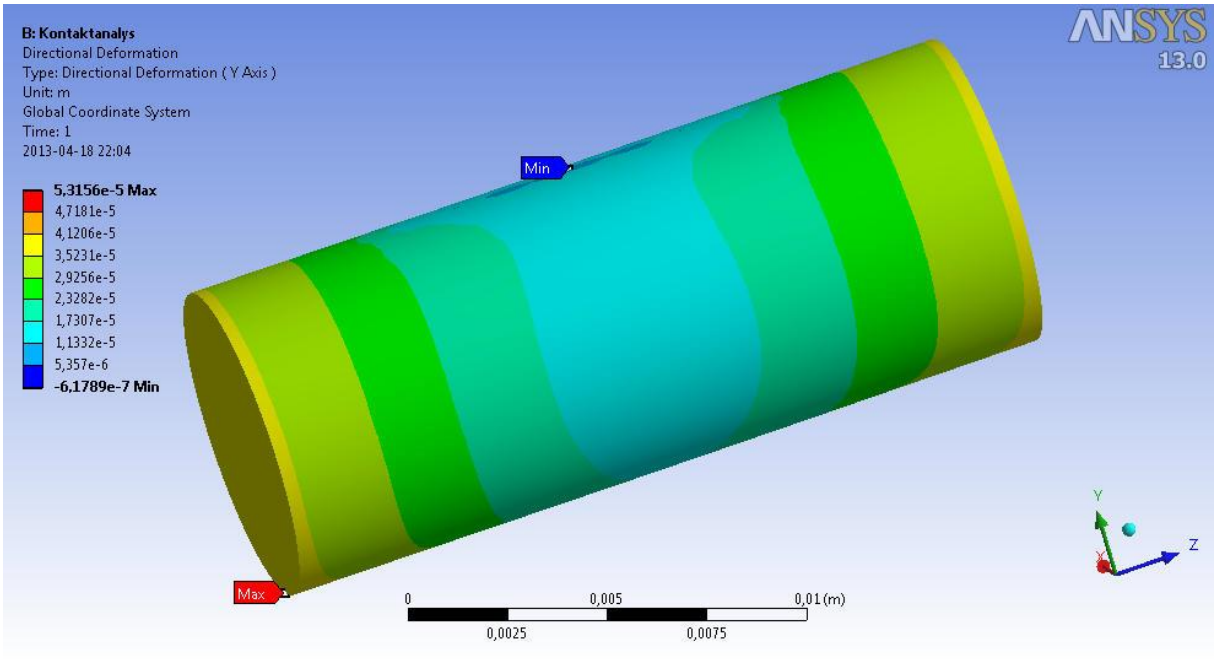

Figure 3.2.13: *Deflection of the pin.*

3.3 Simulations conclusions

It can be seen in the pictures above that the model with a small radius is the one that has the best properties with regard to the Hertzian pressure. The other models have a greater Hertzian pressure, which may be because of the hard edges that the chamfer creates in the structure.

The reason that the model with the small radius of 0.2 mm has the best properties and not the model with a radius of 1 mm may be due to the significant reduction of contact length created by the radius. It may be seen that although stresses on the edges decrease, the stress concentration grows larger in the center as the radius increase.

4. Calculations

4.1 Geometry

In order to calculate the distribution used to calculate the contact forces the geometry of the disc must be analysed.
The distances used to calculate contact radius r_k are shown in equations 4.1.1-4.1.3 and figure (4.1.1)
Geometry and the law of cosines return the equations:

$$a = \frac{2r_p - e}{2} \tag{4.1.1}$$

$$r_k^2 = r^2 + a^2 - 2ar\cos(180 - \varphi) = r^2 + a^2 + 2ar\cos\varphi \tag{4.1.2}$$

The angle between the hole centre and the contact point δ is derived by use of the sine law.

$$\frac{r_k}{\sin\varphi} = \frac{a}{\sin\delta} \Longrightarrow \delta = \sin^{-1}\frac{a\sin\varphi}{r_k} \tag{4.1.3}$$

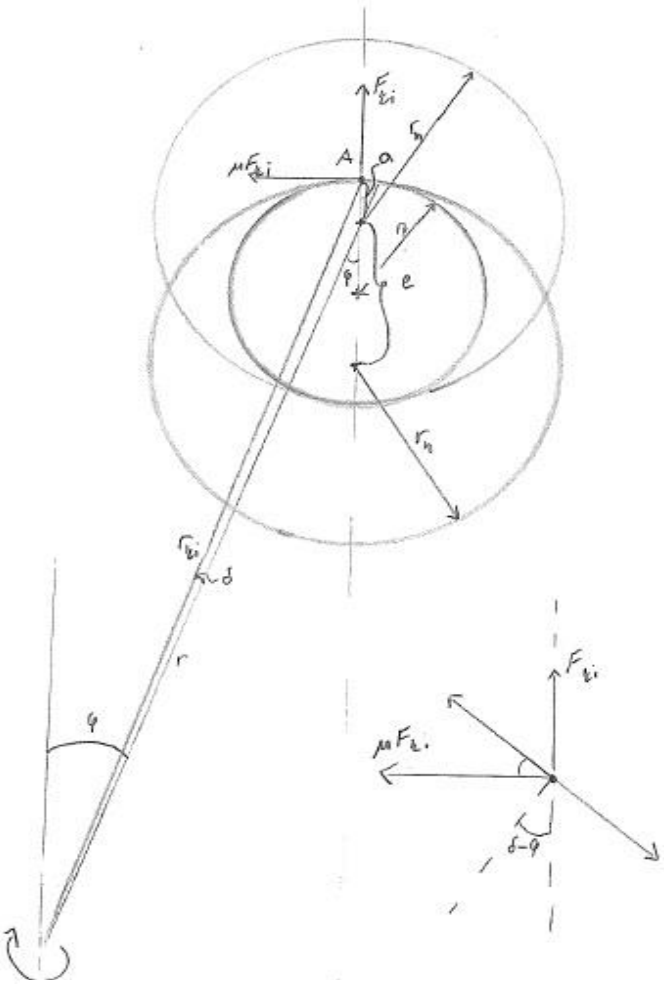

Figure 4.1.1: *Geometry used to calculate* r_k**.**

5.2 Forces

The calculation of the contact forces in the Cyclo Drive were made in two steps. In the first step the distribution (se figure 4.2.2) was calculated. This was made by introducing a deformation to the disc by rotating it a small angle. As the direction of the contact force is vertical, the deformation in this direction must be determined. If it is assumed that the relation between deformation and force is linear (eq. 4.2.1). The relation between contact forces on different pins will be the same as that between deformations on those same pins.

$$F_{ki} = c\Delta \tag{4.2.1}$$

$$\Delta = r_k(\cos(\theta + \varphi - \delta + \psi) - \cos(\theta + \varphi - \delta)) \tag{4.2.2}$$

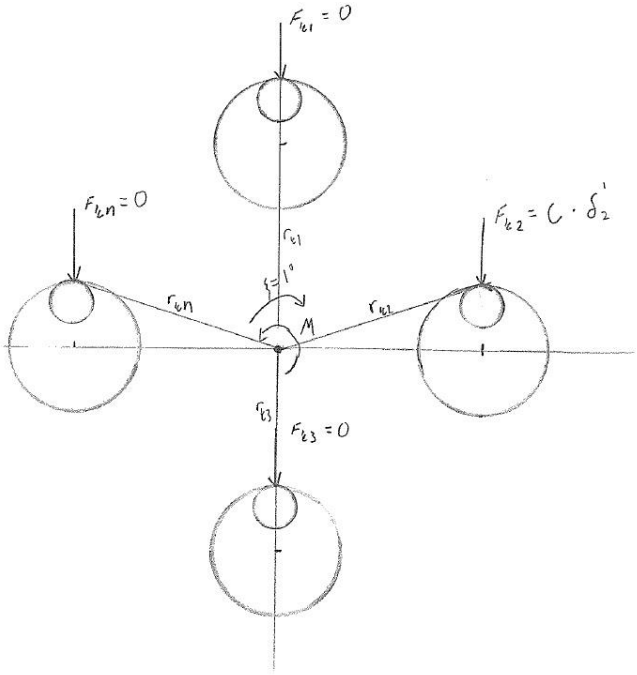

Figure 4.2.1: *Illustration of the deformation criterion*

When the distribution (see figure 4.2.2) was derived the real contact forces could be calculated depending on the actual torque.

$$M = \sum_{i=1}^{n} F_{ki} r_{ki} \sin(\varphi_i - \delta_i) \qquad (4.2.3)$$

With the distribution known this equation may be written:

$$M = \sum_{i=1}^{n} F d_i r_{ki} \sin(\varphi_i - \delta_i) \qquad (4.2.4)$$

Where F is the sum of all contact forces and d_i is the share of that sum on the particular pin.

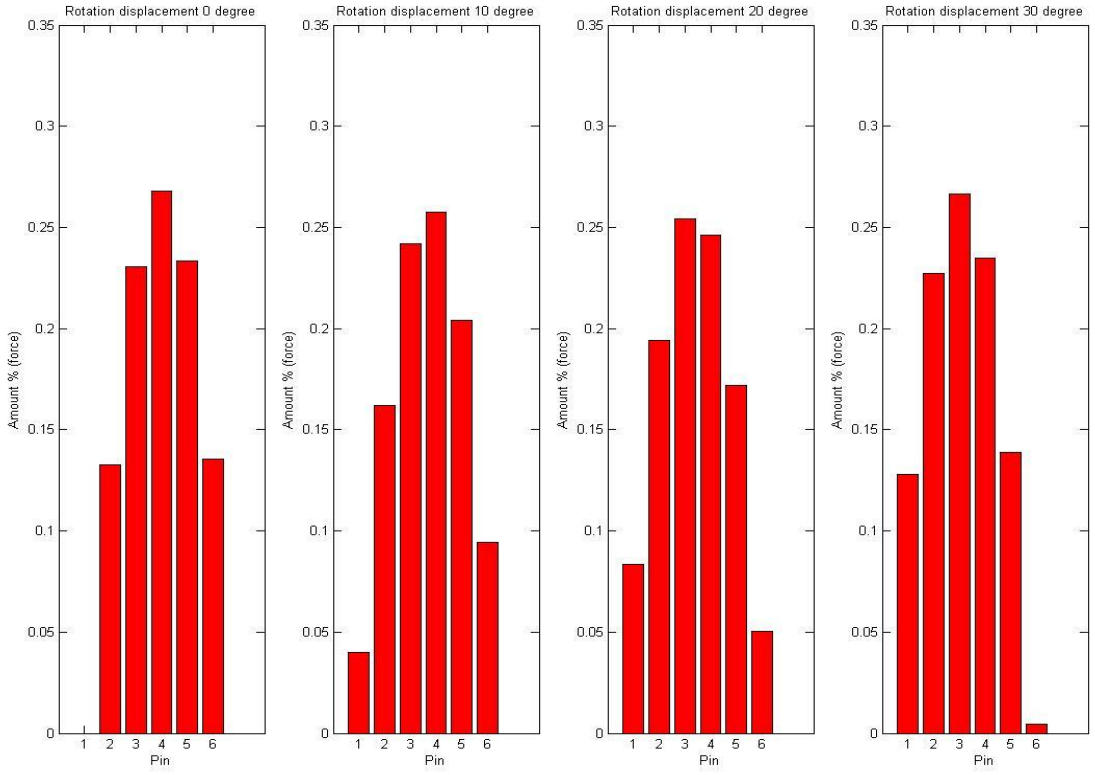

Figure 4.2.2: *The distribution of the force.*

5.3 Stresses

When the forces were calculated the contact force F_{kiR} was used to derive the Hertzian contact pressure as:

$$P = \sqrt{\frac{F_{kiR}}{\pi 2 k_p} \frac{r_p - r_h}{(-r_h) r_p}} \quad (4.3.1)$$

Where

$$k_p = \frac{1-v^2}{E} \quad (4.3.2)$$

r_h and r_p are the radius of the hole and the pin and v is Poisson's ratio.

The Hertzian pressure is used to calculate the shear stress as:

$$\tau_{max} = 0.3 P_{max} \quad (4.3.3)$$

Where τ_{max} is the maximum shear stress arising from contact pressure. The shear stress is then inserted in the Von Misses formula to be converted to equivalent normal stress equation (5.3.4).

$$\sigma_s = \tau_{max} \sqrt{3} \quad (4.3.4)$$

This is the stress that is to be used in the lifetime calculations.

4.4 Variation of geometry

To analyse the structure some values were replaced with variables and then used to plot the stresses. The variables that were plotted in intervals were:

- Hole position
- Hole radius
- Eccentricity
- Pin radius
- Thickness
- Number of holes

During the variation of the different variables the surrounding geometry that was dependent on the changed variable was updated (i.e. when varying the hole radius the pin radius was changed to keep the eccentricity constant) in order to maintain the function of the mechanism.

When varying the number of holes two approaches were chosen. During the first simulation the external measurements are increased as the number of holes increase, in order to keep the arc distance d_3 (se figure 4.4.1) between the holes' endpoints constant. If, on the other hand, the number of holes is less than twelve the hole radius is increased instead.

In the second simulation the external measurements as well as the distance d_3 between holes are preserved, meaning the hole radius will increase if the number of holes decrease and vice versa. Furthermore the distances d_1 and d_2 of the holes was preserved as well.

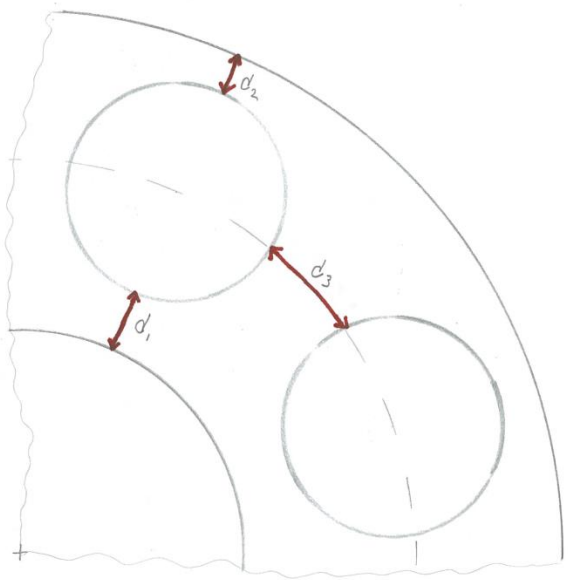

Figure 4.4.1 *Distances d_1, d_2 and d_3*

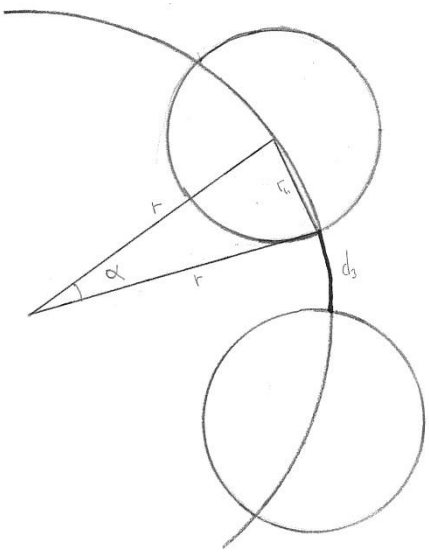

Figure 4.4.2 *Illustration of* d_3.

d_3 is calculated as below:

$$\cos(\alpha) = \frac{2r^2 - r_h^2}{2r^2} \tag{4.4.1}$$

$$12d_3 = 2\pi r - 24\alpha r \tag{4.4.2}$$

$$d_3 = \frac{r\pi}{6} - 2r \arccos\left(1 - \frac{r_h^2}{2r^2}\right) \tag{4.4.3}$$

As for the variation of pin radius, it is apparent that in order to maintain eccentricity and hole radius, the pins will have to be non-circular. It would then be possible for the radii of the holes and pins to be equal, creating a surface contact rather than a line contact (see figure 4.4.3). The radii on the side (r_f in figure 4.4.3) may be chosen to minimize deflection in the pins.

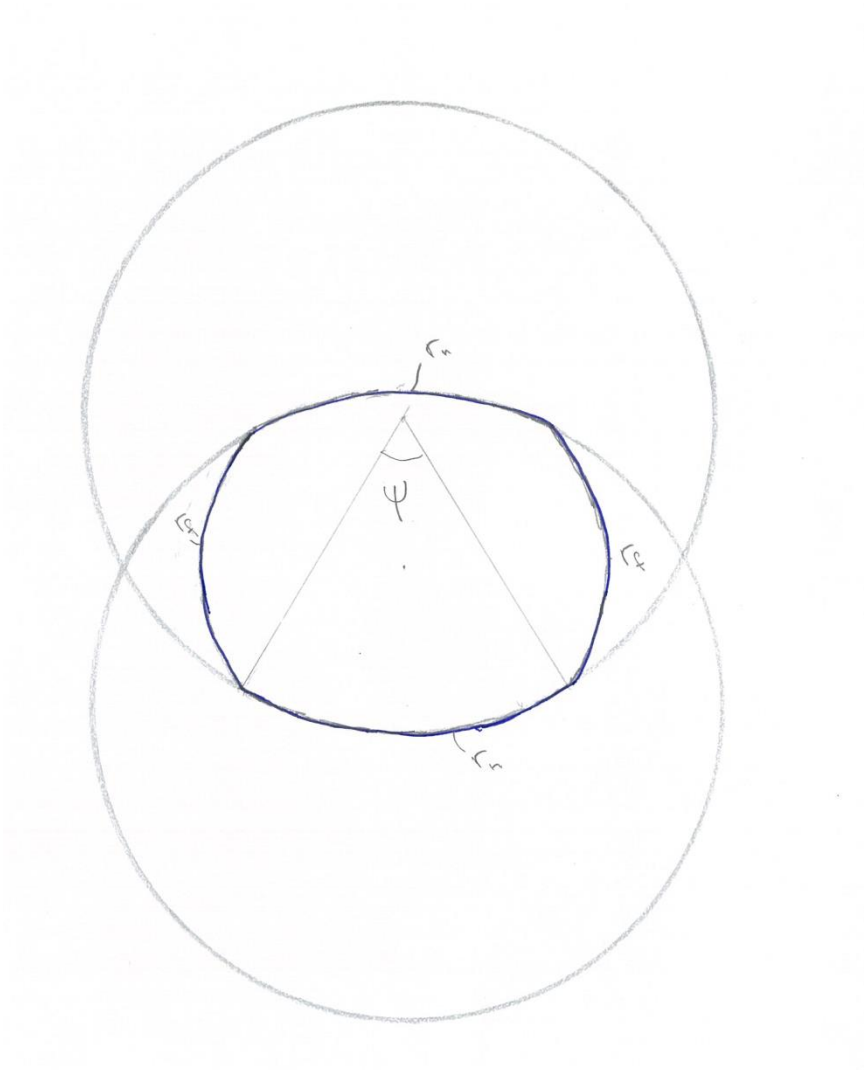

Figure 4.4.3 *Illustration of non-circular pin.*

It is apparent that using non-circular pins as in figure 4.4.3 will affect the efficiency since the pin will be forced to slide. However, theoretically the efficiency will not differ from the case in which the original pins are sliding. Although the contact area will be significantly larger, friction is independent of area (when using the Coulomb friction model) which means the total friction force (and thus total friction loss) will be the same.

4.5 Tolerances

In order to simulate the effect of manufacturing variations, the tolerances are assumed to follow a normal distribution with the excepted value, μ, being the blueprint value and the tolerance limits being 3σ.

As the hole position may deviate in any direction, the position accuracy of the holes will consequently be modelled as a “circular” normal distribution (se figure 4.5.1), with probability decreasing as the radius increases. This is achieved by introducing a uniformly distributed angle in addition to the normally distributed radius.

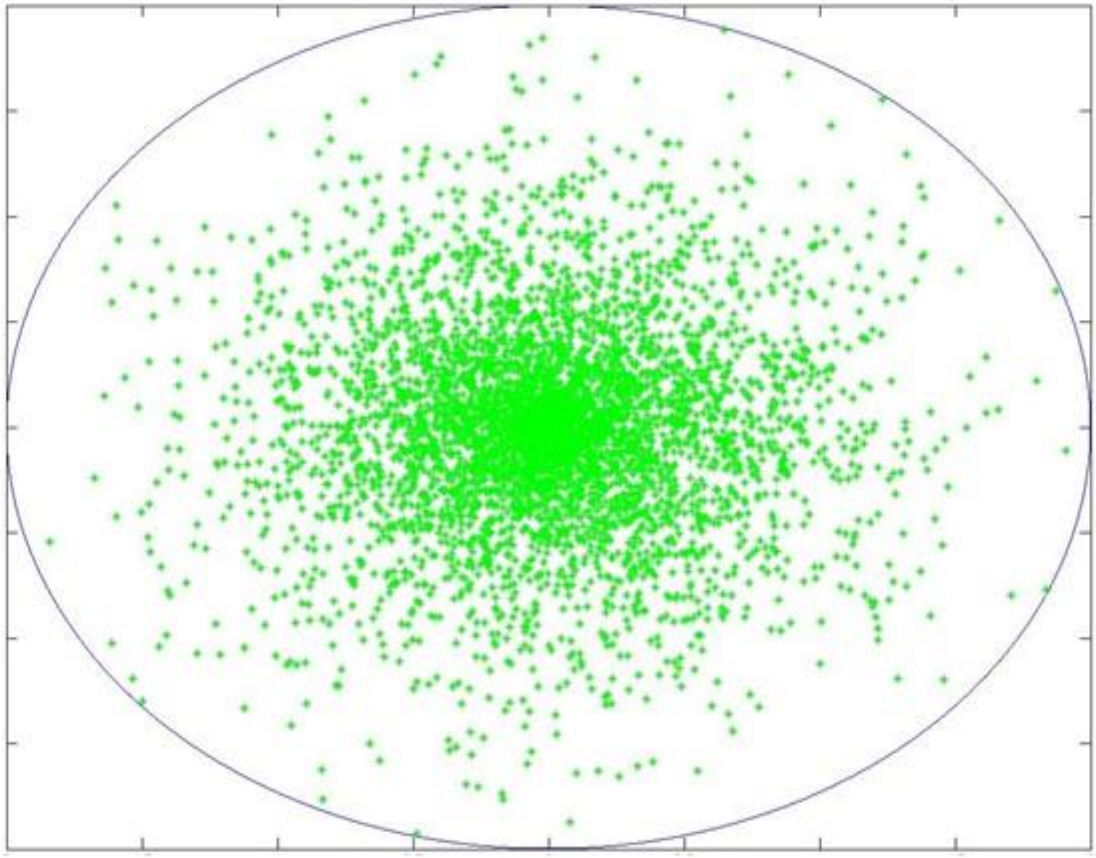

Figure 4.5.1: *Plot after 5000 simulations, each dot indicating the location of hole centre. Blue circle indicates tolerance limits.*

As manufacturing variations are assumed to follow a normal distribution, variations in contact pressure etc. will be assumed to do so as well. Results will thus be presented as a mean value (‘expected value’) as well as the 90-percentile, i.e. the value under which 90 % of values are found.

4.6 Calculations with tolerances

To calculate the distribution with the tolerances included in the calculation the main task is to determine whether the pin and hole are in contact. This may be done by choosing the hole with the smallest horizontal displacement (which may be negative) as a reference and then calculate the displacement of the other holes (see figure 4.6.1).

$$F = \sum_{i=1}^{n} c(u_i - \Delta_i) \qquad (4.6.1)$$

Here F is the sum of all contact forces, c is the constant stiffness, u is the horizontal displacement (caused by loading) and Δ is the horizontal displacement due to manufacturing variations.

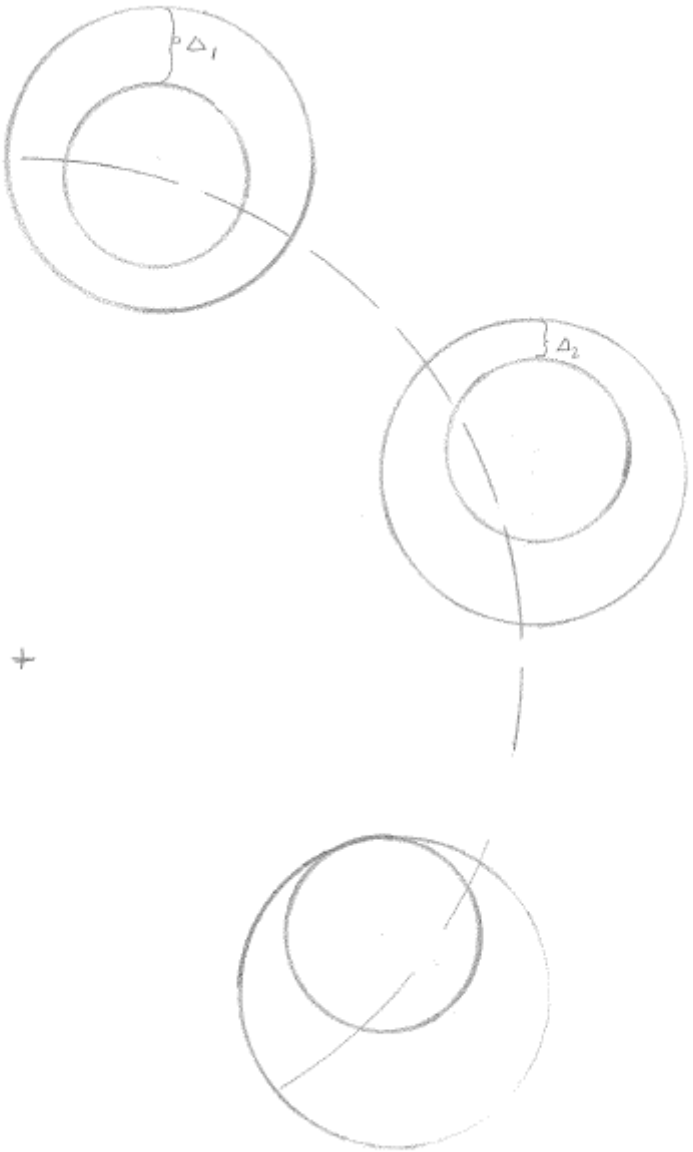

Figure 4.6.1: *Illustration of variation of hole position.*

The contact criterion then becomes

$$\begin{cases} (u_i - \Delta_i) \geq 0 \Rightarrow \ contact \\ (u_i - \Delta_i) < 0 \ \Rightarrow no\ contact \end{cases} \tag{4.6.2}$$

Previously, the disc was rotated a small angle to introduce a deformation. With tolerances, the contact forces will depend on the magnitude of that deformation, because very small deformations mean some holes may not be in contact at all. Thus the rotation angle was increased in steps, producing a different force distribution for each angle until the deformation was large enough to ensure every pin was in contact, at which point the distribution remained constant.

In order to derive the correct distribution the actual displacement must thus be approximated, which was done in the contact simulation (see section 3) analysis where the deformation due to the contact force and the deflection in the pin is was derived. This deformation is now to be used to estimate the correct magnitude of the forced deformation.

With use of these approximations the load distribution over the pins is as shown in figure 4.6.2 to 4.6.6.

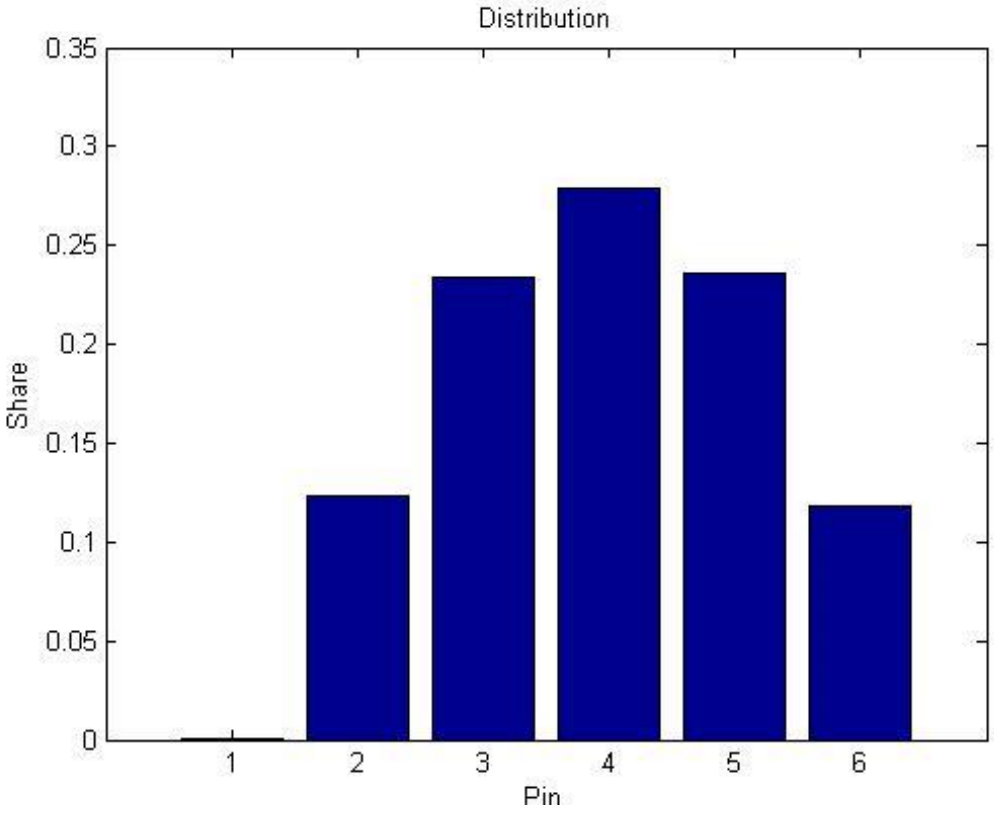

Figure 4.6.2: *Mean distribution with tolerances. After 100 loops.*

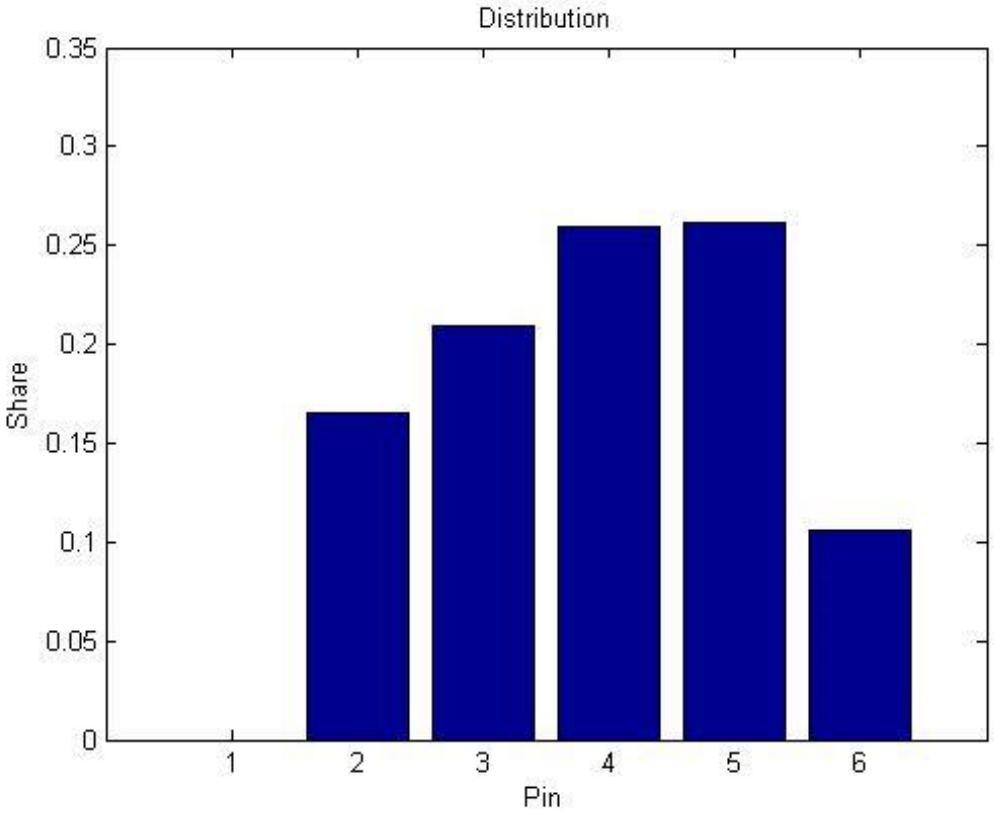

Figure 4.6.3: *Random distribution with tolerances.*

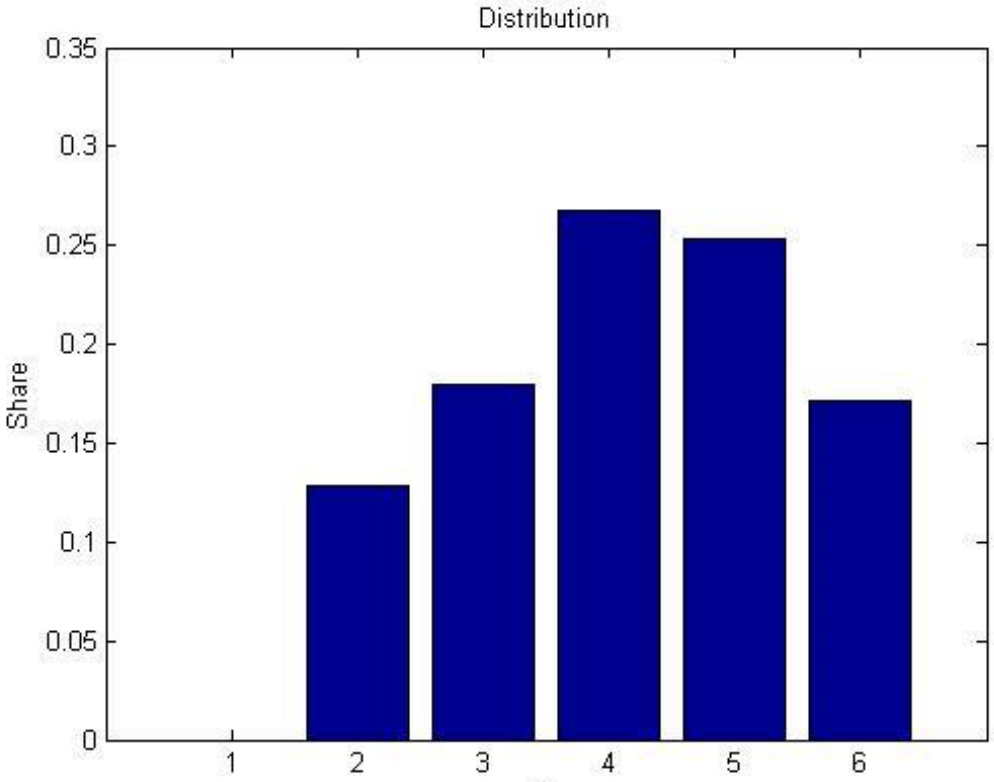

Figure 4.6.4: *Random distribution with tolerances.*

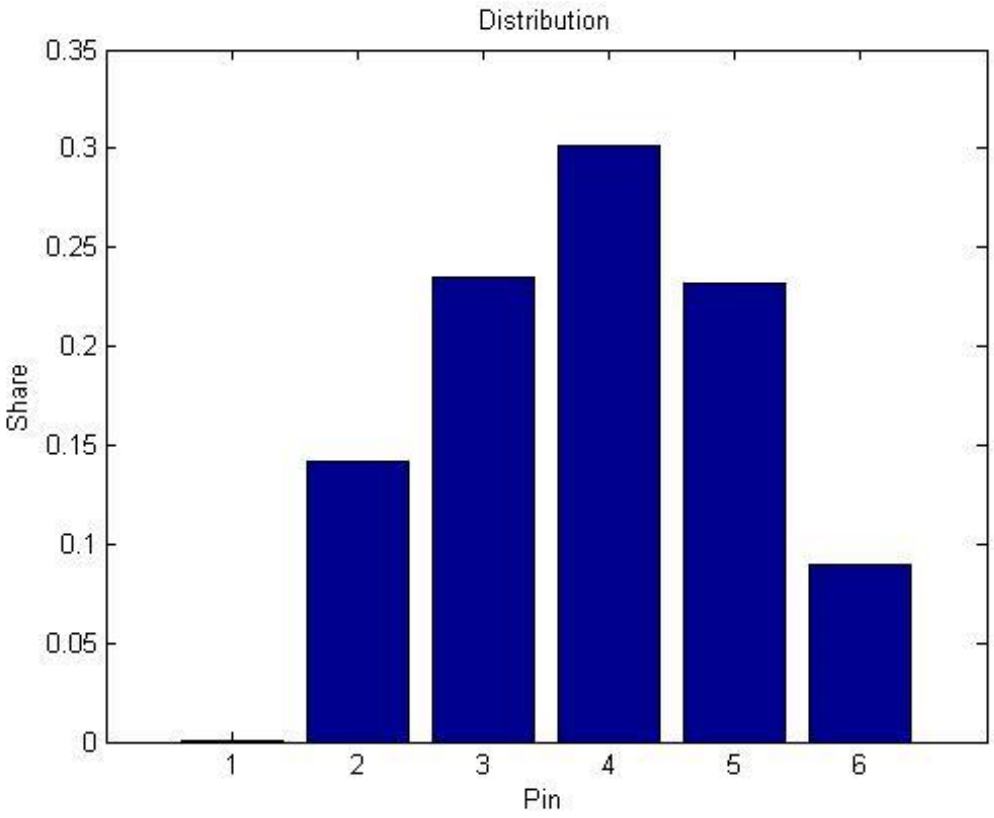

Figure 4.6.5: *Random distribution with tolerances.*

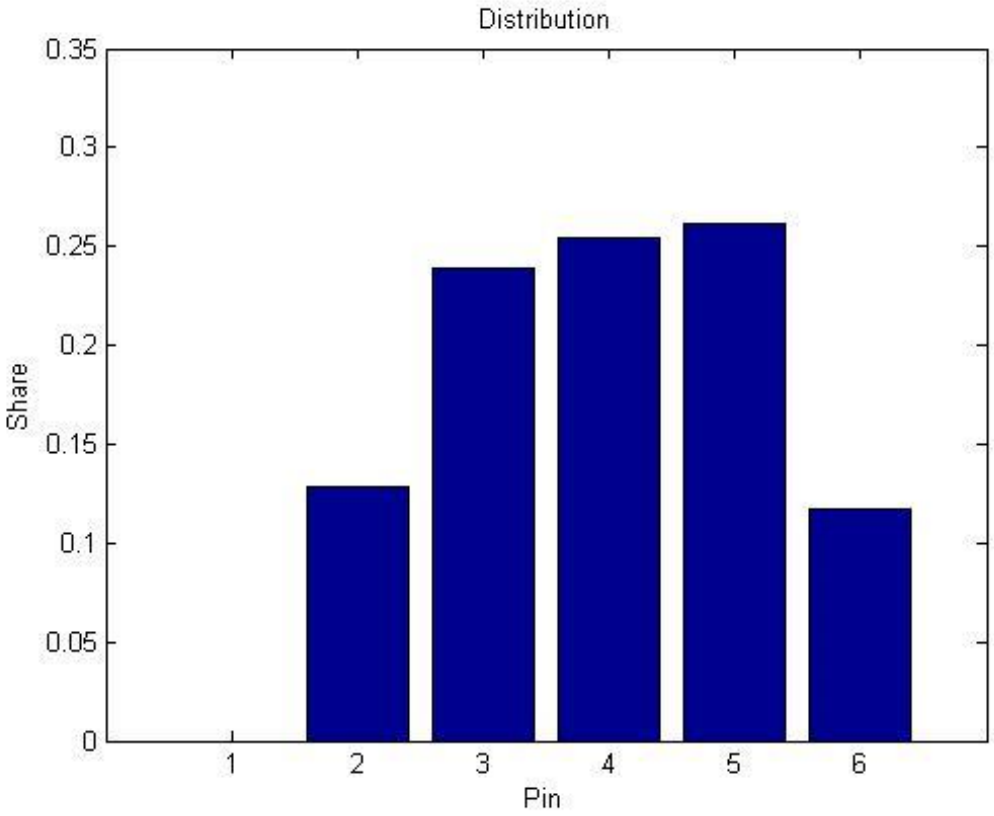

Figure 4.6.6: *Random distribution with tolerances.*

4.7 Fatigue

To estimate the life time of the structure the Palmgren damage rule was used. This rule states that failure occurs when:

$$\sum_{i=1}^{m} \frac{n_i}{N_i} \geq 1 \qquad (4.7.1)$$

Where m is the number of different loads, n_i is the number of cycles during a load and N_i is the cycles to failure during a specific load.
To estimate N_i a Wöhler curve was used (se figure 4.7.1).

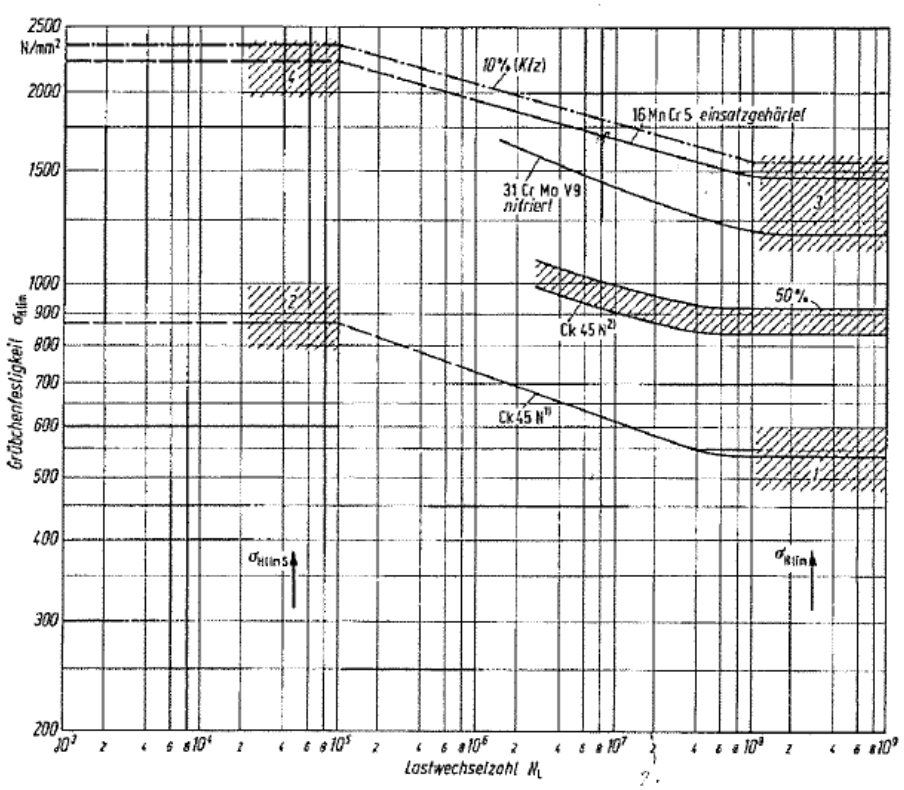

Figure 4.7.1: *Wöhler curve*[3]

Furthermore the value representing the maximum load on the structure was compared to the value of infinite lifetime 1.5 GPa (contact pressure). It should be noted that the value of infinite lifetime used at BorgWarner is 1.65 GPa which indicates there is no absolute certainty. Furthermore, the material compositions are slightly different. Both are however case hardened steels which means it may still be used as a guide line.

The different loads used during the fatigue calculations were given by a load spectrum that was given by BorgWarner.

4.8 Efficiency

When calculating the efficiency it is of great importance whether the pins roll along with the discs or if they are stationary, i.e. slides against the discs. It is possible that both sliding and rolling appear making it virtually impossible to calculate an exact value.
In order to produce some rough value the efficiency has been calculated for both these extremes: pure sliding and pure rolling. When sliding friction will cause losses whereas for rolling losses will be significantly lower. The rolling resistance coefficient used was C=0.0025[4] and friction coefficient μ=0.1.
For sliding, the power loss will be:

$$P_f = \dot{\xi} F_f = \dot{\xi} \mu F_k = \dot{\varphi} r_h \mu F_k \quad (4.8.1)$$

Where $\dot{\xi}$ is the sliding velocity, F_f is the frictional force and F_k is the contact force.
Thus the mean power loss over a revolution becomes:

$$P_{fr} = \frac{1}{2\pi} \int_0^{2\pi} \dot{\varphi} r_h \mu F_k d\varphi \quad (4.8.2)$$

For rolling the expression becomes

$$P_f = \dot{\beta} M_f = \dot{\beta} C F_k r_p = r_h \varphi \dot{C} F_k \quad 4.8.3)$$

Where M_f is the rolling resistance torque and $\dot{\beta}$ is the rotational velocity of the pin.
And the mean loss for rolling:

$$P_{fr} = \frac{1}{2\pi} \int_0^{2\pi} \dot{\varphi} r_h C F_k d\varphi \quad (4.8.4)$$

The results were plotted against the hole radius and for different μ and C.

5 Calculation results

5.1 Initial geometry forces

The analysis yielded the following results:

Maximum contact force: **9.44 kN**

Maximum Hertzian contact pressure: **1.91 GPa**

Maximum equivalent stress (von Mises)**: 994 MPa**

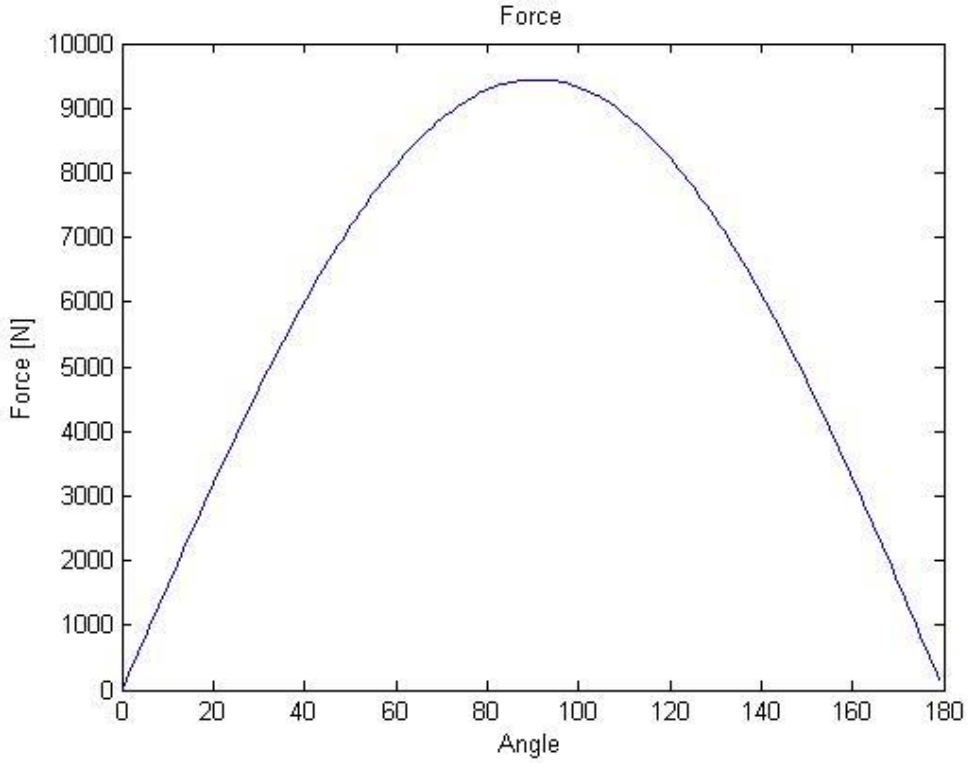

Figure 5.1.1: *The actual force.*

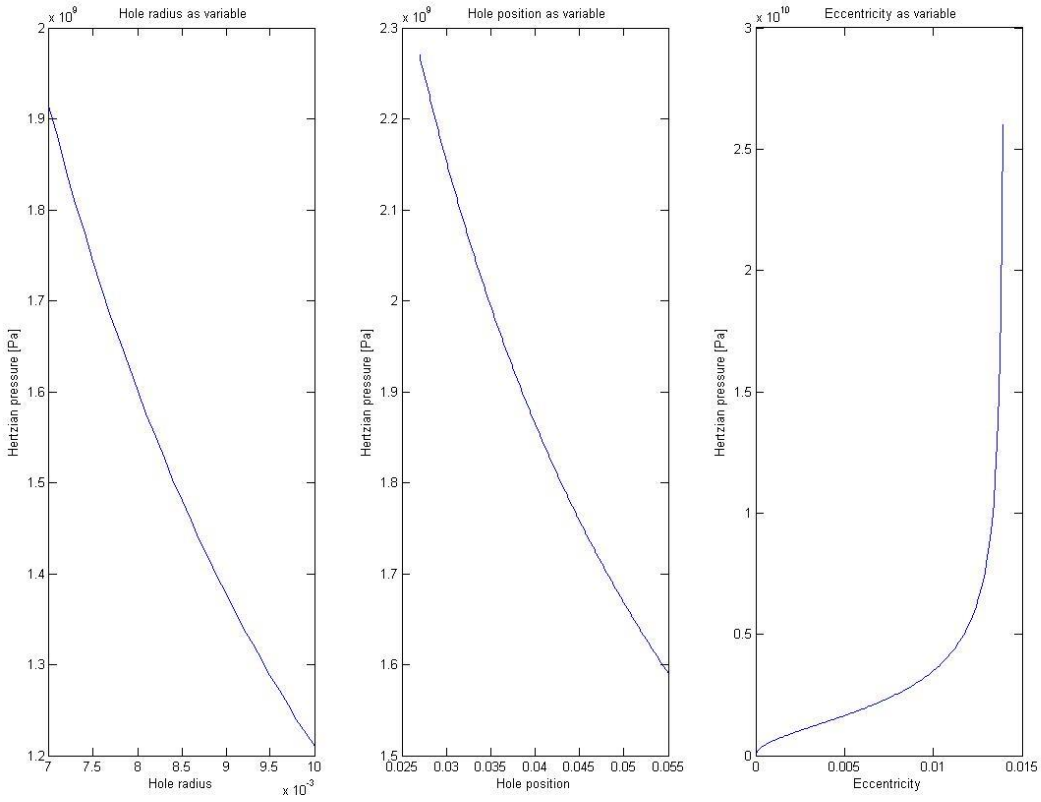

Figure 5.1.2: *Stresses depending on the hole radius, hole position and the eccentricity from left to right.*

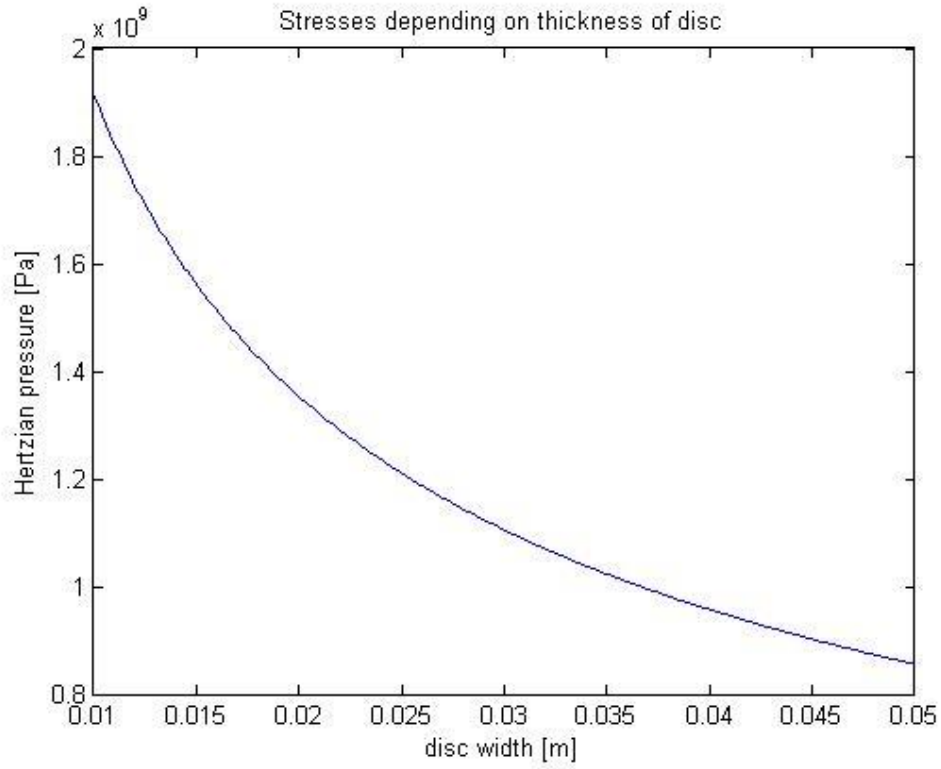

Figure 5.1.3: *Stresses in inner disc depending on width*

5.2 Variable geometry

When the calculation was looped over different parameters the following results in figure 5.2.1-5.2.8 was obtained. In all the figured the curves has been plotted for different thickness (b) of the disc.

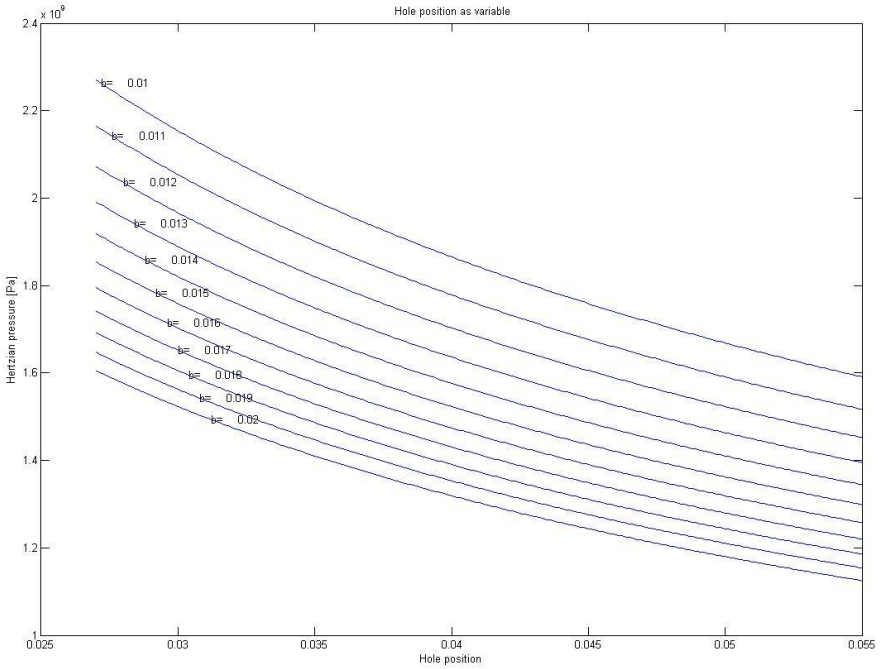

Figure 5.2.1: *Hertzian pressure with the hole position and thickness as variable.*

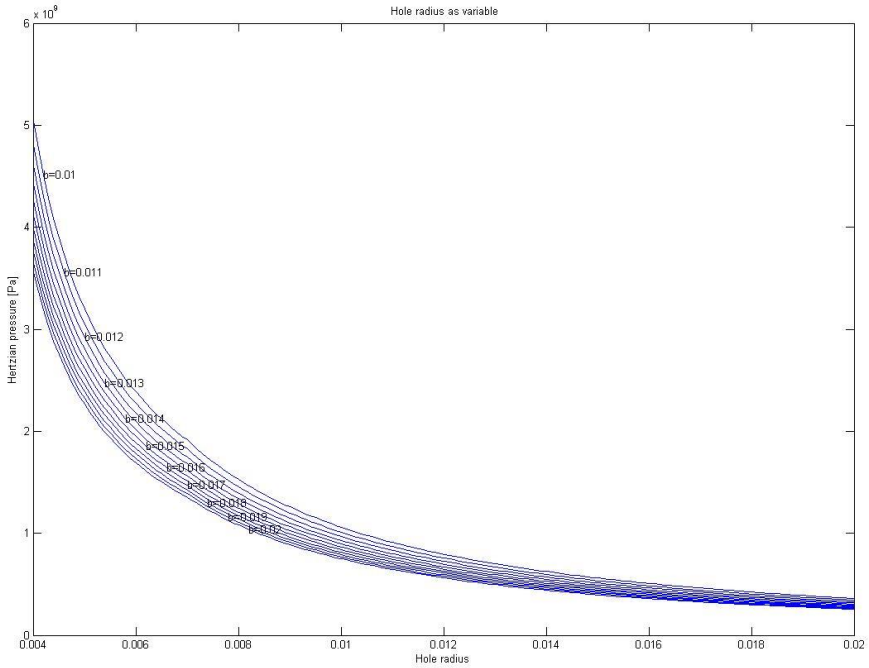

Figure 5.2.2: *Hertzian pressure with the hole radius and thickness as variable.*

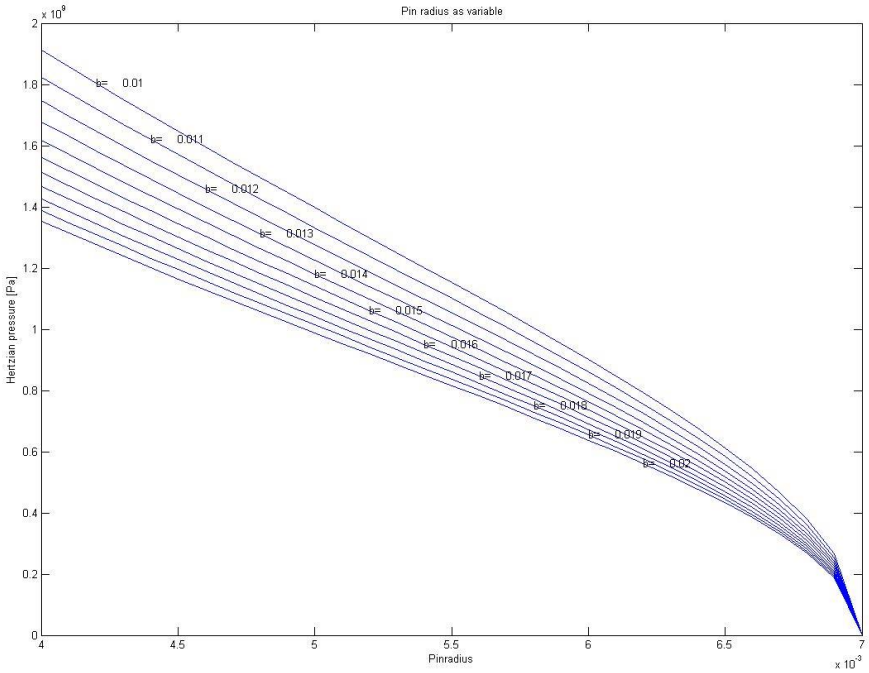

Figure 5.2.3: *Hertzian pressure with the pin radius and thickness as variable.*

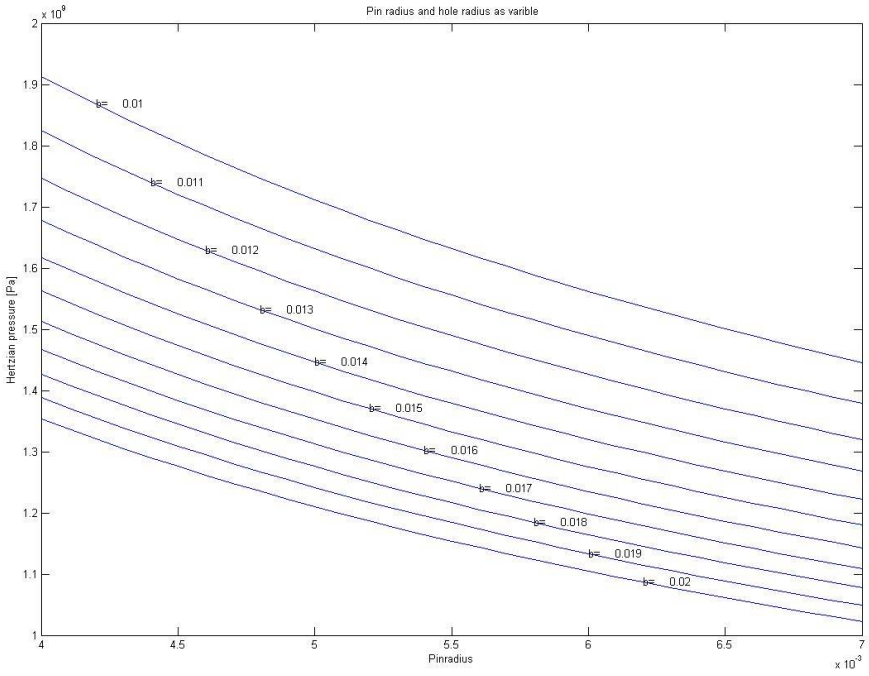

Figure 5.2.4: *Hertzian pressure with the pin and hole radius as variable and thickness. The relation between the hole and the pin radius is constant.*

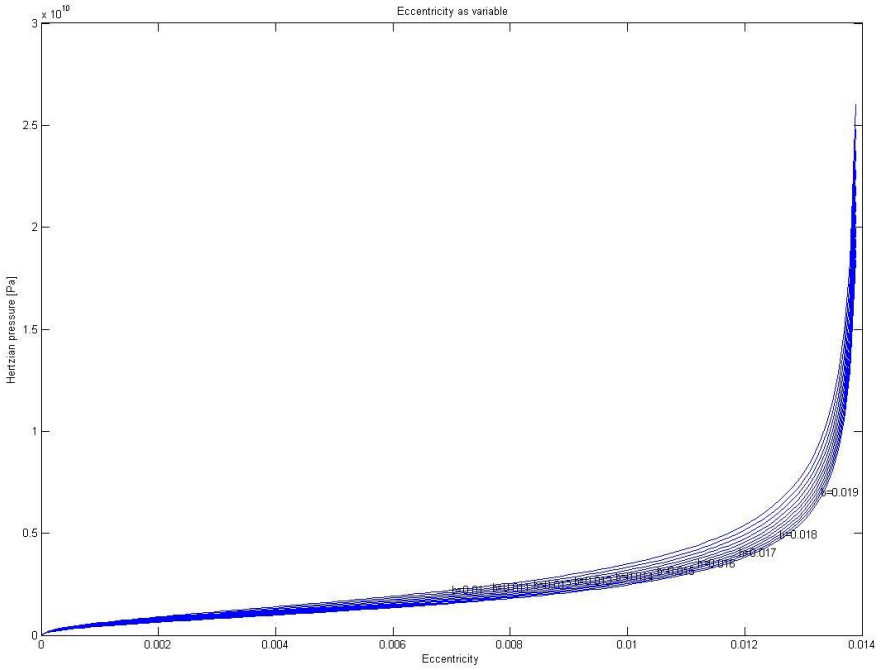

Figure 5.2.5: *Hertzian pressure with eccentricity and thickness as variable.*

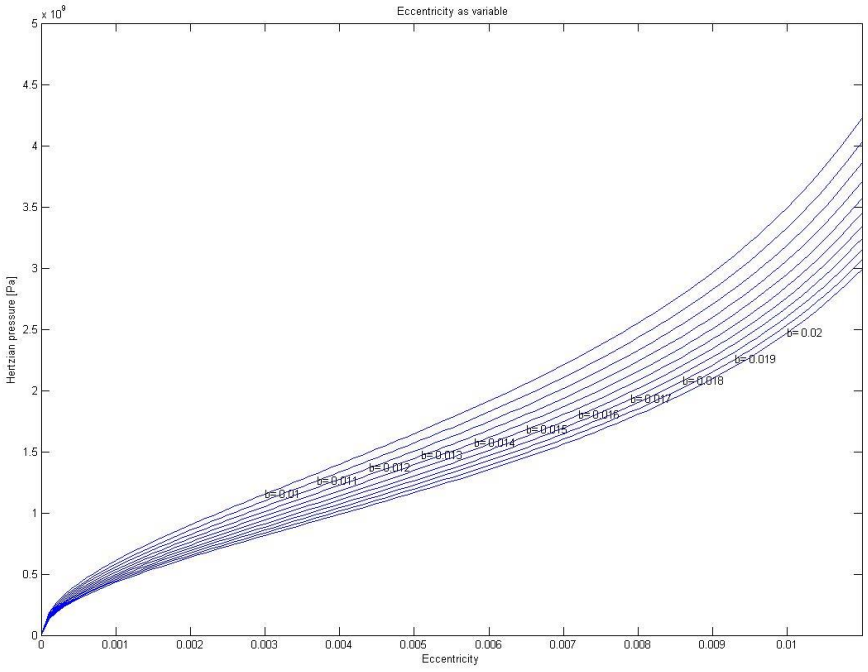

Figure 5.2.6: *Hertzian pressure with eccentricity and thickness as variable (different axes)*

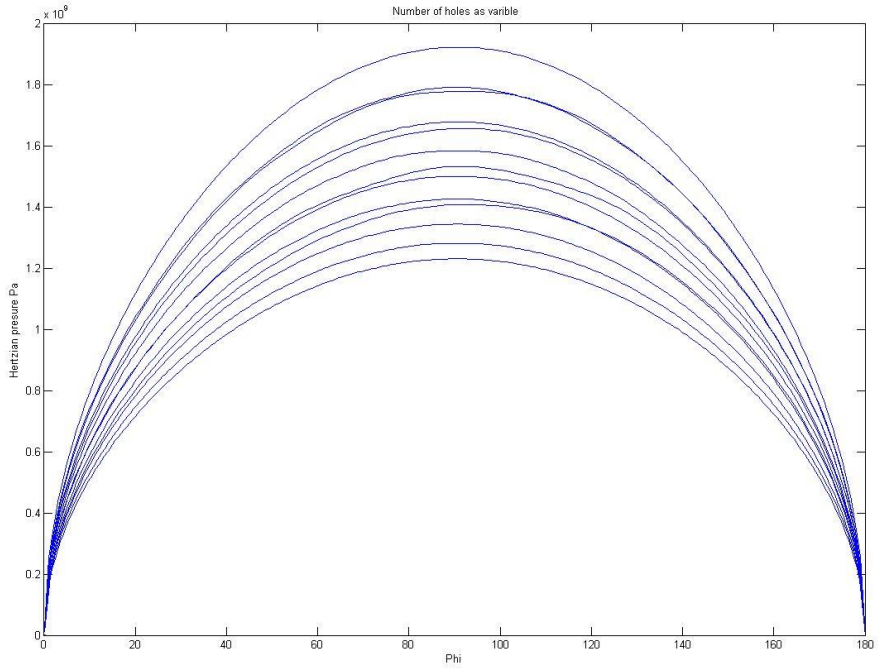

Figure 5.2.7: *Hertzian pressure with number of holes as variable, starting on 8 holes (highest curve) finishing on 20 (lowest curve).*

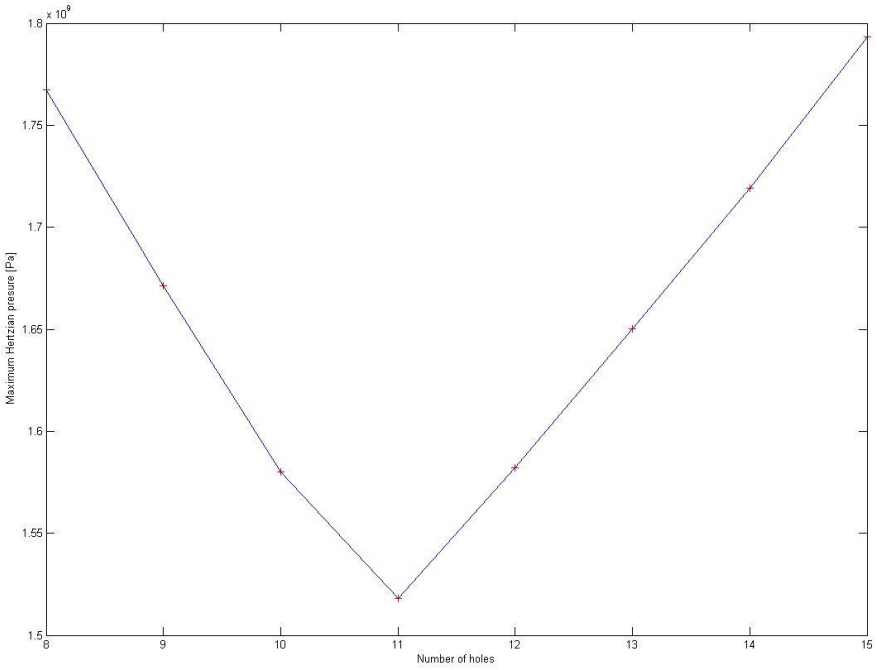

Figure 5.2.8: *Hertzian pressure plotted against number of holes with external measurements preserved*

5.3 Results Geometry with tolerances

The results with the tolerances included in the calculations are shown below, shown as a mean value of 101 loops.

Maximum mean contact Force: **10.2 kN**

Maximum mean Hertzian contact pressure: **1.99 GPa**

The 90-percentile for the Hertzian pressure: **2.07 GPa**

Below the mean contact force is plotted:

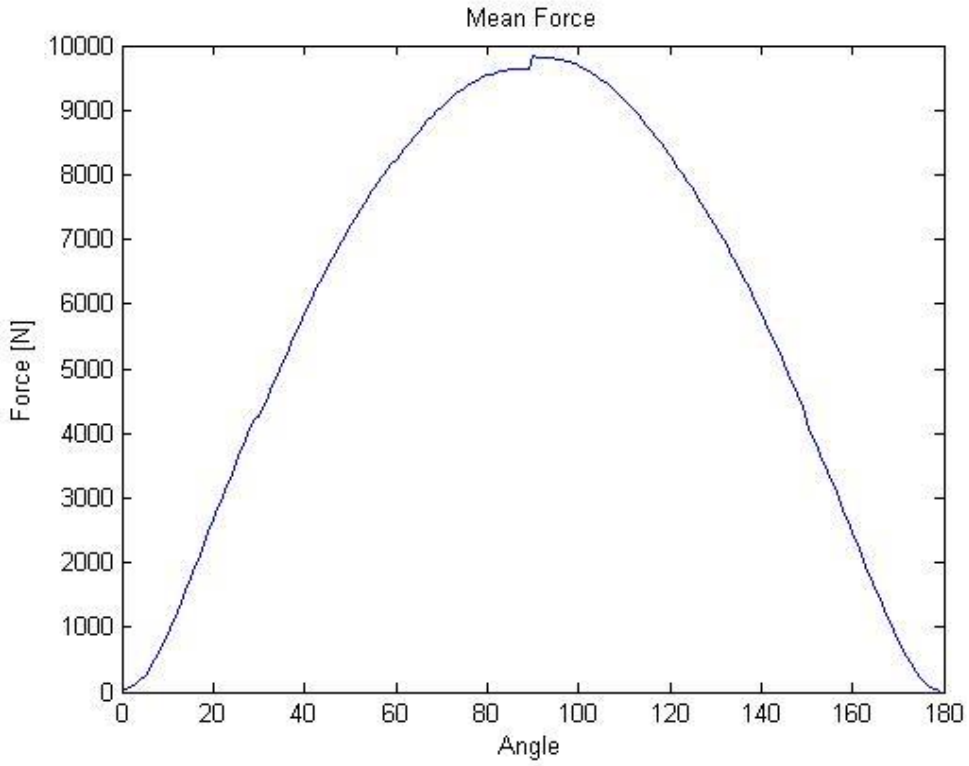

Figure 5.3.1: *Mean contact force.*

In the pictures (5.3.2 to 5.3.4) below shows some random graph of the contact force (the graphs are not associated with each other).

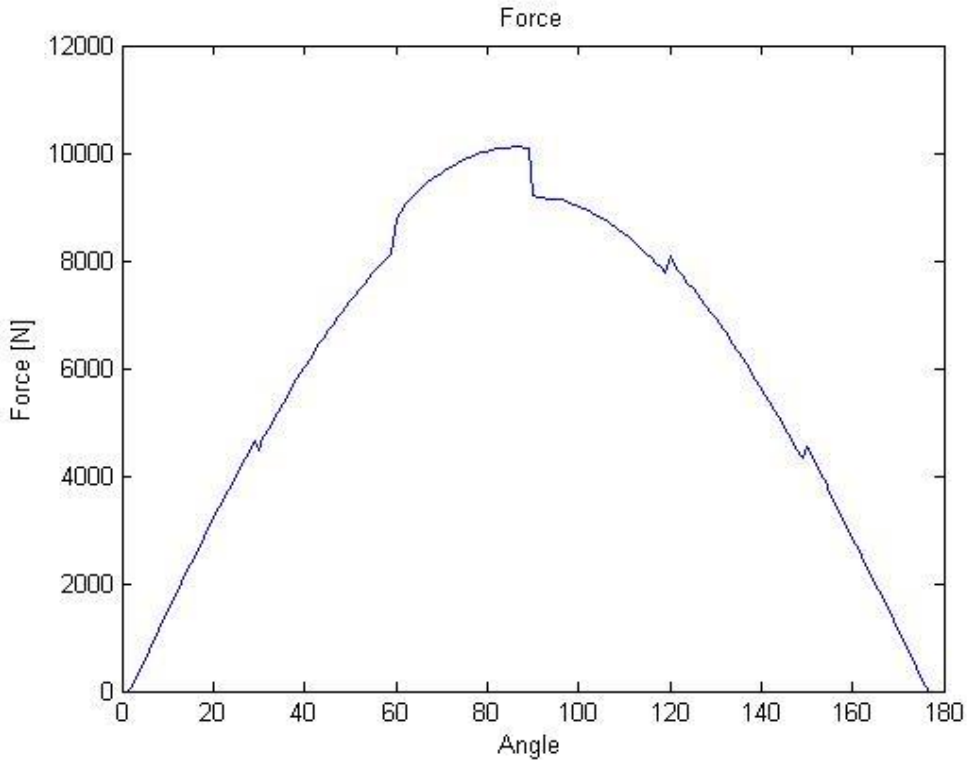

Figure 5.3.2: *Contact force.*

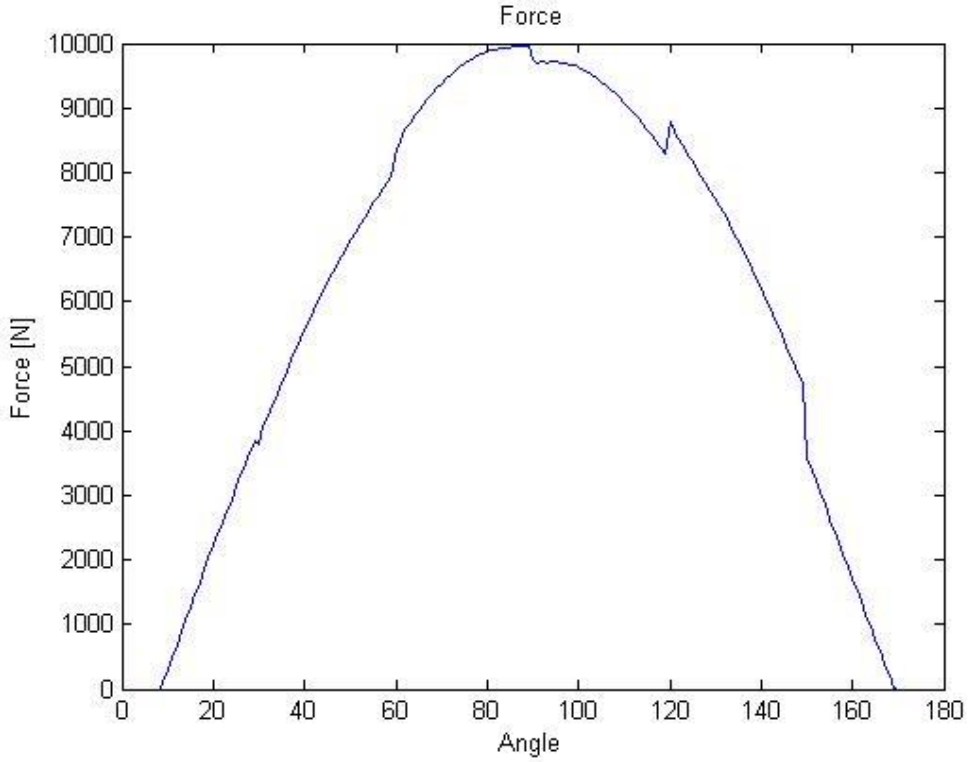

Figure 5.3.3: *Contact force.*

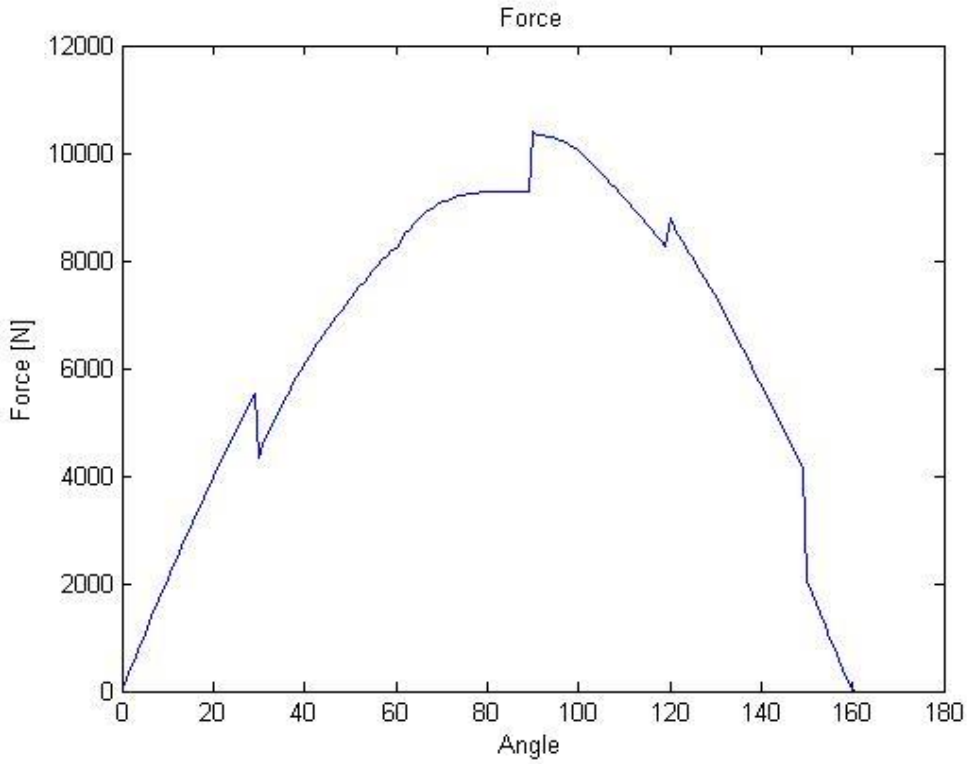

Figure 5.3.4: *Contact force.*

Below the mean Hertzian pressure is plotted:

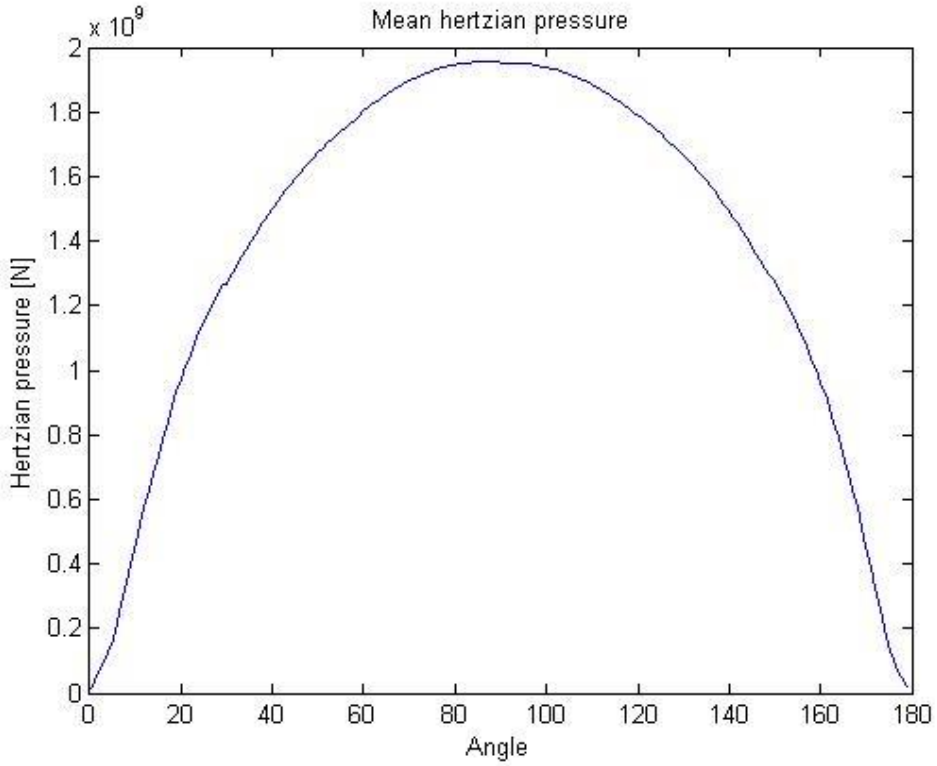

Figure 5.3.5: *Mean Hertzian pressure.*

In the pictures (5.3.6 to 5.3.8) below shows some random graph of the Hertzian pressure (the graphs are not associated with each other).

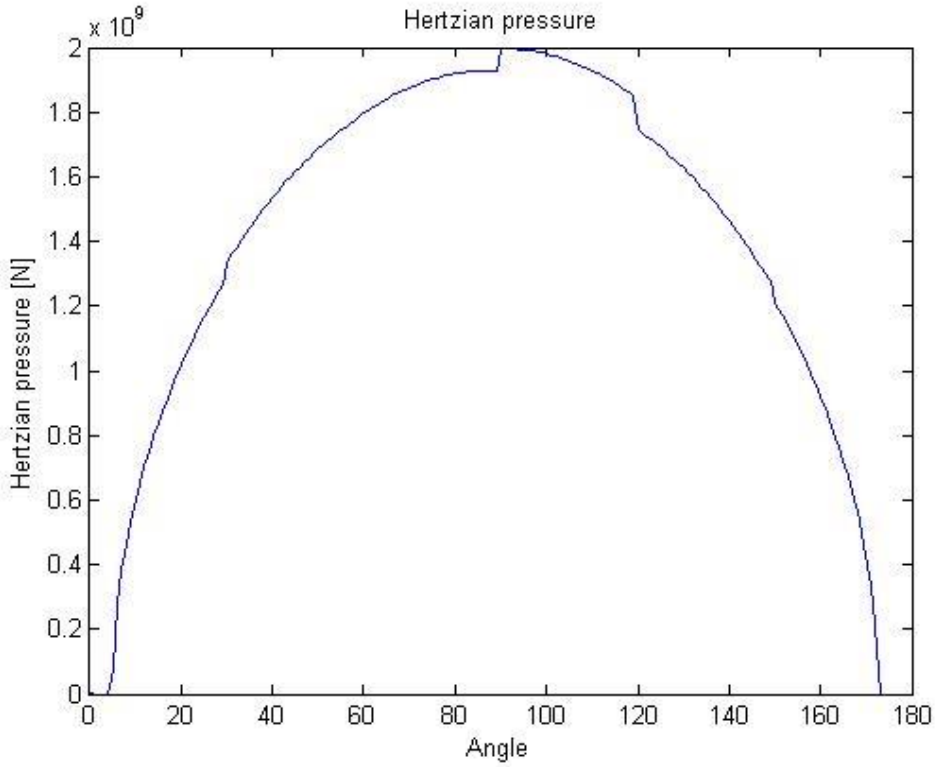

Figure 5.3.6: *Random Hertzian pressure.*

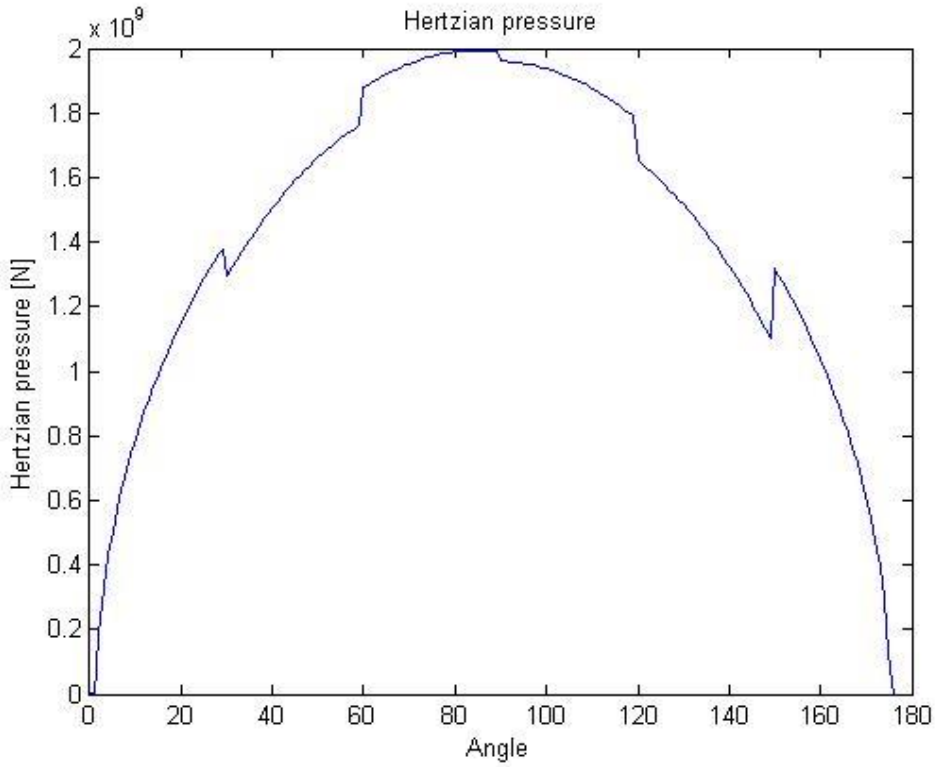

Figure 5.3.7: *Random Hertzian pressure.*

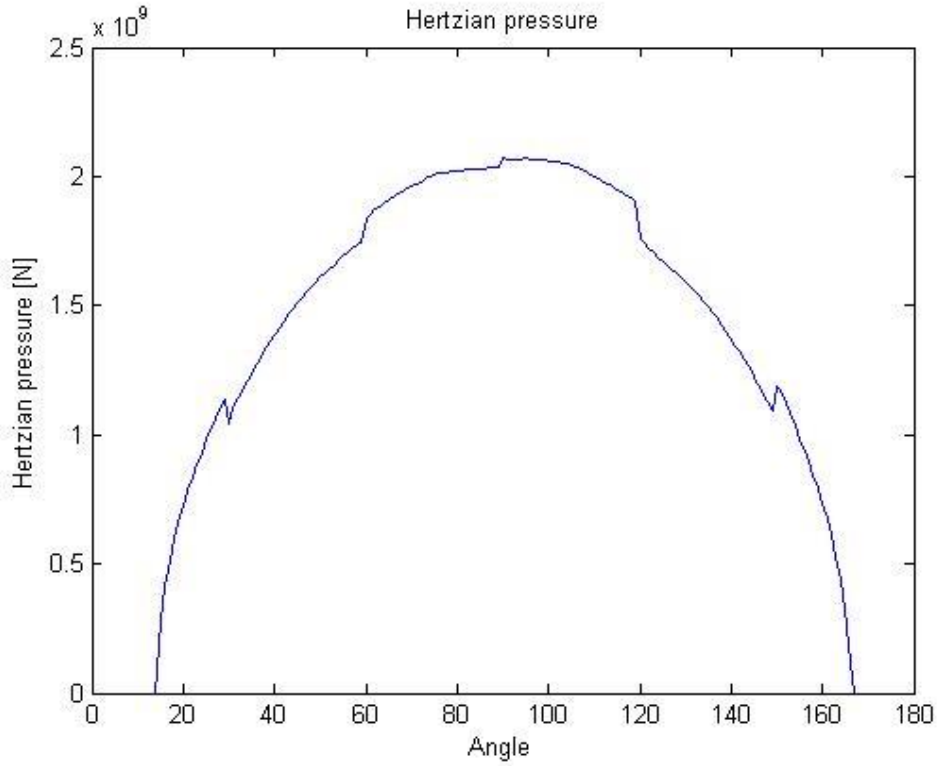

Figure 5.3.8: *Random Hertzian pressure.*

5.4 Fatigue

The Palmgren-damage rule value achieved with the original structure with tolerances included in the calculation was **1.21**, which means that failure occurs.

The mean maximum Hertzian pressure was **1.99 GPa** and the 90-percentile maximum Hertzian pressure was **2.07 GPa** both of which are greater than the 1.5 -1.65GPa that is the infinite fatigue limit.

5.5 Efficiency

The efficiency calculated for the Cyclo Drive is shown in the figures below. The first figure (figure 5.5.1) show the efficiency if the pins were to slide in the hole. The plot is made for different value of my. Figure 5.5.2 shows the efficiency when the pins are rolling in the hole.

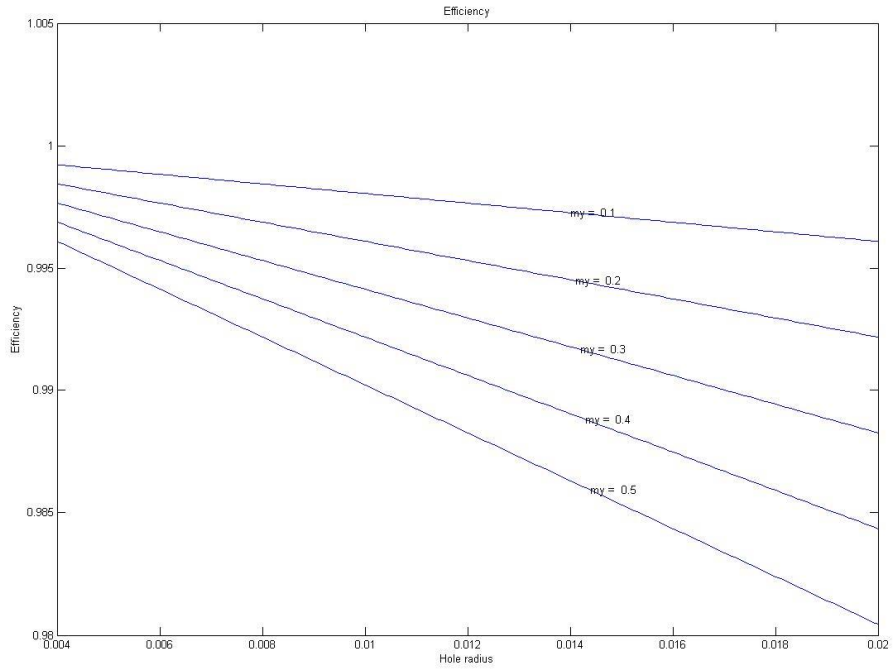

Figure 5.5.1: *Efficiency during sliding, plotted for different μ*

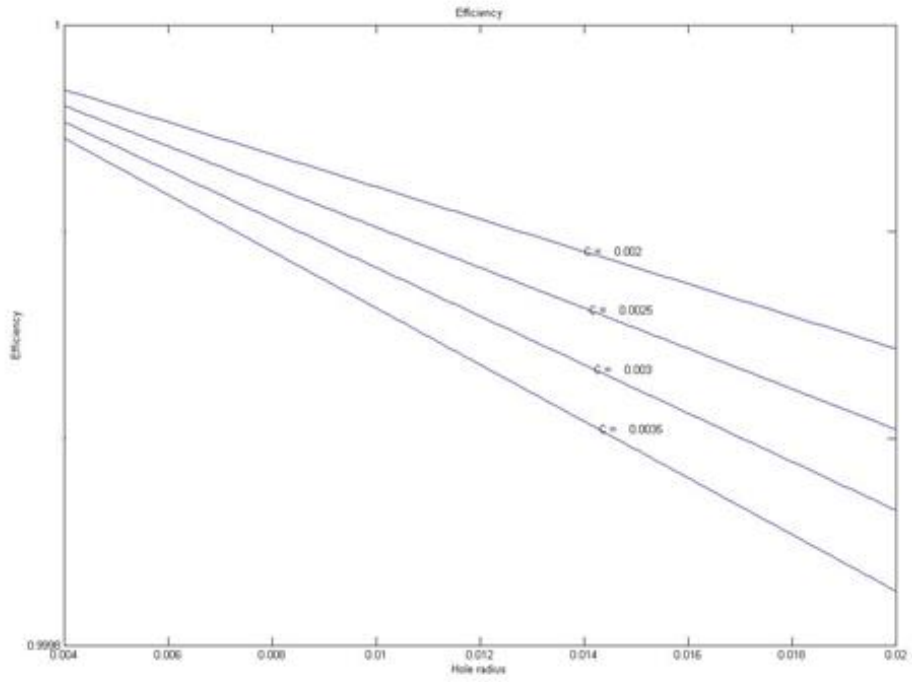

Figure 5.5.2: *Efficiency when the pin is rolling.*

6. Calculation conclusions

The fatigue calculations show that the current structure does not fulfil the requirements due to the high contact pressure, a fact which is confirmed by BorgWarner with real tests. The fact that the tests show the same results as the fatigue calculations serves as an indication that the model might be a reasonable approximation.

To be able to find geometry of the structure that will accomplish the goals the curves and results in section 5.2 is to be consulted. It is evident (see figure 5.1.3) that an increase in thickness is a rather inefficient method as it requires a significant increase to yield results. It might however be used in combination with some other measure to further improve the structure.

Regarding eccentricity, it is possible to greatly reduce contact pressure, but since a certain eccentricity is needed for the function of the overall system, thought must be given to other issues than contact pressure as well.

Changing hole position only yields moderate results, the reason for which being the fact that it mainly serves to reduce contact forces (by increasing the lever arm). As the contact pressure is proportional to the square root of the contact force (see eq. 4.3.1), the effect is reduced.

Increasing hole radius is the most favourable change of geometry. Even small increases will produce significant results, as evident in figure 5.2.2. Similar to hole position modification however, it requires changing the external geometry, unless the number of holes is changed as well.

When it comes to the hole count the variation of these will allow change of the parameters as hole and pin radius without intruding on the size of the disc. As decreasing the number of holes will increase contact pressure on each hole and increasing hole radius will reduce it, it is a matter of finding an optimal configuration, which was found to be eleven holes (see figure 5.2.8).

As for the increase of the pin radius with the hole radius constant (using non-circular pins), it will have a beneficial effect on the contact pressure at the expense of the efficiency (see section 5.5). If efficiency were to be of minor importance, this solution might be appealing. However for practical reasons such as assembling non-circular pins may be difficult to implement, as they would have to be placed in a specific position. Furthermore, if one of the pins were to rotate or otherwise be displaced during load the mechanism might be unable to function properly or even break down. The issue of rotating might be addressed by adding material on the sides of the pin however this would make the pin even more complicated to manufacture and would not resolve the assembly problem.

To reduce stresses due to the pin deflection it can be seen (section 3.2) that the most beneficial edge design is the radius. This is the design that yields the lowest Hertzian pressure. However the model is only an indication of how the stresses due to the deflection will behave.

7. Mechanisms

7.1 Aims

The investigation of a new mechanism that will achieve a conversion between centric and eccentric rotation intends to fulfil the following list of requirements.

- The mechanism must handle a torque of 1000 Nm.
- The mechanism must be small enough to fit in a cylindrical room with the dimensions of approximately 35 mm in height and 105 mm in diameter.
- Gear ratio of $U = 1{:}\,1$.

The different solutions presented are evaluated in accordance with these specifications.

7.2 Mechanisms Presentation

7.2.1 Oldham

The Oldham coupling allows two axes to circle around two different centres using splines (se figure 7.2.1.1). The coupling is made in three parts, one input axis, one output and a disc in between which is connected to the axes by tongue and groove on each side (see figure 7.2.1.1).

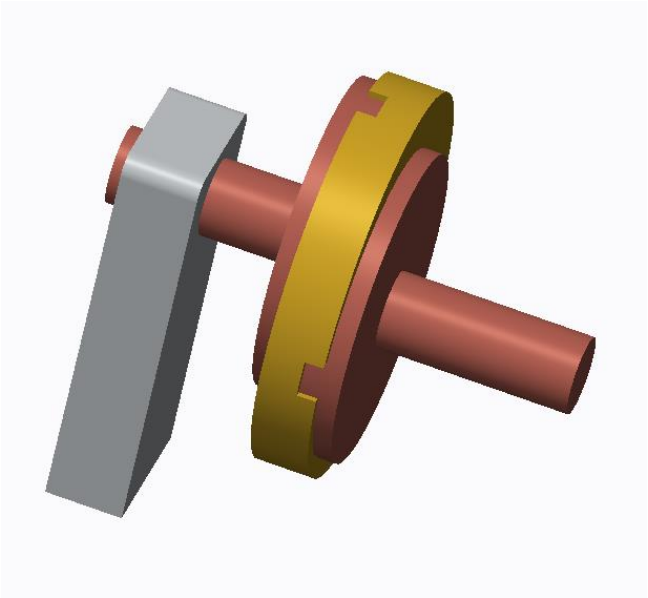

Figure 7.2.1.1: *Oldham coupling illustration, input axis to the right and output axis on the disc.*

7.2.2 Cardan shaft

Much like the Oldham coupling, a cardan shaft allows transfer of motion between two different centres. An angular bar attached with universal joints is used to connect the two axes.

7.2.3 Eccentric ball bearing mechanism

This mechanism transfers the eccentric motion to the input/output axis through a ball bearing mechanism (se figure 7.2.3.1). This allows the eccentric motion of the one cogwheel to rotate with an angle.

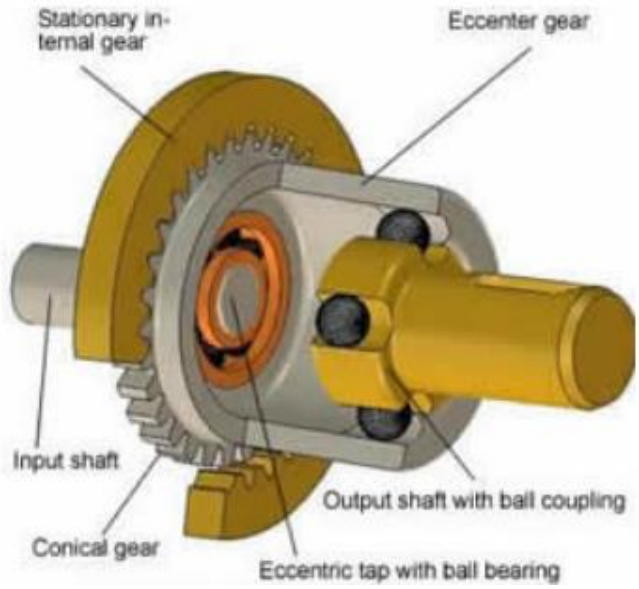

Figure 7.2.3.1: *Eccentric ball bearing*[1]

7.2.4 Chain transfer

This mechanism transfers rotation between two sprockets one of which is eccentrically attached to the output axis.

7.2.5 Eccentric internal gear

This drive is made up of two gears, one internal and one external. The external is attached to the input axis and the internal to the output axis. The eccentric motion is achieved by displacing the rotation centres of the internal gear forcing the output axis to rotate eccentrically. (Figure 7.2.5.1)

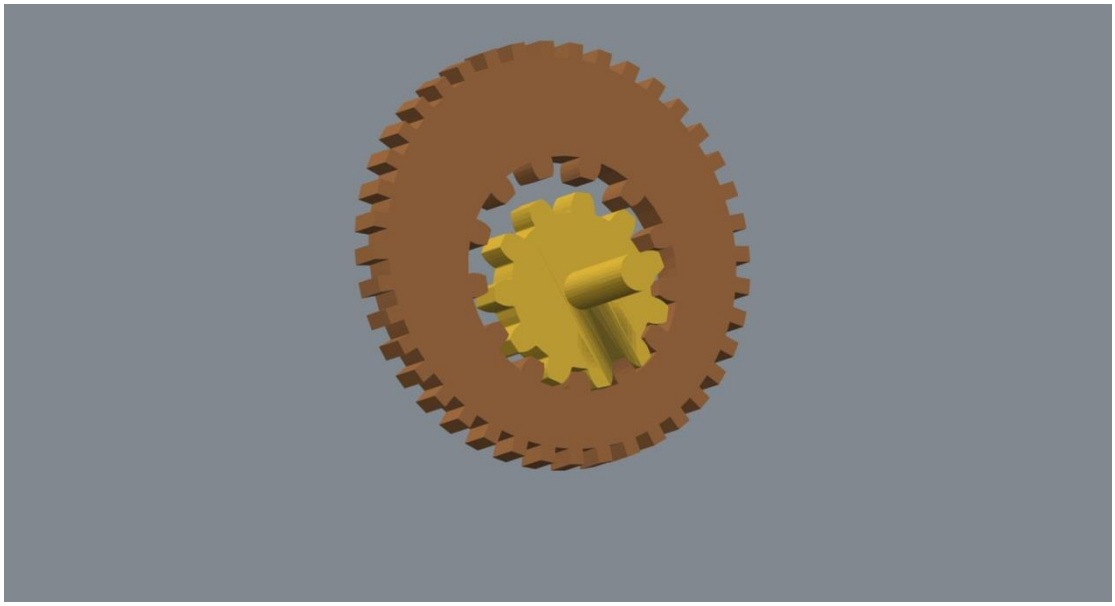

Figure 7.2.5.1: *Eccentric placed internal cogwheel.*

A different but similar design would be two external gears, one of which is eccentrically attached to a disc, which is in turn the output axis (figure 7.2.5.2).

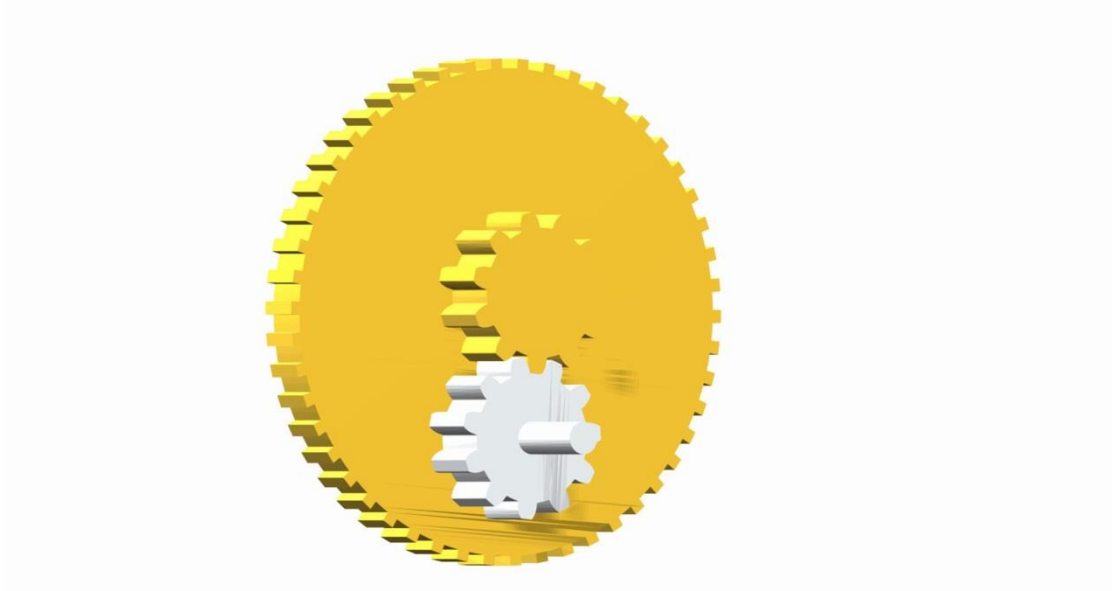

Figure 7.2.5.2: *Eccentric placed external cogwheel.*

7.2.6 Planetary gearing

Works as regular planetary gearing but the planet gears differ in size producing an offset between the sun gear's and the outer ring wheel's axis of rotation (picture 7.2.6.1).
If two epicyclical gearings would be placed into each other and connected with a common annulus the epicyclical gearing would be very compatible. This will enable the gear ratio to be as desired.

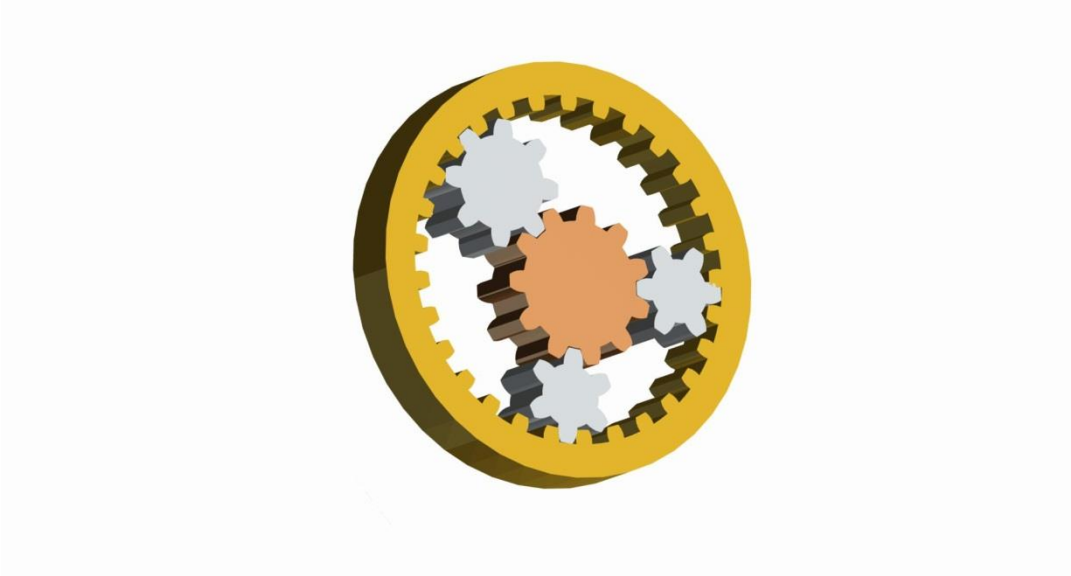

Figure 7.2.6.1: *Eccentric placed internal cogwheel.*

7.2.7 Double planetary gearing

The issue of gear ratio could be managed if two epicyclical gearings (see figure 2.2.7.1) would be placed into each other and connected with a common outer ring. This will enable the gear ratio to be chosen and varied precisely as desired.

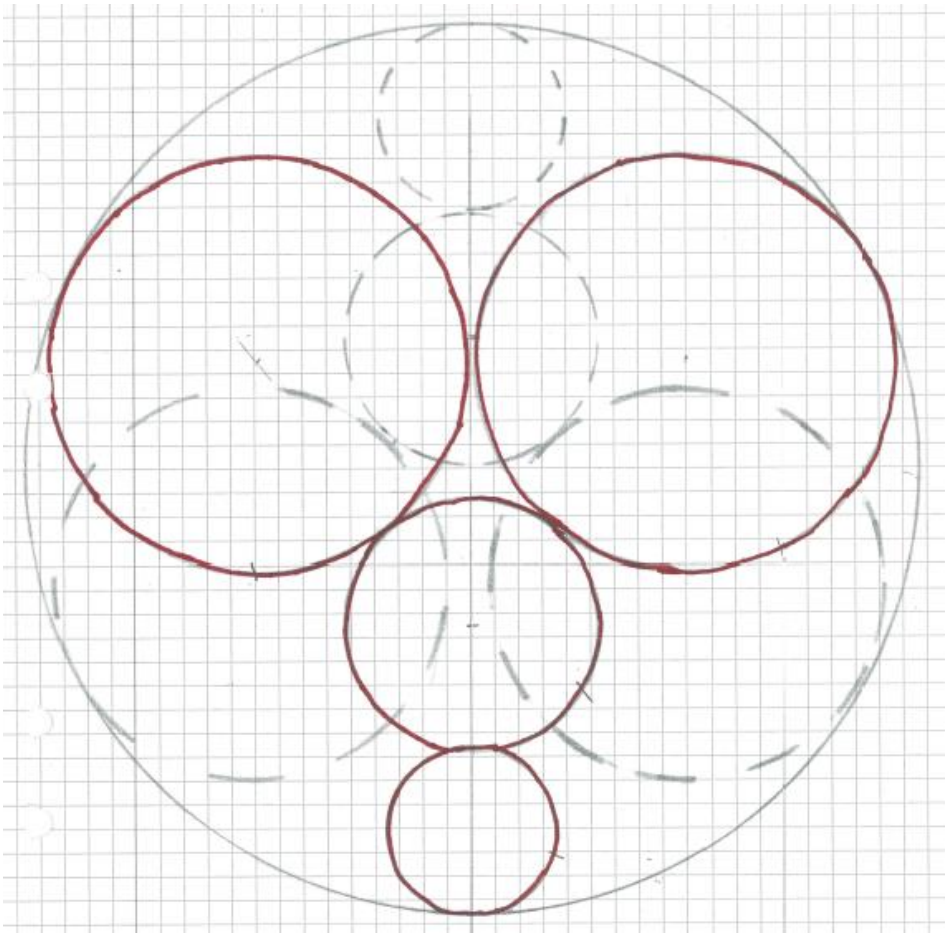

Figure 7.2.7.1: *Illustration of double planetary gearing.*

7.3 Evaluation

To derive which mechanism to use an evaluation is made. This was made to conclude if the mechanism could transfer the eccentric motion.

7.3.1 Oldham

There is some uncertainty as to whether the Oldham fits in the amount of space available. The support of the left disc (see figure 7.2.1.1) will have to be mounted in such a way that the output axis may extend past it.

One other downside of the Oldham is that the centre disc will move and rotate eccentrically in perspective to the inlet and outlet axis, which will create harmful vibrations in the gearing.

After some brief calculation on the motion of the disc and the force between the parts in the Oldham the efficiency was calculated to 0.9-0.95 (se figure 7.3.1.1 and 7.3.1.2 and equations 7.3.1.1-7.3.1.7).

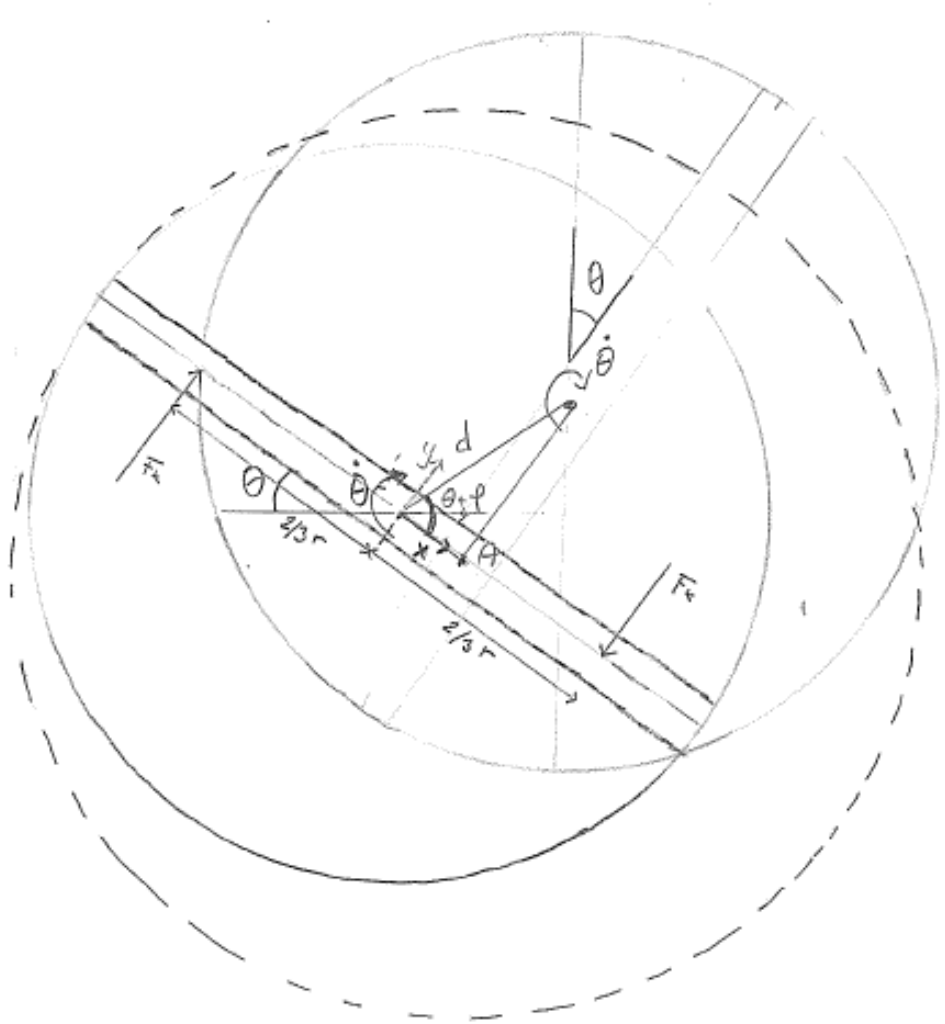

Figure 7.3.1.1: *Illustration of parameters used during calculations on Oldham coupling.*

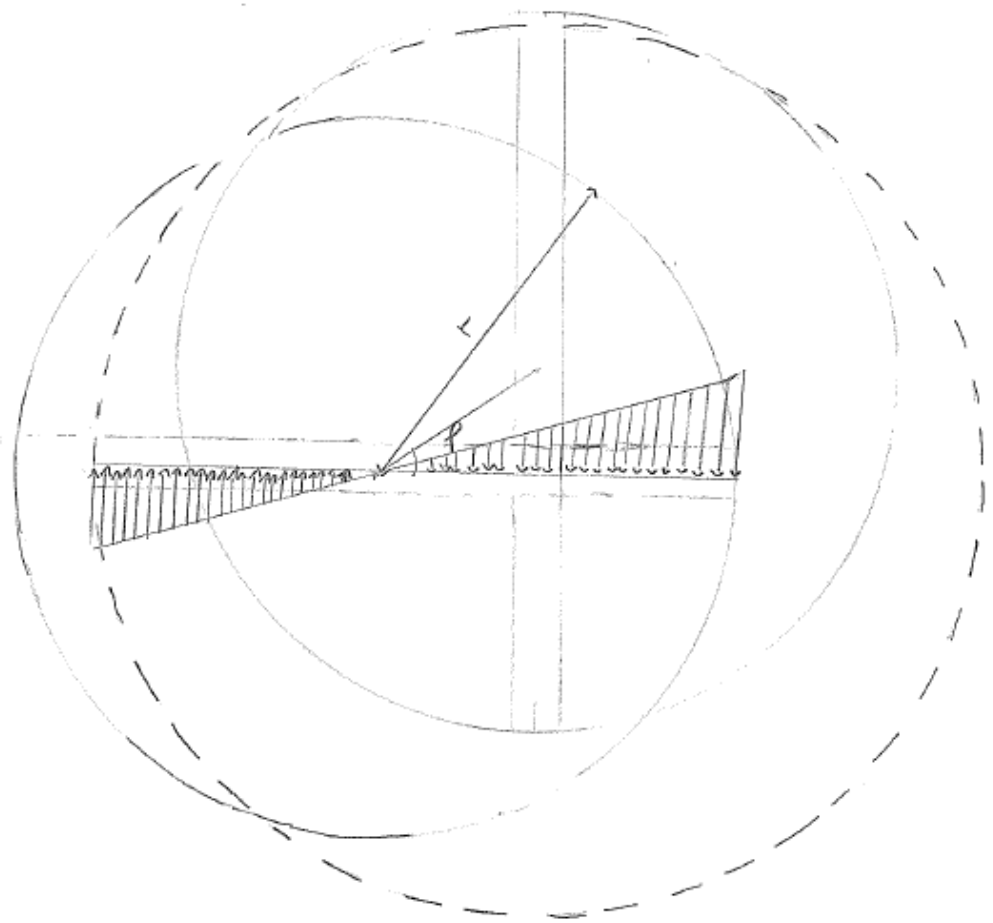

Figure 7.3.1.2: *Illustration of contact force in an Oldham coupling.*

$$\varphi = \arctan(\frac{y}{x}) \tag{7.3.1.1}$$

$$x = dcos(\theta + \varphi) \tag{7.3.1.2}$$

$$\dot{x} = -d\dot{\theta}sin(\theta + \varphi) \tag{7.3.1.3}$$

$$F_k = \frac{3M}{4r} \tag{7.3.1.4}$$

$$P_e = F_k \mu \dot{x} = -d\dot{\theta}sin(\theta + \varphi)\frac{3M}{4r} \tag{7.3.1.5}$$

The loss after 360 degrees of rotation is:

$$-2\mu F_k d\dot{\theta} \int_0^{\pi} \sin(\theta + \varphi)\, d\theta \quad = -\frac{3Mdcso\varphi\mu\dot{\theta}}{r} \tag{7.3.1.6}$$

Choosing the coordinate system wisely may eliminate the angleφ.
The efficiency thus becomes:

$$\eta = \frac{M\dot{\theta} - \frac{3Md\mu\dot{\theta}}{r}}{M\dot{\theta}} = 1 - \frac{3d\mu\dot{\theta}}{r} \approx 0.9 \qquad (7.3.1.7)$$

7.3.2 Cardan shaft

Like the Oldham, a cardan shaft would have to be modified somehow to be suitable for this application. As there appears to be no good way to accomplish that the cardan shaft is deemed unsuitable. Moreover the cardan shaft would have to be 28 mm in diameter to be able to withstand the torque requirements (se equations below).

$$\begin{cases} W_v = \frac{\pi r^3}{2} \\ Mv = 1000\ Nm \\ \tau_{\max} = \frac{M_v}{W_v} \\ \sigma_{yield_{ss2511}} = 415\ Mpa \end{cases} \Rightarrow \qquad \sigma_{yield_{ss2511}} = \sqrt{3\tau_{\max}^2} \qquad \Rightarrow$$

$$\tau_{\max} = \frac{M_v}{W_v} = \left(\frac{\sigma_{yield_{ss2511}}^2}{3}\right)^{\frac{1}{2}} \qquad \Rightarrow$$

$$r = \left(\frac{2M_v}{\pi\tau_{max}}\right)^{\frac{1}{3}} = 0{,}0139 \qquad (7.3.2.1)$$

7.3.3 Eccentric ball bearing mechanism

Since the ball bearing enables a movement with an angle around the axis the output axis in the mechanism must be able to move in the connecting splines. This will however probably be a problem because of the small space needed between the splines at the connecting axis and the axis about from the eccentric mechanism. With regards to this discussion this solution will be excluded from further investigations.

7.3.4 Chain transfer

Because this mechanism would require a massive chain to operate it is deemed unsuitable due to lack of space.

7.3.5 Eccentric internal gear

A rather simple design the main issue of which is keeping the gear ratio close to 1:1. For internal gear transmissions with standard involute teeth the difference in number of teeth should be around ten in order to avoid interference[2], thus limiting the achievable gear ratio.

Gear ratio is not a problem should two external gears be used, however it would require more space than an internal one. Furthermore, the rotation centres of the wheels would have to be further apart.

The main problem is keeping the size of the mechanism sufficiently small while retaining the torque transfer ability.

7.3.6 Planetary drive

For planetary gearing, there are several different configurations possible.

$$R = \frac{\omega_1 - \omega_c}{\omega_2 - \omega_c} = -\frac{z_2}{z_3}\frac{z_3}{z_1} = -\frac{z_2}{z_1} \qquad (7.3.6.1)$$

Where z_1 and z_2 are the number of teeth of the sun gear and the outer ring respectively and $\omega_1, \omega_2 \; and \; \omega_c$ are the rotational speeds of the sun gear, outer ring and planet carrier.

With the planet carrier locked, i.e. $\omega_c = 0$ the sun gear and outer ring are used as input/output axis.

Thus

$$U = \frac{\omega_1}{\omega_2} = -\frac{z_2}{z_1} \qquad (7.3.6.2)$$

Similarly by locking each wheel the gear ratio becomes:

$$\omega_2 = 0 \; => U = \frac{\omega_1}{\omega_c} = 1 + \frac{z_2}{z_1} \qquad (7.3.6.3)$$

$$\omega_1 = 0 => U = \frac{\omega_2}{\omega_c} = 1 + \frac{z_1}{z_2} \qquad (7.3.7.4)$$

As $z_2 > z_1$ it proves difficult to achieve a gear ratio close to 1:1 if either one of the input/output axis is the sun gear, it is preferable to use the outer ring and the planet carrier as input/output axis (whichever is more suitable).

As for the number of planet gears, this will have to be decided with regard to the strength requirements of the drive.

7.3.7 Double planetary drive

If two epicyclical gearings were to be placed after one and other the gearing ratio would be easily modified as desired. More over the double planetary gearing still has the beneficial efficiency, however not quite as good as the simple planetary gearing. Still the torque transfer requirement will have to be achieved by an appropriate number of planet wheels.

7.4. Mechanisms Summary

As seen in the table below the best mechanisms is the planetary gearings, mainly because it only has possible weakness (gear ratio), which may possibly be eliminated by using the double planetary gearing the gear ratio can be as desired.

The Oldham coupling along with the eccentric internal gear comes second as both of those have very significant shortcomings (vibrations and transferable torque respectively).

The remaining mechanisms are disqualified since none of them is deemed to handle the expectations of the mechanism.

Mechanism	***Torque***	***Packing space***	***Gear retio***	***Efficency***	***Pros***	***Cons***
Oldham	+	-	+	-	2	2
Cardan shaft	-	-	+	+	2	2
Eccentric ballbearing	+	-	-		1	2
Eccentric internal gear	-	+	-	+	2	2
Eccentric epicyclical gearing	+	+	-	+	3	1
Double epicyclical gearing	+	-	+	+	3	1

Table 7.4.1: *Evaluation of mechanisms.*

8. Final design

Based on the above discussion, the optimal design was found to be a disc with eleven holes, slightly increased hole radius and thickness and a rounding radius at the holes' edges.
The new design is shown below in table (8.1).

Final design	**mm**	**Hole count**	**Hertz [GPa]**
rh	8		
r	39		
e	6		
rp	5		
b	12		
n		11	
Pmax			1,4245
Rounding radius	0,2		

Table 8.1: *New dimensions.*

Below the new design are evaluated:

Calculations without tolerances:

Maximum force = **9.12 kN**

Maximum Hertzian pressure = **1.44 GPa**

Calculations with the tolerances:

Maximum mean force = **10.78 kN**

Maximum mean Hertzian pressure = **1.57 GPa**

The 90-percentile for the Hertzian pressure: **1.62 GPa**

In figure 8.1 to 8.2 the contact force and the Hertzian pressure are shown (calculations with perfect conditions).

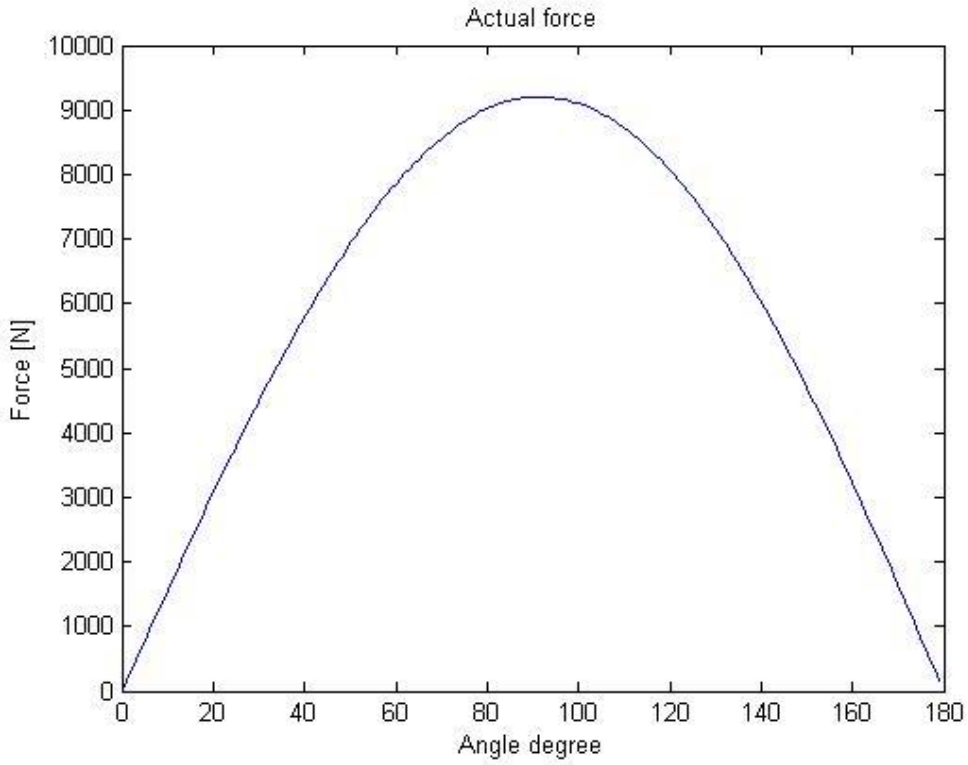

Figure 8.1: *Contact force of one pin during 180^o rotation with new geometry.*

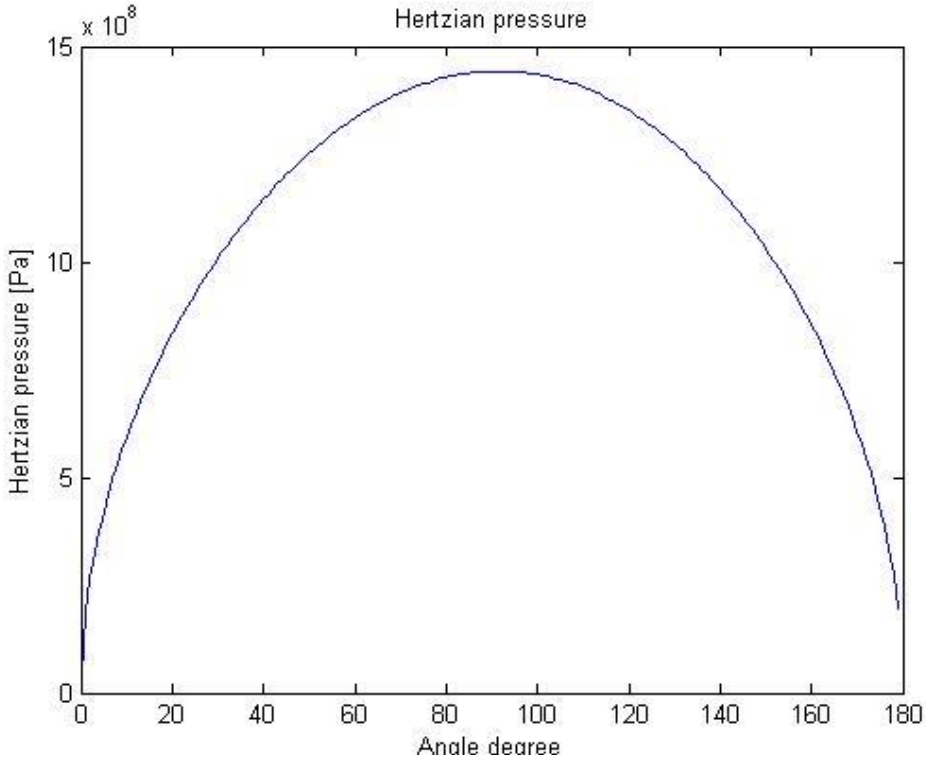

Figure 8.2: *Hertzian pressure of one pin during 180^o rotation with new geometry.*

In picture 8.3 to 8.6 shows the contact force and Hertzian pressures (calculations with tolerances).

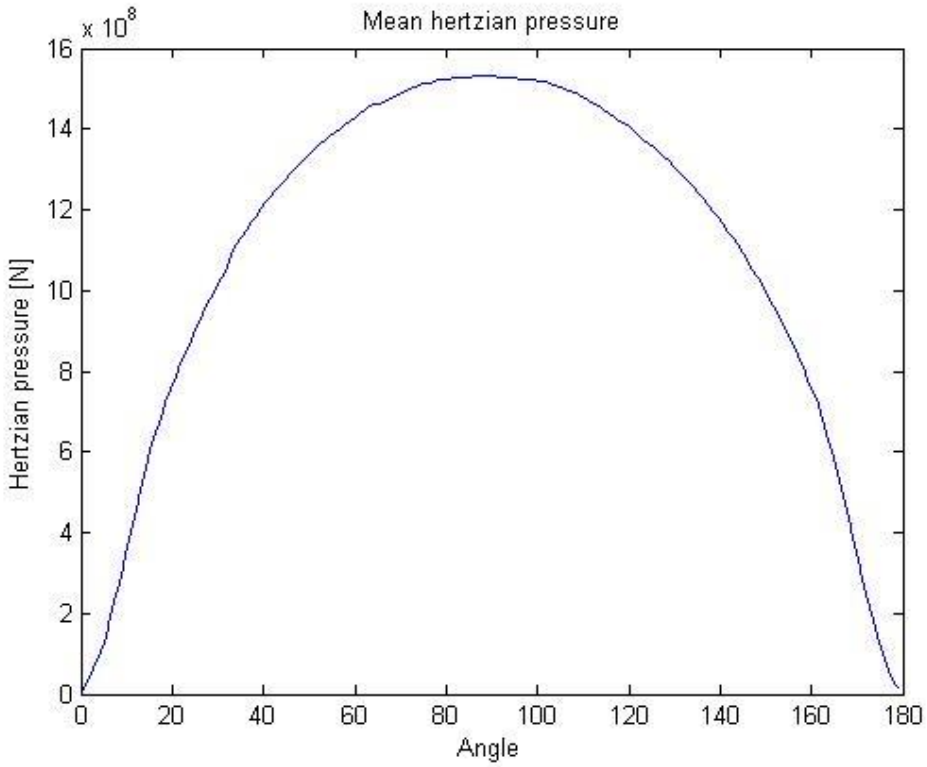

Figure 8.3: *Mean Hertzian pressure of one pin during 180^o rotation with new geometry and tolerances.*

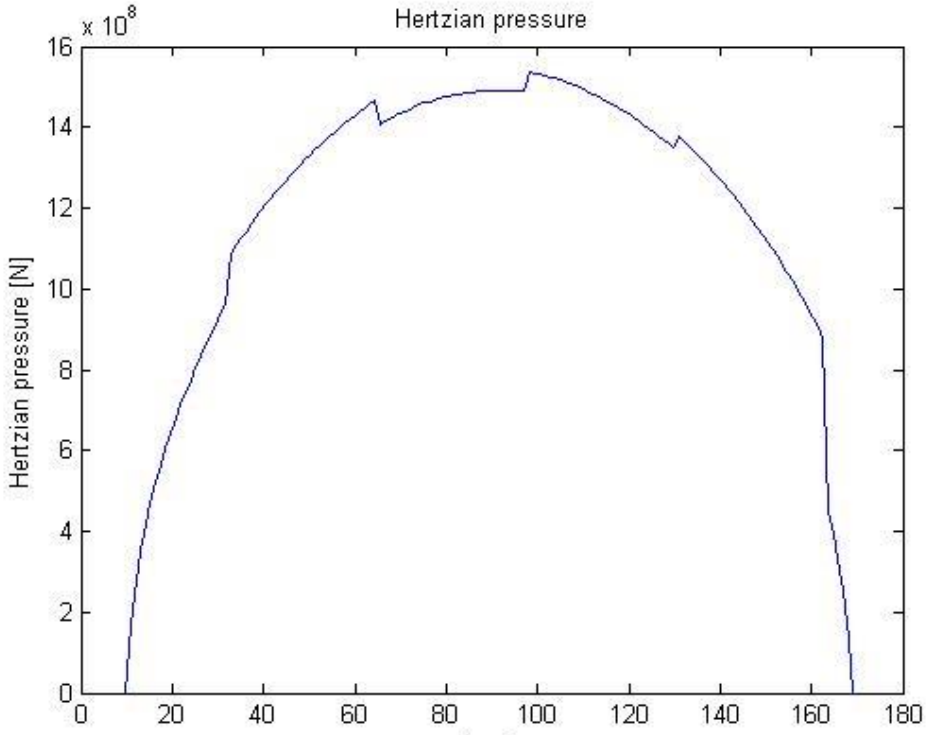

Figure 8.4: *Random Hertzian pressure of one pin during 180^o rotation with new geometry and tolerances.*

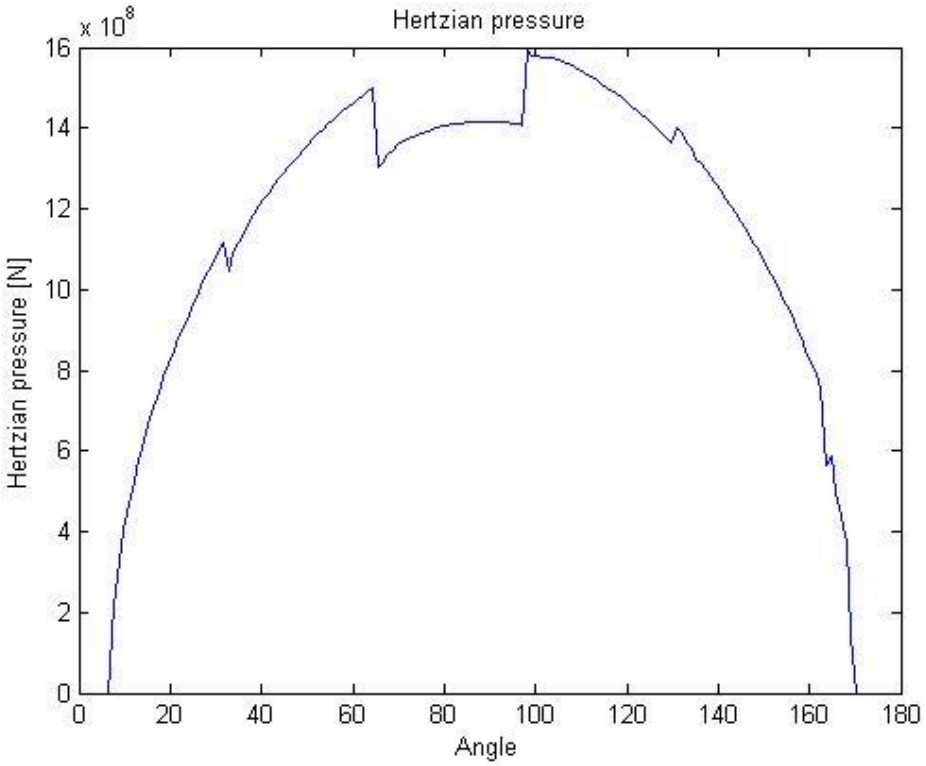

Figure 8.5: *Random Hertzian pressure of one pin during 180^o rotation with new geometry and tolerances.*

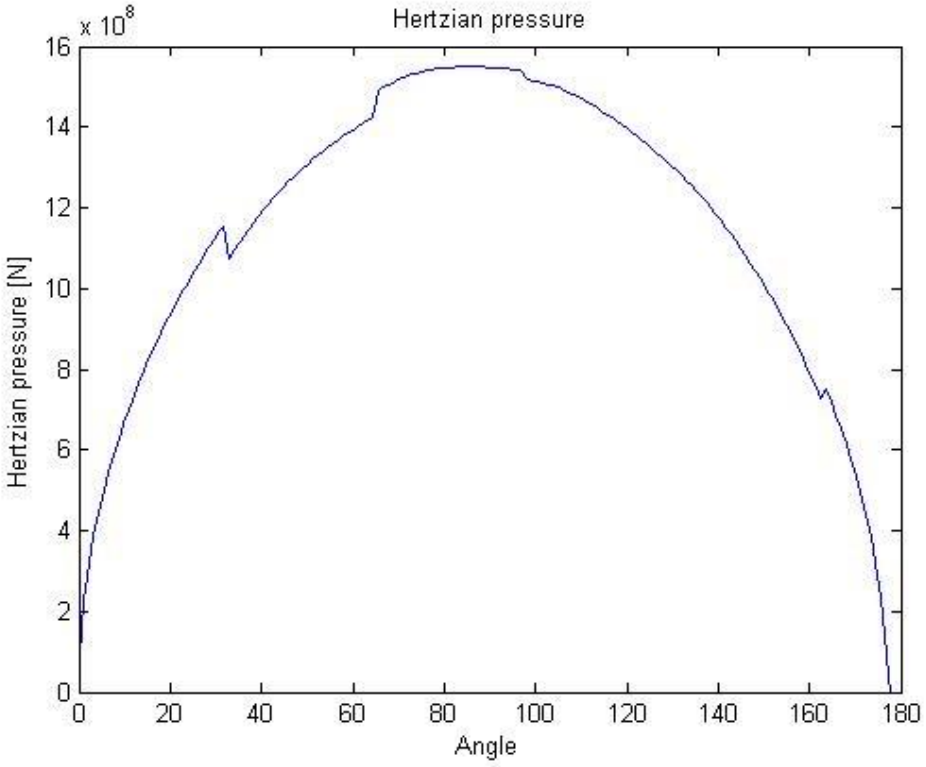

Figure 8.6: *Random Hertzian pressure of one pin during 180^o rotation with new geometry and tolerances.*

The fatigue calculations with the new design and tolerances included to the calculations is illustrated in table 8.2 next to the value of the old design.

Palmgren Value	Original design	New design
	1,16	0,15
	1,21	0,21
	1,2	0,22
	1,3	0,21
	1,17	0,15

Table 8.2: *Result of Palmgren-damage rule.*

The table shows that the Palmgren-damage rule is considerably sensitive regarding the load.

9. Discussion

9.1 Accomplishment

The goal of the project was to design the Cyclo Drive in a way that it can withstand the loads that are expected. It has been shown that the Cyclo Drive is now able to handle the loads and cycles from the load spectrum. However the fatigue evaluation is based on material data that is not exactly the same as used in the Cyclo Drive (although they are both case hardened steels). But the fatigue calculation may be used as an approximation especially if the results from the original design are compared to those of the modified one with fewer holes and different dimensions. Still, to be sure of the function of the Cyclo Drive a life cycle test will have to be conducted.

During the calculations, virtually all measurements have been plotted and illustrated with regard to its effect on stresses, even those that were not changed in the final design. This enables the use of this report in future development of similar projects.

The screening lead to seven concepts that were evaluated. The evaluation produced two similar alternatives to replace the Cyclo Drive, however none of these solutions are an obvious choice. Furthermore, exact calculations of their torque transferability will have to be conducted, as such calculations have been excluded due to time limitations and lack of resources.

9.2 Uncertainties

One major uncertainty of the analysis is that the fact that there will be stresses in the edges of the holes not is included in the analytical calculations.

It is not known how the temperature will affect the structure. The mechanical properties of the steel as well as will the lubrication properties of the oil will both be affected by an elevated temperature.

There is also some uncertainty regarding the accuracy of the fatigue model used, although it has been empathised that it is to be viewed only as a rough estimate.

During the screening of mechanisms there were two similar solutions suggested as the best option. However in both the single planetary gearing and the double there are some uncertainties if the drive will be able to handle the torque and still be small enough to fit in the packing space. Furthermore the single planetary gearing will have problems achieving the gear ratio desired, while the double will have no problems achieving the gear ratio it will have less chances of handling the torque.

10. References

1. *http://odencontrol.se/UcmsFiles/File/Oden_gear(1).pdf* *2013-02-15*
2. G. Niemann, H. Winter: *Maschinenelemente: Band 2*, Springer-Verlag, Berlin Heidelberg, 1989, s.66
3. G. Niemann, H. Winter: *Maschinenelemente: Band 2*, Springer-Verlag, Berlin Heidelberg, 1989, s. 171
4. L. Vedmar, B. Jacobson: *Tribologi*, KFS, Lund, 2011, s.261

Appendix

Appendix A

Matlab code used to solve the distribution:

```
%%Variables %%%%%%%%%%%%%%%%%%%%%%%%%%%%%%%%%%%%%%%%%%%%%%%%%%%%%%%%%%%%%%
r=0.038;                                    %Hole placement              m
rh=0.007;                                   %Hole radius                 m
rp=0.004;                                   %Pin radius                  m
ry=0.1139;                                  %Cyclo disk Outer radius     m
e=0.006;                                    %eccentricity
ri=0.01859;
M=1075;                                     %Total Torque                Nm

my=0.1;                                     %Coefficient of friction     -

by=5e-3;                                    %Thickness of Cyclo disk Outer
bi=10e-3;                                   %Thickness of Cyclo disk inner

v=0.3;                                      %Poisson's ratio             -
E=207E9;                                    %Young's modulus             Pa
del=30;
n=12;                                       %Number of pins
number
pos=1;                                      %position
number
mov=180;                                    %Examination area
degrees
theta=0:360/n*pi/180:2*pi-360/n*pi/180;     %Angle between spacing holes
rad
phi=0:pi/180*360/n/del:mov*pi/180-pi/180;   %Position displacement
rad
si=pi/(180);                                %Turning angle
rad
Fk=zeros(size(phi,2),size(theta,2));        %Contact force               N
deltha=zeros(1,size(theta,2));              %Angle
rad
rki=zeros(size(phi,2),size(theta,2));       %Distance to contact         m
deff=zeros(1,size(theta,2));                %Deformation                 m
Pmax=zeros(size(phi,2),size(theta,2));      %Hertz                       Pa
Mt=zeros(size(phi,2),1);                    %Moment iteration            Nm
C=0.0025;                                   %Rolling resistance coefficient
mt=2*r*(pi-12*acos(1-rh^2/(2*r^2)));
rhv=0.004:0.0001:0.02;                      %Variable hole radius        m

%%Equilibrium/deformation equations%%%%%%%%%%%%%%%%%%%%%%%%%%%%%%%%%%%%%%

%Internal cyclo
t=zeros(size(phi,2),1);
for k=1:size(phi,2)


    for i=1:size(theta,2)

            a=(2*rp-e)/2;
```

```
            rki(k,i)=sqrt(r^2+a^2+r*a*cos(theta(i)+phi(k)));
            deltha(k,i)=abs(asin(a*abs(sin(theta(i)+phi(k)))/rki(k,i)));
            if theta(i)+phi(k)  <= pi  && theta(i)<= pi
                x=si*(rki(k,i)*abs(sin(theta(i)+phi(k)-deltha(k,i))))^2-
C*si*(rki(k,i)*abs(cos(theta(i)+phi(k)-deltha(i))))^2;
            else
                x=0;
            end
            if theta(i)+phi(k)  >= pi  && theta(i)>= pi
                x=rki(k,i)*abs(cos(theta(i)+phi(k)-deltha(i)+si)-
cos(theta(i)+phi(k)-deltha(i)));
            end

            t(k)=t(k)+x;


    end

    c=M/t(k);

    for i=1:size(theta,2);
        deff(k,i)=si*rki(k,i)*abs(sin(theta(i)+phi(k)-deltha(k,i)));
        if theta(i)+phi(k)  <= pi
            Fk(k,i)=c*deff(k,i);
        else
            Fk(k,i)=0;
        end
        Mt(k)=Mt(k)+(-C*Fk(k,i)*cos(theta(i)+phi(k)-
deltha(k,i))+Fk(k,i)*sin(theta(i)+phi(k)-deltha(k,i)))*rki(k,i);
    end
end

%%Plots%%%%%%%%%%%%%%%%%%%%%%%%%%%%%%%%%%%%%%%%%%%%%%%%%%%%%%%%%%%%%%%%

if mov == 180

%Plot based on forces distribution
figure
    m=0;
    o=0;
    for k=1:1:del
        m=m+1;
        for i=1:n/2+0.5
            Ft(m,i)=Fk(k,i);

        end

        t3(k,:)=Ft(m,:)/sum(Ft(m,:));

        if k==1
            o=o+1;
             subplot(1,4,o)
            bar(t3(k,:),'r')
            xlabel('Pin')
            ylabel('Amount % (force)')
            title('Rotation displacement 0 degree')
        end
        if k==10
            o=o+1;
```

```
            subplot(1,4,o)
            bar(t3(k,:),'r')
            xlabel('Pin')
            ylabel('Amount % (force)')
            str1=num2str(120/n);
            title('Rotation displacement 10 degree')
        end
        if k==20
            o=o+1;
            subplot(1,4,o)
            bar(t3(k,:),'r')
            xlabel('Pin')
            ylabel('Amount % (force)')
            str2=num2str(180/n);
            title('Rotation displacement 20 degree')
        end
        if k==30
            o=o+1;
            subplot(1,4,o)
            bar(t3(k,:),'r')
            xlabel('Pin')
            ylabel('Amount % (force)')
            str3=num2str(360/n);
            title('Rotation displacement 30 degree')
        end
    end

end

%Geometry

figure
circle(0,0,0.05)
hold on
circle(0,0,ri)
theta2=0;
for i=1:n
    circle(r*sin(theta2),r*cos(theta2),rh)
    theta2=theta2+2*pi/n;
end
```

Appendix B

Matlab code used to solve the Hertzian pressure and contact forces:

```
clear all
Fanal_Var_Geometry
close all

%Assembling the distribution variations
t3z=zeros(1,size(t3,1));
t32t=[t3(:,1);t3(:,2);t3(:,3);t3(:,4);t3(:,5);t3(:,6)];
T3=zeros(size(t32t,1),size(theta,2));

f=1;
for j=1:size(theta,2)/2+1

    T3(1:size(t32t,1)-f+1,j)=t32t(f:end);
    f=f+360/n;
end
f=360/n+1;
for j=size(theta,2):-1:size(theta,2)/2+1

    T3(f:size(t32t,1),j)=t32t(1:size(t32t,1)-f+1);
    f=f+360/n;
end

%Calculating forces
FKRt=zeros(size(phi,2),1);
FKRt2=zeros(size(phi,2),1);

for k=1:size(phi,2)

    for i=1:size(theta,2)

            FKRt(k)=FKRt(k)+ (T3(k,i)*rki(k,i)*(abs(sin(theta(i)+phi(k)-
deltha(k,i)))-C*abs(cos(theta(i)+phi(k)-deltha(k,i)))) );

    end
    FKRt2(k)=M/FKRt(k);
    for i=1:size(theta,2)
        FKR(k,i)=T3(k,i)*FKRt2(k);
    end
end

%Force plot
plot(phi*180/pi,FKR(:,1))
title('Force')
ylabel('Force [N]')
xlabel('Angle')

%Control
Mk=zeros(size(phi,2),1);
for k=1:size(phi,2)
    for i=1:size(theta,2)
        Mk(k)=Mk(k)+FKR(k,i)*(rki(k,i)*(abs(sin(theta(i)+phi(k)-
deltha(k,i))) -C*abs(cos(theta(i)+phi(k)-deltha(k,i)))) );
    end
end
```

```
%%Hertz pressure
bi=0.01:0.001:0.02;
save=cell([size(bi,2),1]);
savePmax=cell([size(bi,2),1]);
for m=1:size(bi,2)
    for k=1:size(phi,2)
        for i=1:size(theta,2)
            kb=(1-v^2)/E;
            Pmax(k,i)=sqrt(FKR(k,i)/(pi*bi(m)*2*kb) * (rp-rh)/(rp*(-rh)));
            Tau=0.3*Pmax;
            Sm(k,i)=Tau(k,i)*sqrt(3);

        end
    end
    save(m)={Sm};
    savePmax(m)=({Pmax});
end


%Calculations with variable geometry
q=4;
l=360/q;
rv=27e-3:1e-4:55e-3;
FKRtrv=zeros(size(rv,2));
FKRrv=zeros(size(rv,2));
saverv=cell([size(bi,2),1]);
saveev=cell([size(bi,2),1]);
savehv=cell([size(bi,2),1]);
savePmaxrv=cell([size(bi,2),1]);
savePmaxev=cell([size(bi,2),1]);
savePmaxrhv=cell([size(bi,2),1]);
savepv=cell([size(bi,2),1]);
savePmaxpv=cell([size(bi,2),1]);
saverprhv=cell([size(bi,2),1]);
savePmaxrprhv=cell([size(bi,2),1]);


for m=1:size(bi,2)
    FKRrv=zeros(size(rv,1));
    FKRtrv=zeros(size(rv,2),1);
    for k=1:size(rv,2)
        for i=1:size(theta,2)
                e=2*rh-2*rp;
                a=(2*rp-e)/2;
                rki(i)=sqrt(rv(k)^2+a^2+rv(k)*a*cos(theta(i)));
                deltha(i)=abs(asin(a*abs(sin(theta(i))/rki(i))));
                FKRtrv(k)=FKRtrv(k)+( T3(1,i)*rki(i)*(abs(sin(theta(i)-
deltha(i))) -C*abs(cos(theta(i)-deltha(i)))) );

        end
        FKRtrv(k)=M/FKRtrv(k);
        FKRrv(k)=T3(1,q)*FKRtrv(k);
                if rv(k)==0.038
                    FKRrv(k);
                end
        for i=1:size(theta,2)
             kb=(1-v^2)/E;
             Pmaxrv(k)=sqrt(FKRrv(k)/(pi*bi(m)*2*kb) * (rp-rh)/(rp*(-rh)));
             Tau=0.3*Pmaxrv(k);
```

```
            Smrv(k)=Tau*sqrt(3);
        end


    end
    saverv(m)=({Smrv});
    savePmaxrv(m)=({Pmaxrv});



    ev=0:1e-4:14e-3;
    FKRtev=zeros(size(ev,2));
    FKRev=zeros(size(ev,2));
    for k=1:size(ev,2)
        for i=1:size(theta,2)
                rp=rh-ev(k)/2;
                a=(2*rp-ev(k))/2;
                rki(i)=sqrt(r^2+a^2+r*a*cos(theta(i)));
                deltha(i)=abs(asin(a*abs(sin(theta(i))/rki(i))));
                FKRtev(k)=FKRtev(k)+( T3(1,i)*rki(i)*(abs(sin(theta(i)-
deltha(i))) -C*abs(cos(theta(i)-deltha(i)))) );

        end
        FKRtev(k)=M/FKRtev(k);
        FKRev(k)=T3(1,q)*FKRtev(k);

        for i=1:size(theta,2)
             kb=(1-v^2)/E;
             Pmaxev(k)=sqrt(FKRev(k)/(pi*bi(m)*2*kb) * (rp-rh)/(rp*(-rh)));
             Tau=0.3*Pmaxev(k);
             Smev(k)=Tau*sqrt(3);
        end

    end

    saveev(m)=({Smev});
    savePmaxev(m)=({Pmaxev});
    r=0.038;
    FKRtrhv=zeros(size(rhv,2));
    FKRrhv=zeros(size(rhv,2));
    for k=1:size(rhv,2)

        if rhv(k) > rh
            r=fzero(@(x) 2*pi*x-2*x*n*acos(1-rhv(k)^2/(2*x^2))-mt,[0.01
10]);
        end

        for i=1:size(theta,2)
                rp=rhv(k)-e/2;
                test(k)=rhv(k)/rp;
                a=(2*rp-e)/2;
                rki(i)=sqrt(r^2+a^2+r*a*cos(theta(i)));
                deltha(i)=abs(asin(a*abs(sin(theta(i))/rki(i))));
                FKRtrhv(k)=FKRtrhv(k)+( T3(1,i)*rki(i)*(abs(sin(theta(i)-
deltha(i))) -C*abs(cos(theta(i)-deltha(i)))) );

        end
        FKRtrhv(k)=M/FKRtrhv(k);
        FKRrhv(k)=T3(1,q)*FKRtrhv(k);
```

```
        for i=1:size(theta,2)
             kb=(1-v^2)/E;
             Pmaxrhv(k)=sqrt(FKRrhv(k)/(pi*bi(m)*2*kb) * (rp-rhv(k))/(rp*(-
rhv(k))));
             Tau=0.3*Pmaxrhv(k);
             Smrhv(k)=Tau*sqrt(3);
        end

        rtot(k)=r+0.012;
    end
    savehv(m)=({Smrhv});
    savePmaxrhv(m)=({Pmaxrhv});
    rp=0.004;
    r=38e-3;

    rpv=0.004:0.0001:0.007;
    FKRtpv=zeros(size(rpv,2),1);
    FKRpv=zeros(size(rpv,2),1);
    e=0.006;

        for k=1:size(rpv,2)
            for i=1:size(theta,2)
                a=(2*rpv(k)-e)/2;
                rki(i)=sqrt(r^2+a^2+r*a*cos(theta(i)));
                deltha(i)=abs(asin(a*abs(sin(theta(i))/rki(i))));
                FKRtpv(k)=FKRtpv(k)+( T3(1,i)*rki(i)*(abs(sin(theta(i)-
deltha(i))) -C*abs(cos(theta(i)-deltha(i)))) );

            end
            FKRtpv(k)=M/FKRtpv(k);
            FKRpv(k)=T3(1,q)*FKRtpv(k);

            for i=1:size(theta,2)
                 kb=(1-v^2)/E;
                 Pmaxpv(k)=sqrt(FKRpv(k)/(pi*bi(m)*2*kb) * (rpv(k)-
rh)/(rpv(k)*(-rh)));
                 Tau=0.3*Pmaxpv(k);
                 Smpv(k)=Tau*sqrt(3);
            end
        end
    savepv(m)=({Smpv});
    savePmaxpv(m)=({Pmaxpv});

    FKRtrprhv=zeros(size(rpv,2));
    FKRrprhv=zeros(size(rpv,2));
    e=0.006;

        for k=1:size(rpv,2)
            for i=1:size(theta,2)
                a=(2*rpv(k)-e)/2;
                rki(i)=sqrt(r^2+a^2+r*a*cos(theta(i)));
                deltha(i)=abs(asin(a*abs(sin(theta(i))/rki(i))));

FKRtrprhv(k)=FKRtrprhv(k)+( T3(1,i)*rki(i)*(abs(sin(theta(i)-deltha(i))) -
C*abs(cos(theta(i)-deltha(i)))) );

            end
            FKRtrprhv(k)=M/FKRtrprhv(k);
            FKRrprhv(k)=T3(1,q)*FKRtrprhv(k);
```

```
        for i=1:size(theta,2)
             kb=(1-v^2)/E;
             Pmaxrprhv(k)=sqrt(FKRrprhv(k)/(pi*bi(m)*2*kb) * (rpv(k)-
rpv(k)*rh/rp)/(rpv(k)*(-rpv(k)*rh/rp)));
             Tau=0.3*Pmaxrprhv(k);
             Smrprhv(k)=Tau*sqrt(3);

        end
    end
    saverprhv(m)={Smrprhv};
    savePmaxrprhv(m)={Pmaxrprhv};


end

% Plots
i=0;
for m=1:size(bi,2)
    plot(rhv,savePmaxrhv{m})
    title(' Hole radius as variable')
    xlabel('Hole radius')
    ylabel('Hertzian pressure [Pa]')
    str=num2str(bi(m));
    text(rhv(m+2+i),savePmaxrhv{m}(m+2+i),'b=')
    text(rhv(m+2+i)+0.00025,savePmaxrhv{m}(m+2+i),str)
    i=i+3;
    hold on
end
i=0;
figure
for m=1:size(bi,2)
    plot(rv,savePmaxrv{m})
    title(' Hole position as variable')
    xlabel('Hole position')
    ylabel('Hertzian pressure [Pa]')
    str=num2str(bi(m));
    text(rv(m+2+i),savePmaxrv{m}(m+2+i),'b=')
    text(rv(m+2+i)+0.001,savePmaxrv{m}(m+2+i),str)
    i=i+3;
    hold on
end
i=0;
figure
for m=1:size(bi,2)
    plot(ev,savePmaxev{m})
    title(' Eccentricity as variable')
    xlabel('Eccentricity')
    ylabel('Hertzian pressure [Pa]')
    str=num2str(bi(m));
    text(ev(m+30+i),savePmaxev{m}(m+30+i),'b=')
    text(ev(m+30+i)+0.0002,savePmaxev{m}(m+30+i),str)
    i=i+6;
    hold on
    axis([ev(1) 11e-3 0 5e9])
end

%Efficiency calculations
 i=0;
 figure
```

```
for m=1:size(bi,2)
    if savepv{m}(1:end) == 0
        break
    end
    plot(rpv,savePmaxpv{m})
    title(' Pin radius as variable')
    xlabel('Pinradius')
    ylabel('Hertzian pressure [Pa]')
    str=num2str(bi(m));
    text(rpv(m+2+i),savePmaxpv{m}(m+2+i),'b=')
    text(rpv(m+2+i)+0.0001,savePmaxpv{m}(m+2+i),str)
    i=i+1;
    hold on
end
i=0;
figure
for m=1:size(bi,2)
    if saverprhv{m}(1:end) == 0
        break
    end
    plot(rpv,savePmaxrprhv{m})
    title(' Pin radius and hole radius as varible')
    xlabel('Pinradius')
    ylabel('Hertzian pressure [Pa]')
    str=num2str(bi(m));
    text(rpv(m+2+i),savePmaxrprhv{m}(m+2+i),'b=')
    text(rpv(m+2+i)+0.0001,savePmaxrprhv{m}(m+2+i),str)
    i=i+1;
    hold on

end

t4=0;
for i=1:size(phi,2)
     if i>1
            t4=t4+(phi(i)-phi(i-1))*Fk(i,1);
     else
            t4=t4+(phi(i)-0)*Fk(i,1);
     end
end
figure
myv=0.1:0.1:0.5;
rhv=0.004:0.0001:0.02;
for i=1:size(myv,2);
    for j=1:size(rhv,2)
        Pf(j)=2*n*t4*myv(i)*rhv(j)/(2*pi);
        eta(j)=1-Pf(j)/M;
    end
    plot(rhv,eta)
    title('Efficiency')
    hold on
    xlabel('Hole radius')
    ylabel('Efficiency')
    str=num2str(myv(i));
    text(rhv(i+100),eta(i+100),'my =')
    text(rhv(i+100)+0.0006,eta(i+100),str)
end
Cv=0.002:0.0005:0.0035;
figure
for i=1:size(Cv,2)
    for j=1:size(rhv,2)
```

```
            PfC(j)=2*n*t4*Cv(i)*rhv(j)/(2*pi);
            etaC(j)=1-PfC(j)/M;
    end

    plot(rhv,etaC)
    title('Efficiency')
    hold on
    xlabel('Hole radius')
    ylabel('Efficiency')
    str=num2str(Cv(i));
    text(rhv(i+100),etaC(i+100),'C =')
    text(rhv(i+100)+0.0006,etaC(i+100),str)

end
```

Appendix C

Matlab code used to solve the distribution with tolerances in the geometry:

```
clc
clear all
close all

%%Variabler %%%%%%%%%%%%%%%%%%%%%%%%%%%%%%%%%%%%%%%%%%%%%%%%%%%%%%%%%%%%%%%%
rg=0.038;                                   %Hole placement              m
rhg=0.007;                                  %Hole radius                 m
rp=0.004;                                   %Pin radius                  m
ry=0.1;                                     %Cyclo disk Outer radius     m
e=0.006;                                    %eccentricity
ri=0.01859;
M=1075;                                     %Total Torque                Nm

my=0.1;                                     %Coefficient of friction     -

by=5e-3;                                    %Thickness of cycloidisk Outer
big=10e-3;                                  %Thickness of cycloidisk inner

v=0.3;                                      %Poisson's ratio             -
E=207E9;                                    %Young's modulus             Pa

n=12;                                       %Number of pinns          number
pos=1;                                      %position                 number
mov=180;                                    %Examination area        degrees
thetag=0:360/n*pi/180:2*pi-360/n*pi/180;    %Angle between spacingholes rad

del=30;
phi=0:pi/180*360/n/del:mov*pi/180-pi/180*360/n/del;

Fk=zeros(size(phi,2),size(thetag,2));       %Contact force               N
deltha=zeros(1,size(thetag,2));             %Angle                      rad
rki=zeros(size(phi,2),size(thetag,2));      %Distance to contact         m
deff=zeros(1,size(thetag,2));               %Deformation                 m
Pmax=zeros(size(phi,2),size(thetag,2));     %Hertz                       Pa
Mt=zeros(size(phi,2),1);                    %Moment iteration            Nm
C=0.0025;                                   %Rolling resistance coefficient
z=1e-1;                                     %Constant
siv=z:z:10*z;                               %Displacement degree
siv=siv*pi/180;
zx=0;

% Calculation of the distribution
mr=0;
w2=1;
while mr<100
    %Updating geometry
    for i=1:size(thetag,2)
        [r(i),theta(i),ea,ycoord(i)]=tcirkel(rg,thetag(i),0.00002);
         bi=tbredd(big,-25e-6);
    end
    Fk=0;
    diff=ycoord-ones(size(ycoord,1))*min(ycoord);
    w=1;
```

```
    for tol=1:size(siv,2)
        si=siv(tol);
        t=0;
        for k=1:size(phi,2)

            for i=1:size(theta,2)
                    a=(2*rp-e)/2;
                    rki(k,i)=sqrt(r(i)^2+a^2+r(i)*a*cos(theta(i)+phi(k)));

deltha(k,i)=abs(asin(a*abs(sin(theta(i)+phi(k)))/rki(k,i)));
                    if theta(i) <= pi
                        x=rki(k,i)*abs(cos(theta(i)+phi(k)-deltha(i)+si)-
cos(theta(i)+phi(k)-deltha(i)));
                    else
                        x=0;
                    end

                    if abs(x)-diff(i) >= 0
                        x2=abs(x)-diff(i);
                    else
                        x2=0;
                    end

                    t=t+x2;

                    xs(k,i)=x2;

                     if cos(si)*rki(1,4) >= 2e-4 && w==1
                        saverki(w2)=({rki});
                        savetheta(w2)=({theta});
                        savebi(w2)=({bi});
                    end



            end

        end

        for k=1:size(phi,2)
            for i=1:size(theta,2);
                zx=zx+1;
                deff(i)=si*rki(k,i)*abs(sin(thetag(i)+phi(k))-deltha(i));
                if theta(i)+si <= pi
                    Fk(k,i)=xs(k,i);
                else
                    Fk(k,i)=0;
                end

                %Control
                Mt=Mt+(-my*Fk(k,i)*cos(theta(i)+phi(k)-
deltha(i))+Fk(k,i)*sin(theta(i)+phi(k)-deltha(i)))*rki(k,i);
            end

        end

        m=0;
        for k=1:1:del
```

```
            m=m+1;
            t3(k,:)=Fk(m,:)/sum(Fk(m,:));
        end

        [MaxFord(tol) pos(tol)]=max(max(t3));
        if cos(si)*rki(1,4) >= 2e-4 && w==1
            savet3(w2)=({t3});
            w=w+1;
            w2=w2+1;
            meant3(w2,:)=t3(1,1:n/2);

            break
       end

    end
    mr=mr+1;
    MFM(:,mr)=MaxFord;

end
 FMV=zeros(size(siv,2),1);

% Distribution plot
bar(mean(meant3))
title('Distribution')
xlabel('Pin')
ylabel('Share')
```

Appendix D

Matlab code used to calculate the forces and pressures with the tolerances in the geometry:

```
Loads
for mom=1:size(torque,1)

   Final_geom_tol
   M=torque(mom);



   C_ansys=9440/5.3003e-7;
   lo=0;
   for po=1:size(saverki,2)

   %Assembling the distribution matrix
   t3=savet3{po};

   theta=savetheta{po};
   t32=zeros(1,size(phi,2));
           h=1;

           T3=zeros(size(t32,2),size(theta,2));
           if mod(n,2)==0
               for i=1:n/2
               t32(h:h+del-1)=t3(:,i);
               h=h+del;
               end
               f=1;
               for j=1:size(theta,2)/2+1

                   T3(1:size(t32,2)-f+1,j)=t32(f:end);
                   f=f+del;
               end
               f=del+1;
               for j=size(theta,2):-1:size(theta,2)/2+1

                   T3(f:size(t32,2),j)=t32(1:size(t32,2)-f+1);
                   f=f+del;
               end
           else
               lo=lo+1;
               for i=1:n/2+0.5
                   t32(h:h+del-1)=t3(:,i);

                   h=h+del;
               end
               t32=t32(1:size(phi,2));

               f=1;
               for j=1:size(theta,2)/2+0.5

                   T3(1:size(t32,2)-f+1,j)=t32(f:end);
                   f=f+del;
               end
               f=del+1;
```

```
                for j=size(theta,2):-1:size(theta,2)/2+1.5

                    T3(f:size(t32,2),j)=t32(1:size(t32,2)-f+1);
                    f=f+del;
                end

            end
            if n==11
                T3t=T3;
            end

        %Calculation forces and Hertzian pressures
        rki=saverki{po};
        rh=tradie(rhg,2e-5);
        rp=rh-e/2;
        bi=tbredd(big,-25e-5);
        FKRt=zeros(size(phi,2),1);
        FKRt2=zeros(size(phi,2),1);
        for k=1:size(phi,2)

                    for i=1:size(theta,2)

                            FKRt(k)=FKRt(k)+
(T3(k,i)*rki(k,i)*(abs(sin(theta(i)+phi(k)-deltha(k,i)))-
C*abs(cos(theta(i)+phi(k)-deltha(k,i)))) );
                    end
                    FKRt2(k)=M/FKRt(k);
                    for i=1:size(theta,2)
                        FKR(k,i)=T3(k,i)*FKRt2(k);
                    end
        end

            %%Control
            Mk=zeros(size(phi,2),1);
            for k=1:size(phi,2)
                for i=1:size(theta,2)

Mk(k)=Mk(k)+FKR(k,i)*(rki(k,i)*(abs(sin(theta(i)+phi(k)-deltha(k,i))) -
C*abs(cos(theta(i)+phi(k)-deltha(k,i)))) );

                end
            end

            %%Hertz
                kb=(1-v^2)/E;
                Pmax=sqrt(FKR./(pi*bi*2*kb) * (rp-rh)/(rp*(-rh)));
                for k=1:size(phi,2)
                        Tau=0.3*Pmax(k,i);
                        Sm(k)=Tau*sqrt(3);
                end
           % Values are saved
            savePmax(po)={Pmax};
            saveFKR(po)={FKR};
            MPmax(po)=max(max(Pmax));
            MFKR(po)=max(max(FKR));
    end
    mean(MFKR);
    mean(MPmax)
    Pmax90=prctile(MPmax,90)
    PmaxF90(mom)=Pmax90;
```

```
 end

%deriving the mean values of Pmax and the contact force
tPmax=zeros(size(Pmax,1),size(Pmax,2));
tFKR=zeros(size(FKR,1),size(FKR,2));
for i=1:po
    tPmax=tPmax+savePmax{i};
    tFKR=tFKR+saveFKR{i};
end
meanPmax=tPmax/po;
meanFKR=tFKR/po;

%Plots
close all
plot(phi*180/pi,saveFKR{1}(:,1))
title('Force')
xlabel('Angle')
ylabel('Force [N]')
figure
for i=1:5
plot(phi*180/pi,savePmax{i}(:,1))
title('Hertzian pressure')
xlabel('Angle')
ylabel('Hertzian pressure [N]')
figure
end
plot(phi*180/pi,meanPmax(:,1))
title('Mean hertzian pressure')
xlabel('Angle')
ylabel('Hertzian pressure [N]')
figure
plot(phi*180/pi,meanFKR(:,1))
title('Mean Force')
xlabel('Angle')
ylabel('Force [N]')
```

Appendix E

Matlab code used to handle the fatigue calculations:

```
clear all
close all
clc
Final_forces_tol
wholer
clc

palmG=0;
Koll=0;
for p=1:size(torque)

     P=PmaxF90(p)*ones(size(wy,2),1);
        S=abs(wy-P');
        [s,o]=min(S);

        if wy(o)<=min(wy)
            o=size(wy,2);
        end
        t5(p)=LoadColl(p,4)/wx(o);
        palmG=palmG+t5(p);
        Koll=Koll+1;

end
Koll
palmG
```

Appendix F

Matlab code creating the Wöhler curve:

```
close all
clc
wxt=[1 10^5 10^8 10^9];
wyt=[2250 2250 1490 1490];


k=(1490-2250)/log10(10^8/10^5);
m=2250-k*log10(10^5);



wx=[0:1000:10^5 10^5:1000:10^8 10^8:1000:10^9];


for i=1:size(wx,2)
    if wx(i)<=10^5
        wy(i)=2250;
    end

    if wx(i)>10^5 && wx(i)<=10^8
        wy(i)=(log10(wx(i))*k+m);
    end
    if wx(i)>10^8
        wy(i)=1490;
    end
end

wy=wy*10^6;
```